Generation and characterization of a porcine model for Becker muscular dystrophy

Von Michael Maximilian Stirm

Inaugural-Dissertation zur Erlangung der Doktorwürde
der Tierärztlichen Fakultät der
Ludwig-Maximilians-Universität München

Generation and characterization of a porcine model for Becker muscular dystrophy

von

Michael Maximilian Stirm

aus Bietigheim-Bissingen

München 2023

Aus dem Veterinärwissenschaftlichen Department der Tierärztlichen Fakultät der Ludwig-Maximilians-Universität München

Lehrstuhl für Molekulare Tierzucht und Biotechnologie

Arbeit angefertigt unter der Leitung von: Univ.-Prof. Dr. Eckhard Wolf

Gedruckt mit Genehmigung der Tierärztlichen Fakultät

der Ludwig-Maximilians-Universität München

Dekan:	Univ.-Prof. Dr. Reinhard K. Straubinger, Ph.D.
Berichterstatter:	Univ.-Prof. Dr. Eckhard Wolf
Korreferent/en:	Univ.-Prof. Dr. Laurent Frantz
	Univ.-Prof. Dr. Dusan Palic
	Prof. Dr. Frank Ebel
	Priv.-Doz. Dr. Susanne Zöls

Tag der Promotion: 22.07.2023

Für meine Familie

During the preparation of this thesis, the following publications have been published:

Stirm M, Fonteyne LM, Shashikadze B, Lindner M, Chirivi M, Lange A, Kaufhold C, Mayer C, Medugorac I, Kessler B, Kurome M, Zakhartchenko V, Hinrichs A, Kemter E, Krause S, Wanke R, Arnold GJ, Wess G, Nagashima H, Hrabě de Angelis M, Flenkenthaler F, Kobelke LA, Bearzi C, Rizzi R, Bähr A, Reese S, Matiasek K, Walter MC, Kupatt C, Ziegler S, Bartenstein P, Fröhlich T, Klymiuk N, Blutke A, Wolf E. **A scalable, clinically severe pig model for Duchenne muscular dystrophy. Dis Model Mech. 2021** Dec 1;14(12):dmm049285. doi: 10.1242/dmm.049285. Epub 2021 Dec 16. PMID: 34796900; PMCID: PMC8688409.

Stirm M, Fonteyne LM, Shashikadze B, Stöckl JB, Kurome M, Keßler B, Zakhartchenko V, Kemter E, Blum H, Arnold GJ, Matiasek K, Wanke R, Wurst W, Nagashima H, Knieling F, Walter MC, Kupatt C, Fröhlich T, Klymiuk N, Blutke A, Wolf E. **Pig models for Duchenne muscular dystrophy - from disease mechanisms to validation of new diagnostic and therapeutic concepts. Neuromuscul Disord. 2022** Jul;32(7):543-556. doi: 10.1016/j.nmd.2022.04.005. Epub 2022 Apr 25. PMID: 35659494.

TABLE OF CONTENTS

INDEX OF ABBREVIATIONS

µl	Microliter
µmol	Micromole
AAV	Adeno-associated virus
ACE	Angiotensin-converting enzyme
AI	Artificial insemination
ALT	Alanine aminotransferase
ASO	Antisense oligonucleotide
AST	Aspartate aminotransferase
BAC	Bacterial artificial chromosome
BMD	Becker muscular dystrophy
bmx	Murine Becker muscular dystrophy model with a deletion of exon 45-47 of the *DMD* gene
bp	Base pair
BW	Body weight
CACNA1S	Calcium channel,voltage-dependent, L type, alpha 1S subunit
CAG	Synthetic promoter
Cas9	CRISPR associated protein 9
CASA	Computer assisted semen analyses
cDNA	Complementary DNA, DNA synthesized by reverse transcription from a single stranded RNA
CiMM	Center for Innovative Medical Models
CK	Creatine kinase
CKCS-MD	Cavalier King Charles muscular dystrophy

CNS	Central nervous system
CPT2	Carnitine O-palmitoyltransferase 2
CRISPR	Clustered regularly interspaced short palindromic repeats
CXMD	Canine X-linked muscular dystrophy
DAB	Diaminobenzidine-tetrahydrochloride-dehydrate
deltaE50-MD	Canine Duchenne muscular dystrophy model with a deletion of exon 50 of the *DMD* gene
DGC	Dystrophin glycoprotein complex
DMD	Duchenne muscular dystrophy
DMD	Dystrophin gene
Dmd	Murine dystrophin gene
$DMD^{+/-}$	Heterozygous Duchenne carrier sow = *DMD*Δ52_het
$DMD^{+/+}$	Wild type (WT) pig
DMD^{mdx}	Rat model for Duchenne muscular dystrophy with a nonsense mutation in exon 23 of the *DMD* gene
$DMDX^{KO}Y \leftrightarrow X^{WT}X^{WT}$	Chimeric boar, carrying Duchenne muscular dystrophy affected cells and unaffected cells
$DMD^{Y/-}$	Duchenne muscular dystrophy pig
*DMD*Δ51-52	Porcine Becker muscular dystrophy model with a deletion of exon 52 in *DMD* gene
*DMD*Δ51-52/52	Carrier sow for Duchenne and Becker muscular dystrophy
*DMD*Δ51-52_het	Heterozygous Becker muscular dystrophy carrier sow
*DMD*Δ52	Porcine Duchenne muscular dystrophy model with a deletion of exon 52 in *DMD* gene
*DMD*Δ52_het	Heterozygous Duchenne muscular dystrophy carrier sow = $DMD^{+/-}$

DMEM	Dulbecco's Modified Eagle's Medium, synthetic cell culture medium
DNA	Deoxyribonucleic acid
dNTPs	Nucleoside triphosphates containing deoxyribose for DNA
Dp	Dystrophin proteins
DTT	Dithiothreitel
ECG	Electrocardiography
EDTA	Ethylenediaminetetraacetic acid, anticoagulant for blood samples
EPO	Electroporation
ET	Embryo transfer
F0	Animals generated by somatic cell nuclear transfer
F1	First filial generation
F2	Second filial generation
FCS	Fetal calf serum
FFPE	Formalin-fixed paraffin-embedded
g	Gram
GRMD	Golden retriever muscular dystrophy
gRNA	Guide RNA
h	Hour
hDMD	Human *DMD* gene
HDR	Homology-directed repair, correction of a double-strand break in the DNA by homologous recombination using a DNA template
HE	Hematoxylin and eosin, principal tissue stain for histology
HFMD	Hypertrophic feline muscular dystrophy

i.m.	Intramuscular
IgG	Immunoglobulin G
IHC	Immunohistochemistry
JAG1	Jagged1 gene
JSMD	Japanese Spitz muscular dystrophy
kb	Kilobase = 1,000 bases
kDa	Kilodalton, unified atomic mass unit
LbCpf1	RNA-guided endonuclease isolated from Lachnospiraceae bacterium
LRMD	Labrador retriever muscular dystrophy
LTBP4	Gene coding for latent TGF-beta binding proteins
LVEF	Left ventricular ejection fraction
LVFS	Left ventricular fractional shortening
LVG	Lehr- und Versuchsgut Oberschleißheim of the LMU Munich
M	Molar
Mb	Megabase = 1 million bases
mdx	Murine Duchenne muscular dystrophy model with a nonsense mutation in exon 23 of the *DMD* gene
*mdx*52	Murine Duchenne muscular dystrophy model with a deletion of exon 52 of the *Dmd* gene
mg	milligram
min	Minutes
ml	milliliter
MLPA	Multiplex ligation-dependent probe
mM	Millimolar

mRNA	Messenger ribonucleic acid
MYH3	Embryonic myosin = myosin heavy chain 3
neo®	Neomycin resistance cassette, widespread selection gene in molecular biology coding for the kanamycin kinase,
ng	Nanogram
NGS	Next generation sequencing
NHEJ	Non-homologous end joining, correction of a double-strand break in the DNA by direct ligation of the break ends
NLRP3	NLR family pyrin domain containing 3 gene
p.p.	Postpartum = after birth
PAM	Protospacer adjacent motif
PBS	Phosphate-buffered saline
PCR	Polymerase chain reaction
PCV2	Porcine circovirus type 2
PNS	Peripheral nervous system
rAAV	Recombinant adeno-associated virus
RNA	Ribonucleic acid
RT	Room temperature
RYR1	Ryanodine receptor 1
RYR2	Ryanodine receptor 2
SCNT	Somatic cell nuclear transfer
SDS	Sodium dodecyl sulfate
sgRNA	Single guide RNA
SPF	Specific-pathogen-free
SPP1	Secreted phosphoprotein 1 gene = Osteopontin gene

SRY	Gen coding for the sex-determining region Y protein
ssODN	Single-stranded donor oligonucleotides
TALENs	Transcription activator-like effector nucleases
Taq	Thermus aquaticus
U/l	International unit for enzymes per liter
UTRN	Utrophin, ubiquitous dystrophin
WT	Wild type, unmodified animal
x g	Centrifugal force = number of times the gravitational force
XLDCM	X-linked dilated cardiomyopathy

I. INTRODUCTION

Duchenne muscular dystrophy (DMD) is a severe neuromuscular disorder, affecting, due to its X-chromosomal location, almost exclusively boys. The disease is caused by various mutations in the dystrophin gene (*DMD*), mostly frame-shift mutations or nonsense mutations, which lead to premature stop codons and thus to the absence of functional dystrophin protein, which causes a progressive muscle weakness and cardiomyopathy. In-frame mutations, in contrast, result usually in a milder type of dystrophinopathy, the Becker muscular dystrophy (BMD) (DUAN et al., 2021). To date, no cure for DMD exists, but countless different approaches were tested *in-vitro* and *in-vivo* in cell culture, animal models, and human patients. Among these approaches, exon skipping is the most widespread (TAKEDA et al., 2021). In 2020, our research group demonstrated the possibility to restore the reading frame of the *DMD* gene *in-vivo* in our *DMD*Δ52 pig model for Duchenne muscular dystrophy, by additional deleting exon 51. AAV vectors were used to transfer the genetic information for the Cas9 protein and two guide RNAs, flanking exon 51. The therapeutic approach resulted in a partial restoration of dystrophin expression. However, only a shortened dystrophin (*DMD*Δ51-52) was expressed in the injected pigs (MORETTI et al., 2020). To simulate the best possible outcome of this therapy, we generated a *DMD*Δ51-52 pig model by CRISPR/Cas9 gene editing. At the same time, this new pig model represents, due to its in-frame mutation in the *DMD* gene, a model for the Becker muscular dystrophy and thus is the first tailored, genetically modified porcine model for this disorder.

II. LITERATURE

1. Duchenne and Becker muscular dystrophy

1.1. The dystrophin protein and its isoforms – one gene, many peptides

The *DMD* gene, coding for the dystrophin protein, is one of largest protein coding genes in mammalian genomes, with a total length of about 2.4 million base pairs (Mb), located on the X-chromosome. The coding sequence, formed by 79 exons, is about 11.4 kilobases (kb) and the resulting protein is up to 427 kilodaltons (kDa). Within the *DMD* gene, eight known promoter sequences form the starting points of transcripts for at least eight dystrophin isoforms. Three different full-length Dp427 isoforms were discovered (Dp427m, Dp427c and Dp427p) of which the Dp427m is the main isoform in skeletal and heart muscle, while Dp427c and Dp427p are expressed in the central nervous system (CNS). The promoters of the shorter isoforms are distributed over the entire gene. For the Dp260, the retinal dystrophin isoform, it is located between exons 29 and 30, for Dp140, another central nervous system associated isoform, which is additionally expressed in the kidney, the starting sequence is between exons 44 and 45, while Dp116 (peripheral nervous system (PNS)) starts at exon 56. The last two, Dp71 (ubiquitously expressed) and Dp40, both start with exon 63, but Dp40 already ends after exon 70 (DUAN et al., 2021). Dp40, the shortest isoform, is a further CNS specific isoform (TOZAWA et al., 2012).

Among all these isoforms, Dp427m is certainly the most prominent and best studied, as it has the characteristic function of the dystrophin protein. Dp427m connects the cytoskeleton of myocytes and cardiomyoctes, via the dystrophin glycoprotein complex (DGC), to the surrounding extracellular matrix and thus is essential for the membrane stability (**Figure 1**) (GAO & MCNALLY, 2015).

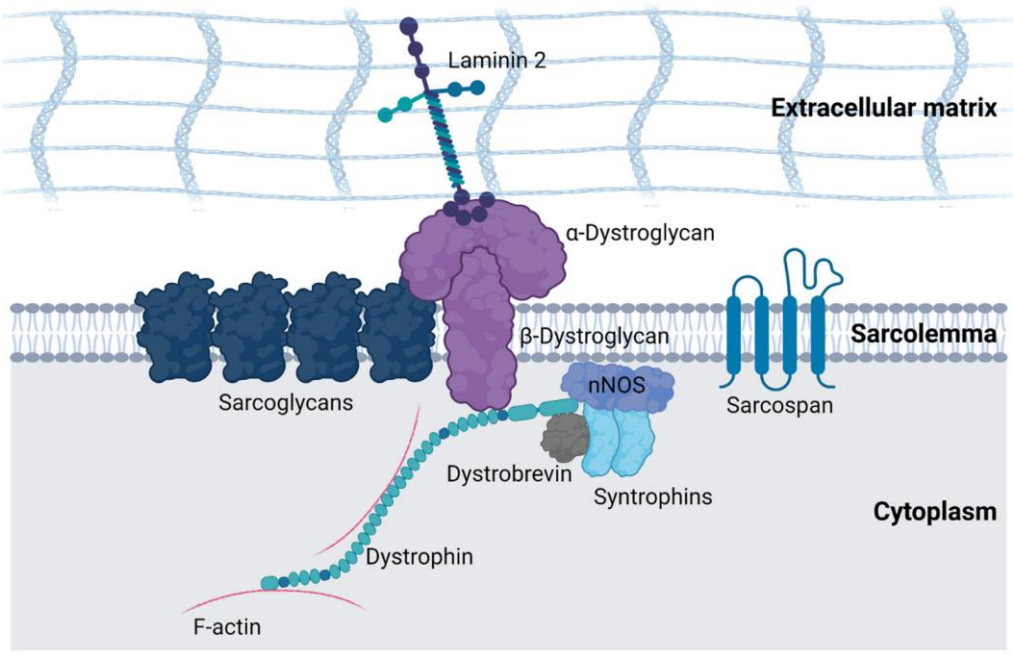

Figure 1: Schematic illustration of the dystrophin glycoprotein complex (DGC). Dystrophin binds the F-actin of the cytoskeleton in myocytes and connects it via the DGC to the surrounding extracellular matrix. Figure published in (STIRM et al., 2022).

1.2. Dystrophinopathies and the reading-frame rule

Considering the size of the *DMD* gene, mutations within this gene occur frequently. Bladen et al. analyzed 7,149 patient mutations, of which 80% were large mutations, affecting one or more exons, while the other 20% mutations were at most one exon in size or smaller. The large mutations were dominated by deletions, while the short mutations were mainly point mutations, mostly nonsense mutations (BLADEN et al., 2015). Mutations in the *DMD* gene could cause different diseases. Reading-frame mutations, insertions or deletions of a number of nucleotides, not divisible by three, or nonsense mutations, which both cause premature stop codons in the *DMD* gene leading to the more severe Duchenne muscular dystrophy. The relationship between dystrophin and Duchenne muscular dystrophy was discovered by Louis M. Kunkel's lab and published for the first time in 1987 (HOFFMAN et al., 1987). In-frame mutations, in contrast, produce a milder disease phenotype, with a later onset and slower progression, the so-called Becker muscular dystrophy. The mutations, with an intact reading-frame usually enable the expression of a shortened, partially functional dystrophin protein, while the premature stop codons

result in loss-of-function mutations, with an absence of dystrophin protein in the Duchenne patients (MONACO et al., 1988). According to the Leiden DMD database, which contains more than 4,700 patients' mutations, 91% of BMD and DMD mutations agree with this reading-frame rule on the DNA level, while up to 99.5% correlation between genotype and phenotype were detected, when the RNA level was considered (AARTSMA-RUS et al., 2006). X-linked dilated cardiomyopathy (XLDCM) is another disorder caused by *DMD* mutations, which is characterized by the absence of skeletal muscle weakness, while substantial heart symptoms are present. The leading symptom is dilated cardiomyopathy, which could even result in heart failure. XLDCM is related to various mutations, affecting the transcription or splicing specific in the myocardium, but not in skeletal muscle or reduce the functionality of regions of the dystrophin protein, which are more relevant in the heart (COHEN & MUNTONI, 2004). Thus, depending on the location and type of mutation, mutations in the *DMD* gene can produce very different clinical pictures: from asymptomatic, to milder BMD and XLDCM with an exclusive cardiac phenotype, to severe DMD (FLANIGAN et al., 2009).

1.3. Clinical manifestation of dystrophinopathies

The incidence of Duchenne muscular dystrophy varies significantly between different countries and ranges between 27.8 per 100,000 male births in Canada and 10.71 in Italy (MAH et al., 2014). Becker muscular dystrophy occurs less frequently with an incidence of only 7.2 out of 100,000 male newborns (MOSTACCIUOLO et al., 1993). DMD is characterized by a progressive muscle weakness and by an early onset of symptoms at an average age of 2-3 years. First symptoms are walking difficulties, frequent falls during walking and the Gower's sign. The Gowers sign describes a maneuver in which the affected boys use their hands to get up from the ground because their hind limbs are too weak (KAMDAR & GARRY, 2016). The patients usually lose their ability to walk, due to progressive muscle weakness, around an age of 12 and suffer from respiratory and cardiac failure in their twenties (MERCURI et al., 2019). The cardiac manifestations are dominated by progressive fibrosis of myocardium, reduced function of the cardiac conduction system, arrhythmias and dilated cardiomyopathy (KAMDAR & GARRY, 2016).

In many DMD patients, muscle weakness is followed by scoliosis of the spine,

especially after becoming wheelchair bound (RYDER et al., 2017). Cognitive impairment and learning difficulties are common symptoms, found not only in DMD, but also in BMD patients (YOUNG et al., 2008; DOORENWEERD et al., 2017).

Life expectancy for DMD patients was ~19 years without artificial ventilation, respectively ~30 years with respiratory support. Most patients die from respiratory or heart failure (LANDFELDT et al., 2020). In BMD patients, disease symptoms appear later, on average at an age of 11.2 years and are in general milder, with a slower progression compared to DMD. Although depending on the causing mutation, BMD phenotypes variate extremely, between asymptomatic to severe, almost DMD-like phenotype (BUSHBY & GARDNER-MEDWIN, 1993). Typical symptoms found in BMD patients are calf pain and hypertrophy, often falling while walking, slower walking than age-matched, difficulties of climbing stairs, a waddling gait, toe-walking, older age when starting to walk, myoglobinuria and muscle wasting (BUSHBY & GARDNER-MEDWIN, 1993).

The CINRG Becker Natural History Study including 83 BMD patients between 5.6 and 75.4 years found no patient younger than 20, who lost his ambulation. In the age group of over 40 years, 50% (12 of 24) of the patients were still able to complete the 6-minute walk test, a diagnostic test for the disease progression (CLEMENS et al., 2020).

Creatine kinase (CK) levels, a muscle and myocardium specific serum marker for cell damage, were elevated ranging between mildly to extremely increased (630-35,340 U/l; mean 5,202 U/l) in a group of 52 patients, compared to less than 150 U/l in unaffected (BUSHBY & GARDNER-MEDWIN, 1993). In a cohort of 28 BMD patients with subclinical or mild muscular involvement, some patients showed increased serum CK activity levels, cramps, myalgia, myoglobinuria, hypertrophy of the calf and cardiac involvement. None of these symptoms were present in all of the investigated individuals. In some of the affected males, heart impairment was at an advanced stage. Specifically, arrhythmias and signs of dilated cardiomyopathy, like reduced ejection fraction were observed (MELACINI et al., 1996).

After all, due to the late onset of the disease, the BMD patients had on average 1.07 children. However, fewer than their healthy brothers, which had 1.63 (BUSHBY &

GARDNER-MEDWIN, 1993). Busby et al. identified in 1993 a mean age of death for BMD patients of 47.3 years ranging from 23 to 89 years (BUSHBY & GARDNER-MEDWIN, 1993). Thus, life expectancy in BMD patients is increased by 50%, compared to DMD patients (~30 years) (LANDFELDT et al., 2020).

1.4. Pathophysiology

The dystrophin protein stabilizes the membrane of myocytes and cardiomyocytes, by connecting the actin cytoskeleton with various membrane proteins, the so-called dystrophin glycoprotein complex, and the surrounding extracellular matrix. In myocytes lacking dystrophin, the contraction of the musculature causes cellular membrane damage, followed by pathological calcium influx, which finally causes cell death (KAMDAR & GARRY, 2016). In BMD, the shortened but partially functional dystrophin protein can maintain muscle and cardiac function for a longer period and thus slow down the disease progression (MONACO et al., 1988). In XLDCM it is speculated, that the mutation influences *DMD* transcription and splicing in a tissue-specific manner and thus leads to an isolated cardiac phenotype, without muscle wasting and weakness. Other mutations seem to involve the stability of some regions, which are more important for the dystrophins' function in the myocardium than in the skeletal muscle (COHEN & MUNTONI, 2004). In some XLDCM patients, the muscle specific full-length dystrophin isoform (Dp427m) is missing, but is restored by an upregulation of the brain and Purkinje fiber specific isoforms (Dp427c +Dp427p) in the skeletal muscle, but not in the heart (MUNTONI et al., 2003).

The progressive muscle and heart muscle cell death is followed by replacement by fat and connective tissue. The progressive fibrosis impairs the muscle and heart function, specifically the contractility of the ventricles and the cardiac conduction system. The myocyte damage leads to increased levels of the cytoplasmic proteins creatine kinase (CK), alanine aminotransferase (ALT) and aspartate aminotransferase (AST) in the serum (DUAN et al., 2021).

Especially the absence of the shorter dystrophin isoforms Dp140 and Dp71 affects the cognitive function in many patients (NAIDOO & ANTHONY, 2020). Although the shorter isoforms dominate in the brain, even full-length dystrophin is expressed in brain tissue (Dp427). Histologically, changes in dendritic development and

arborisation are found in the brains of some dystrophinopathy patients (MUNTONI et al., 2003).

1.5. Inheritance of Duchenne and Becker muscular dystrophy – dystrophinopathies in women

Due to the localization of the *DMD* gene on the X-chromosome, the inherited diseases, caused by mutation it this gene, affect almost exclusively males. Most female carriers for BMD or DMD are asymptomatic, due to their unaffected *DMD* allele on the second X-chromosome. Nevertheless, some of these carriers present symptoms, in most cases signs of cardiomyopathy. In a cohort of 56 DMD carriers, 12% had symptoms of muscle weakness, while cardiac abnormalities, most of them asymptomatic, were present in 18% (GRAIN et al., 2001). There is much evidence to suggest that severe symptomatology in carriers is related to skewed X-chromosome inactivation (VIGGIANO et al., 2016). Further, single cases of DMD or BMD cases in females are described, either by two mutated *DMD* genes on both sex chromosomes (QUAN et al., 1997; FUJII et al., 2009), or by a combination of the carrier stage for a dystrophinopathy and Turner syndrome (VERMA et al., 2017; CHEN et al., 2020). Turner syndrome is caused by the absence of parts or the entire second X-chromosome in women (SYBERT & MCCAULEY, 2004).

About two-third of the DMD patients receive the mutated dystrophin gene from their mother, while the other third resulted from *de novo* germline mutations (DUAN et al., 2021). According, Lee et al. found in 57.6% of DMD patients' mothers the same mutation as in their sons but a significant higher percentage for BMD patients' mothers (89.5%) (LEE et al., 2014).

1.6. Diagnosis of dystrophinopathies

Albeit DMD patients present their first symptoms at an average age of 2.5 years, there is often a delay until the correct diagnosis is made (CIAFALONI et al., 2009).

In contrast to DMD, the mean age, when BMD patients show first disease specific symptoms is at 11.2 years and the diagnosis is even more delayed, with a mean age of 17.7 years. It is noteworthy that some BMD patients did not show onset of muscle weakness until 38 years of age (BUSHBY & GARDNER-MEDWIN, 1993).

Usually CK level check is used as first diagnostic tool (ZALAUDEK et al., 1999), followed by muscle biopsy and genetic testing. CK levels are elevated 10 to 100 times in most DMD and BMD patients. Normally, it takes on average 2 years from first symptoms to the first CK check and referral to a neuromuscular specialist (CIAFALONI et al., 2009). If dystrophinopathy is present in the newborns' family, either male siblings or near relatives are affected, or the mother or an aunt is a carrier for BMD or DMD, a CK measurement is obligatory (NASCIMENTO OSORIO et al., 2019). Further serum markers, which are usually increased in dystrophinopathy patients, are lactate dehydrogenase, alanine aminotransferase and aspartate aminotransferase, of which the both last mentioned lead often the false suspicion of liver involvement (TAY et al., 2000).

Biopsy material could be used to detect the absence of dystrophin in the skeletal muscle of DMD patients or rather to analyze the expression level of dystrophin in BMD patients by immunohistochemistry. Additionally, western blot analysis of dystrophin expression level allows not only a qualitative but also a quantitative detection of dystrophin protein (ANTHONY et al., 2011).

An outdated method, but still used in some cases, is multiplex PCR, which can still detect the majority of large mutations, but often cannot determine the exact boundaries of the mutation. It also cannot reliably differentiate between in-frame and out-of-frame mutations (BEGGS et al., 1990; AARTSMA-RUS et al., 2016).

Multiplex ligation-dependent probe amplification (MLPA) analysis is performed to detect, which *DMD* exons are mutated, using a pair of probes, for each *DMD* exon. Each pair of probes hybridizes next to each other and one of the probes is connected to a "stuffer sequence", with a various length for each exon pair. Only hybridized probe pairs can amplify during the following PCR, indicating missing exon or duplications (OKIZUKA et al., 2009; AARTSMA-RUS et al., 2016). In recent years, Sanger sequencing and next-generation sequencing have gained in importance as they represent the gold standard for small mutation detection, as they also detect point mutations and not only large deletions and duplications affecting entire exons (AARTSMA-RUS et al., 2016). **Figure 2** shows an exemplary diagnostic algorithm.

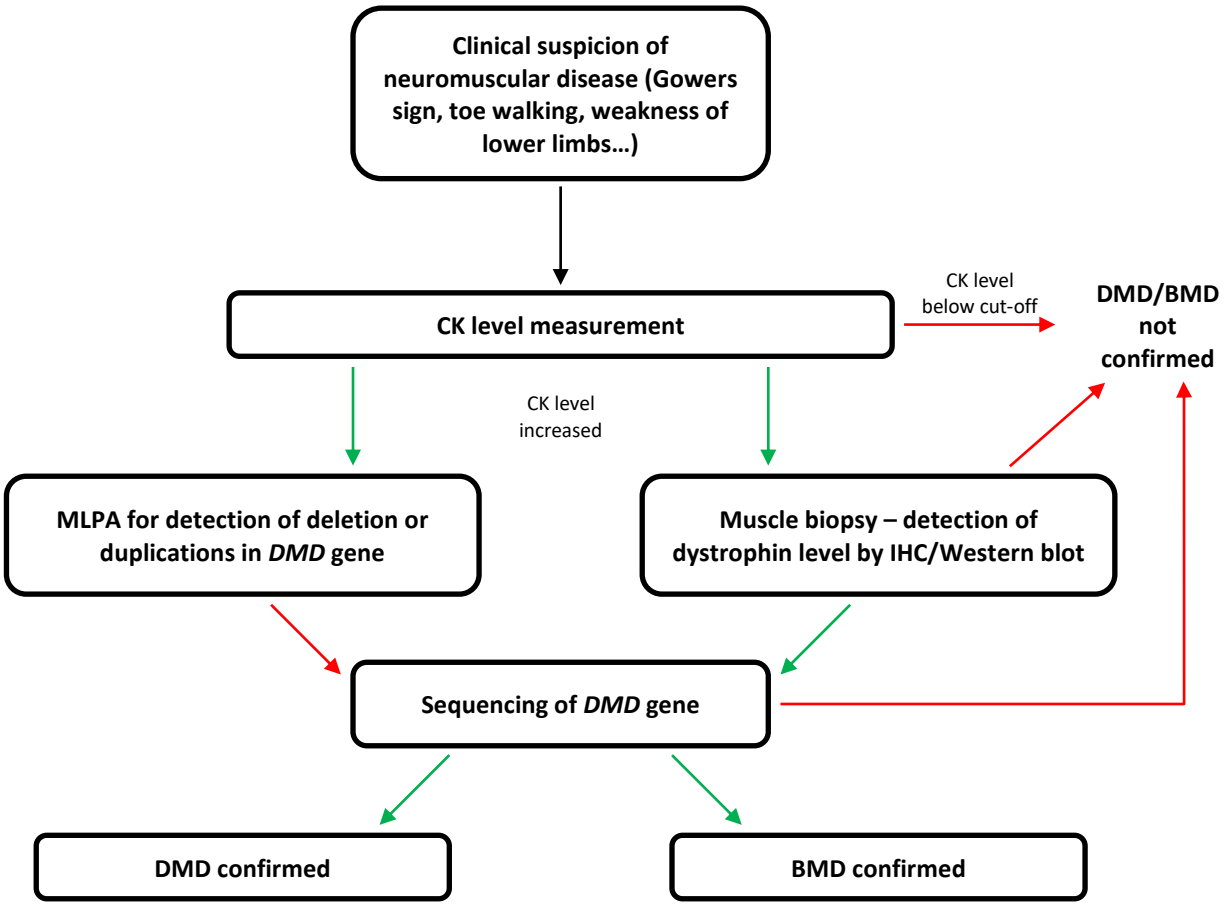

Figure 2: Adapted diagnostic algorithm for the identification of neuromuscular diseases. Modified from (NASCIMENTO OSORIO et al., 2019). CK = Creatine kinase; MLPA = Multiplex ligation-dependent probe amplification; IHC = Immunohistochemistry

In various countries, newborn-screenings were started by checking CK levels from dried blood spots (BIRNKRANT et al., 2018). For example, in New York State, a newborn-screening for neuromuscular disorders was established. Newborns with identified hyperCKemia were again tested after a few days and if values were still above the cut-off, molecular testing were done from cells from blood or buccal swab. In specific, next generation sequencing (NGS) for mutations in the *DMD* gene was performed, followed by NGS for 45 other neuromuscular disorder-related genes, if no causal mutation was found in the *DMD* gene. In some patients, gene-panels for up to 151 genes were done. In total, 15,754 babies were screened, of which three were diagnosed with mutations in the *DMD* gene. Two of these patients were identified as DMD and one as BMD. The postnatal screening enables an early diagnosis, periodic checkups and thus a timely start of treatment (HARTNETT et al., 2022).

In women, who are identified as carriers for one of the dystrophinopathies, preimplantation testing or prenatal tests are available, using either chorionic villi or amniotic fluid (PRIGOJIN et al., 1993).

2. Therapies - today and in the future

2.1. Treatment of Duchenne and Becker muscular dystrophy patients

Up to the present day, no cure for DMD or BMD is available. But nevertheless, different therapeutic strategies are able to slow down the disease progression and could improve life expectancy in the last decades. For example, artificial ventilation extended the average lifespan in Duchenne patients for more than 10 years (LANDFELDT et al., 2020).

State of the art treatment is still the long-term glucocorticoid therapy, with either prednisone/prednisolone (initially 0.75 mg/kg BW per day) or deflazacort (initially 0.9 mg/kg BW per day) (BIRNKRANT et al., 2018). Glucocorticoids seem to slow down the loss of ambulation and respiratory function as well as they could avoid scoliosis (LEBEL et al., 2013). The ability to walk is preserved by almost 4 years with daily deflazacort and about 1.2 years with daily prednisone, compared to DMD patients who have not received glucocorticoids for more than one year. However, the deflazacort treatment had significant increased side effects (growth delay, cushingoid appearance and cataracts (Bello, 2015 #306)). As in DMD patients, glucocorticoid treatment (deflazacort) could delay the muscle wasting and preserve the ability to walk, as well as heart and respiratory function in BMD patients. Prednisone was also used in BMD patients, but was less successful than deflazacort (ANGELINI et al., 2019).

Scoliosis is a common burden that many DMD patients, who lost their ambulation, suffer from. To delay the development of scoliosis, it is important that affected patients stay mobile as long as possible, which could be realized by an early start of glucocorticoid treatment. In patients, in which the scoliosis is already present, only surgery promises alleviation, provided that respiratory and cardiac function of the patients still allows the anesthesia (ARCHER et al., 2016).

The ATS Consensus Statement recommends respiratory muscle training, airway clearance and the use of artificial respiration (FINDER et al., 2004). Especially the

artificial respiration was able to extend life expectancy in DMD by 11 years (LANDFELDT et al., 2020). In contrast to DMD, even adult BMD patients have just a mildly reduced respiratory function compared to unaffected (DE WEL et al., 2021).

Pharmacological treatment is essential for DMD and BMD patients who exhibit cardiac symptoms. Angiotensin-converting enzyme inhibitors (ACE inhibitors), angiotensin receptor blockers, aldosterone antagonists and beta blockers are used to preserve heart function (KASPAR et al., 2009a). Especially the combination of ACE inhibitors and beta blockers showed beneficial results in clinical trials (BUSHBY et al., 2003; KAJIMOTO et al., 2006). Early initiation of therapy with ACE inhibitors is particularly effective in preserving cardiac output in BMD (STALENS et al., 2021). Heart transplantation is another option, but it is used almost exclusively in BMD patients but not in DMD patients (CONNUCK et al., 2008; WU et al., 2010).

Physiotherapy is essential to improve respiratory muscle force and prevent an early loss of ambulation, contractures and scoliosis (DUAN et al., 2021). Physiotherapy including respiration musculature ameliorates respiratory symptoms not only in BMD patients (YELDAN et al., 2008) but also in DMD patients (WANKE et al., 1994). Another important point of physical activity is to keep the body weight low, or to lower it, which should be supplemented by an optimized diet. Due to reduced exercise, but also due to the long-term administration of glucocorticoids, many patients also suffer from obesity, which additionally aggravates some symptoms (WILLIG et al., 1993; MOXLEY et al., 2010). Davis et al. recommend avoiding malnutrition and hypercaloric diets to prevent obesity and not accelerate muscle wasting (DAVIS et al., 2015).

2.2. New treatments

Three different antisense oligonucleotides (ASOs) have a conditional approval by the FDA for the treatment of DMD. These ASOs cause a post-transcriptional modification of the dystrophin pre-mRNA, more precisely the restoration of the correct reading frame and thus the expression of a shortened dystrophin in the treated Duchenne muscular dystrophy patient, corresponding to Becker muscular dystrophy. Eteplirsen skips exon 51 of the dystrophins' pre-mRNA, applicable to

up to 14% of DMD patients, while golodirsen and viltolarsen both skip exon 53, still suitable for 8% of patients (DUAN et al., 2021). A clinical study with eight DMD patients presented an about 16-fold increase of dystrophin expression, which corresponds to just 1% of the dystrophin level of an unaffected person, after weekly treatment with golodirsen (FRANK et al., 2020). Eteplirsen seems to slow down the loss of respiratory function (IFF et al., 2022). Viltolarsen improves not only dystrophin expression, but limb muscle force too (CLEMENS et al., 2022).

However, the effect of such treatments is controversial, since only small amounts of dystrophin are produced and this only at an advanced disease stage (AARTSMA-RUS & ARECHAVALA-GOMEZA, 2018).

2.3. Preclinical experimental treatments

Although the treatment of muscular dystrophy patients has achieved significant improvements in life expectancy and quality of life in recent years and decades, there is still no cure and research is still needed (SUN et al., 2020). In the following section, the most common therapeutic approaches are discussed, but no claim to completeness can be made due to the abundance and heterogeneity of the approaches.

One obvious approach is to introduce the dystrophin gene into myocytes *in vivo*, but due to the size of the full-length dystrophin of 2.4 million bases, respectively 11.4 kb of coding sequence, the delivery of the full-length dystrophin is almost impossible with today's techniques. However, the structure of the dystrophin protein, with its repetitive sequences, allows parts to be excluded and still have a partially functional protein. The resulting mini- and microdystrophins are small enough to be transferred by conventional vectors like retroviral, adenoviral or adeno-associated viral vectors (AAVs) (DUAN, 2018). In dystrophic dogs, for example, the treatment with a microdystrophin construct resulted in reduced muscle histopathology (YUE et al., 2015).

Among the various approaches, which were tested *in vitro* or *in vivo* in animal models in the past years, exon skipping might be the most prominent, but at least as challenging, trial. This only became possible with the discovery of CRISPR/Cas in 2012 (GASIUNAS et al., 2012; JINEK et al., 2012). Three groups published independently the first preclinical exon skipping trials in the *mdx* mouse, the murine

model for DMD, in 2016. All used AAV as vectors to transfer CRISPR/Cas9 approaches into the murine cells. Pairs of guide RNAs, flanking exon 23 of the murine *Dmd* gene, deleted this exon *in vivo* and thus restored the dystrophin expression by deleting the premature stop-codon of the *mdx* mouse model. The investigated mice presented not only elevated dystrophin levels, but also improved muscle force (LONG et al., 2016; NELSON et al., 2016; TABEBORDBAR et al., 2016). This was later followed by experiments in the large animal model dog (AMOASII et al., 2018) and by our research group in the Duchenne pig model (*DMD*Δ52 pig) (MORETTI et al., 2020). Amoasii et al. used the deltaE50-MD dog model, which carries a deletion of exon 50 of the *DMD* gene, resulting in a frame-shift. Via two different AAV vectors, they transferred the information for a single guide RNA and the Cas9 protein to the affected dogs. Two dogs were injected intramuscularly, while the two others got a high dose systemic delivery. The single guide RNA targeted the splice acceptor site of exon 51, and thus restored the open reading frame. In the correct modified cells, a shortened dystrophin transcript, without exons 50 and 51 was produced. Dystrophin levels varied between the tissues, but reached up to 92% of wild type (AMOASII et al., 2018). Moretti et al. pursued a different goal in the *DMD*Δ52 pig (**Figure 3**). They selectively deleted exon 51 *in vivo*, to restore the reading-frame of the pigs, lacking exon 52 of the *DMD* gene. As in the previous trials, AAV were used as vectors for the delivery. Due to the size of the Cas9 plasmid and the two guide RNAs, an intein-split Cas9 was used and divided between two AAVs. The chosen guide RNAs targeted the regions upstream and downstream of the porcine exon 51 and together deleted this exon. Local intramuscular treatment of the pigs showed only a local amelioration in the injected muscle, while high-dose systemic treated pigs presented milder disease symptoms in skeletal muscle and heart compared with untreated controls. However, due to the limited transduction capacity of AAVs, the treated pigs have the shortened, partially functional dystrophin (*DMD*Δ51-52) only in a proportion of their skeletal muscle cells and cardiomyocytes (MORETTI et al., 2020). That is why we decided to generate a new pig model with this mutation, simulating the best possible outcome of the exon skipping therapy, the *DMD*Δ51-52 pig.

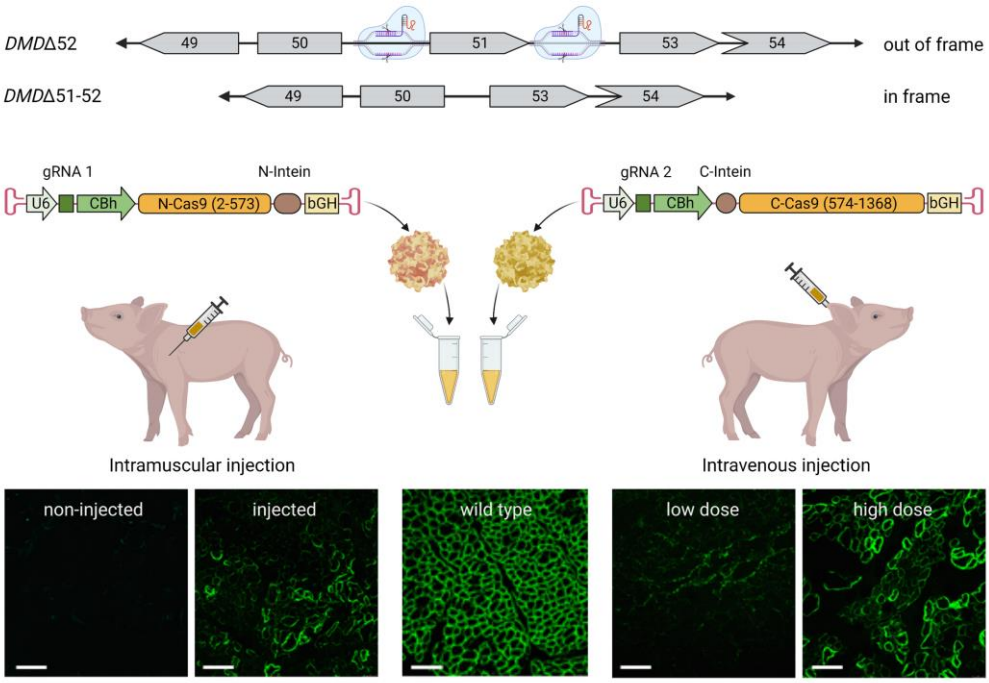

Figure 3: AAV-mediated exon 51 skipping in DMDΔ52 pigs for the restoration of the reading frame of the DMD gene. (a) For the selective deletion, two gRNAs targeted the regions upstream and downstream of exon 51 in the DMDΔ52 pig, resulting in the expression of a truncated dystrophin protein (DMDΔ51-52). (b) Due to the length, the information for the two gRNAs and the Cas9 protein were splitted between two AAV vectors, using an intein split Cas9. Piglets were coinjected with both vectors either local (intramuscular (i.m.)) or systemically (intravenous) with different dosages. (c) While dystrophin protein could not be detected by immunofluorescence against dystrophin in untreated DMDΔ52 skeletal muscle, the treated animals presented different proportion of dystrophin expression. i.m. injected DMDΔ52 had good expression only in the treated muscle, while high dose systemically treated DMDΔ52 expressed well in various investigated muscles. The low dose intravenous resulted only in weak restoration of the dystrophin expression. Figure from (STIRM et al., 2022).

3. Animal models for Duchenne muscular dystrophy

3.1. Murine models

The first time, when a mouse with symptoms, similar to the human Duchenne muscular dystrophy was identified, was in 1984 by the group of Bulfield and Moore. They named their discovered mouse line *mdx* mouse, for X chromosome-linked muscular dystrophy in the mouse (BULFIELD et al., 1984). This was the birth of the first murine model for DMD. The *mdx* mouse shaped DMD research for decades, as evidenced by the frequency of citations of the first publications alone (1,114 citations in March 2023). The spontaneously mutated mice, originated from

a C57BL/10 line, presented disease characteristic symptoms like increased creatine kinase serum levels and skeletal muscle morphology correlating to some histopathological findings in human patients. Further, they discovered by breeding these mice, that the mutation had to be linked to the X chromosome. However, the underlying mutation could not be identified at that time (BULFIELD et al., 1984). This is not surprising as it took another three years for the dystrophin protein to be discovered, by Louis Kunkel's lab. They also identified the link between mutations in the *DMD* gene and Duchenne muscular dystrophy. They found that they could not detect the dystrophin protein either in the muscle of patients or in the *mdx* mouse (HOFFMAN et al., 1987). Finally, two years later, a nonsense mutation in *Dmd* exon 23, causing a premature stop codon in the coding sequence, was identified as causal mutation in the *mdx* mouse model (SICINSKI et al., 1989). The muscle force in the *mdx* model is slightly reduced compared to WT control animals (LYNCH et al., 2001). The upregulation of utrophin (UTRN, ubiquitous dystrophin), a homologue protein to dystrophin, in the *mdx* muscles, could explain almost maintained muscle function (TINSLEY et al., 1998). For this reason, multiple transgenic mouse lines were created, like the *Dmd*/*Utrn* double-knockout mouse, which correlates well to human disease on the phenotype level, but not on the genotype (DECONINCK et al., 1997). In addition, mouse models carrying mutations commonly found in human patients have been generated and are suitable for example for simulating exon skipping trials, which show promise for treating a large proportion of patient mutations simultaneously. Araki et al. generated a murine model with the deletion of exon 52 of the *Dmd* gene (ARAKI et al., 1997). In recent years, humanized mouse models carrying the human *DMD* gene (h*DMD*), integrated in murine chromosome 6 and specific mutations in the h*DMD* have gained importance (T HOEN et al., 2008; YOUNG et al., 2017).

3.2. Rat models

The *Dmd* mutated rat (*Dmd*^{mdx}) model, first described in 2014, carries an 11bp deletion in exon 23 of the *Dmd* gene, correlating to a frameshift mutation. The mutation results in almost complete absent dystrophin expression, not detectable by western blot and less than dystrophin 5% positive fibers in immunohistochemical (IHC) studies. Skeletal muscles presented progressive fibrosis and fatty infiltrations and affected rats had reduced muscle force, compared to unaffected. Further, this model had signs of dilated cardiomyopathy, found in echocardiography

(LARCHER et al., 2014). While the former model was created using transcription activator-like effector nucleases (STALENS et al.), Nakamura et al. already used the newer technique CRISPR/Cas9 to generate their rat model. They coinjected the Cas9 mRNA with two gRNAs, of which one targets exon 3 and the other exon 16 of the rat *Dmd* gene, in zygotes, resulting in the birth of 10 male rats, of which 9 carried a mutation in at least one of the two targeted exons. However, some of the rats carried in-frame mutations, correlating to the human BMD and presented the expression of a truncated dystrophin protein. Fibrosis, central nuclei, regenerating fibers and reduced muscle strength, all signs of muscular dystrophy, were found in the F0 rats. Additionally, the rat model exhibited a more severe cardiac involvement, compared to the *mdx* mouse (NAKAMURA et al., 2014).

3.3. Canine X-linked muscular dystrophy (CXMD)

The first dog diagnosed with symptoms similar to the human Duchenne muscular dystrophy was a male Golden Retriever. This dog showed symptoms of muscle weakness and stiffness, as well as increased serum creatine kinase levels. Skeletal muscle histology presented necrosis and regeneration of muscle fibers (VALENTINE et al., 1986). This founder dog was used for the establishment of a laboratory breeding colony for further research. Some of the resulting pups had severe phenotypes and died after birth, while others could be raised and presented symptoms of progressive muscle wasting (VALENTINE et al., 1988). The absence of dystrophin was identified as the disease origin and due to the *DMD* gene location on the X chromosome and the specific inheritance pattern, the disease was called “Canine X-linked muscular dystrophy” (CXMD) (VALENTINE et al., 1992). Cardiac involvement was identified in dogs older than 6.5 months, but not in puppies younger than 3 months (VALENTINE et al., 1989). However, other dog breeds besides Golden Retrievers, with their Golden Retriever muscular dystrophy (GRMD), were not spared spontaneous cases of CXMD. Thus, among others, cases were found in Labradors (LRMD)(BARTHELEMY et al., 2020), Cavalier King Charles Spaniels (CKCS-MD) (WALMSLEY et al., 2010), and Japanese Spitz (JSMD) (ATENCIA-FERNANDEZ et al., 2015). The causal mutations differ not only with respect to the localization within the *DMD* gene, but also with respect to the type of mutation. In the original GRMD model, which by the way was also bred to a Beagle background, the cause of the disease is a point mutation in the acceptor

splice site of *DMD* intron 6, resulting in the absence of exon 7 in the mRNA and thus a frame-shift and premature stop codons (DUAN, 2015). A 2.2-Mb inversion causes the LRMD, by interrupting the reading frame in intron 20. In CKCS-MD the disease is caused by a point mutation in the splice donor site of exon 50, resulting in an out-of-frame mutation, by deleting exon 50 (WALMSLEY et al., 2010). As in the LRMD dogs, an inversion causes the CXMD in the Japanese Spitz dogs. Specifically, the inversion starts in *DMD* intron 19 and involves additionally the *RPGR* gene and thus interrupt the *DMD* sequence (ATENCIA-FERNANDEZ et al., 2015). CXMD dogs and in especially the GRMD model are widely used in DMD research (KORNEGAY et al., 2012).

3.4. Hypertrophic feline muscular dystrophy (HFMD)

Different publications described cats, with muscular dystrophy symptoms (CARPENTER et al., 1989; GASCHEN et al., 1992). The leading pathological findings in these cats were the hypertrophy of the skeletal musculature, but also of the muscle fibers, which were doubled in diameter, resulting in progressive stiffness. Echocardiography on affected cats indicated symptoms of dilated cardiomyopathy. In contrast to human patients, the affected cats showed no fatty infiltration and increase in fibrosis of musculature (CARPENTER et al., 1989). Gaschen et al. (1992) who established the name “Hypertrophic feline muscular dystrophy” described in their affected cats hypertrophy of tongue, diaphragm and skeletal musculature. Consistent with Carpender et al. (1989) they diagnosed stiffness and in the histology hypertrophic muscle fibers and calcium accumulation (GASCHEN et al., 1992).

3.5. Porcine models

The first porcine model for Duchenne muscular dystrophy, the *DMD*Δ52 pig, was generated and published by our research group in 2013. By deleting exon 52 the *DMD* reading frame of these pigs was interrupted, which resulted in a premature stop codon in exon 53 and the total absence of dystrophin protein. The deletion of exon 52 was chosen, since it represents one of the most common mutations in human Duchenne patients and thus predestinates the model for therapeutic research. The original model was generated by deleting exon 52 in a fibroblast cell line of a

male WT German Landrace pig, by homologous recombination, using a bacterial artificial chromosome (BAC), in which exon 52 was replaced by a selection gene (neomycin resistance cassette), followed by somatic cell nuclear transfer (SCNT) and embryo transfer of the SCNT embryos (**Figure 4A,B**). However, many piglets presented a severe disease phenotype and died within the first week after birth and none of the remaining pigs, with a milder phenotype, could be raised to fertility to establish a breeding herd (KLYMIUK et al., 2013). To overcome the limitation of reproducing the model only by the time and cost intensive method of SCNT, a heterozygous carrier sow was generated the same way, as the male *DMD*Δ52 pigs before and mated with WT boars, resulting in litters of 25% affected animals and 25% female carriers for the establishment of a breeding herd (STIRM et al., 2021) (**Figure 4D**). Nagashimas Lab chose another way to overcome the early mortality and establish a breeding herd, by generating a chimeric boar. Somatic cell nuclear transfer embryos, in the morula stage, generated from a male *DMD*Δ52 fibroblast cell line, were injected with WT blastomeres and resulted in the birth of five piglets, of which three where chimeras (*DMD*$X^{KO}Y \leftrightarrow X^{WT}X^{WT}$) and two *DMD*Δ52. They described a correlation between the proportion of mutated cells (*DMD*Δ52) in the chimeras and the disease severity. One chimeric boar could be raised to fertility (MATSUNARI et al., 2018) (**Figure 4C**).

Another group generated a porcine model, with the same mutation, the deletion of *DMD* exon 52 on a Yucatan mini pig background. They used recombinant adeno-associated virus (rAAV)-mediated gene targeting to delete exon 52 in a male fetal cell line and thus interrupt the reading frame of the *DMD* gene. The correct modified cells were used for SCNT and resulted in the birth of seven piglets (ECHIGOYA et al., 2021).

Two other groups used the more advanced technic of CRISPR/Cas9 gene editing to generate pig models for DMD. Yu et al. used the less efficient technique of zygote injection to generate mutant Chinese Diannan miniature pigs. They coinjected porcine zygotes with Cas9 mRNA and a single guide RNA (sgRNA), targeting exon 27 of the porcine *DMD* gene, which resulted in the birth of two piglets (YU et al., 2016).

Zou et al. used the CRISPR/Cas9 approach for the disruption of the reading-frame in exon 51 of the *DMD* gene in a fibroblast cell line of a male Bama miniature pig. After clonal separation, the resulted fibroblasts were used for SCNT and nine

piglets were born, which carried a mutation in exon 51 (ZOU et al., 2021).

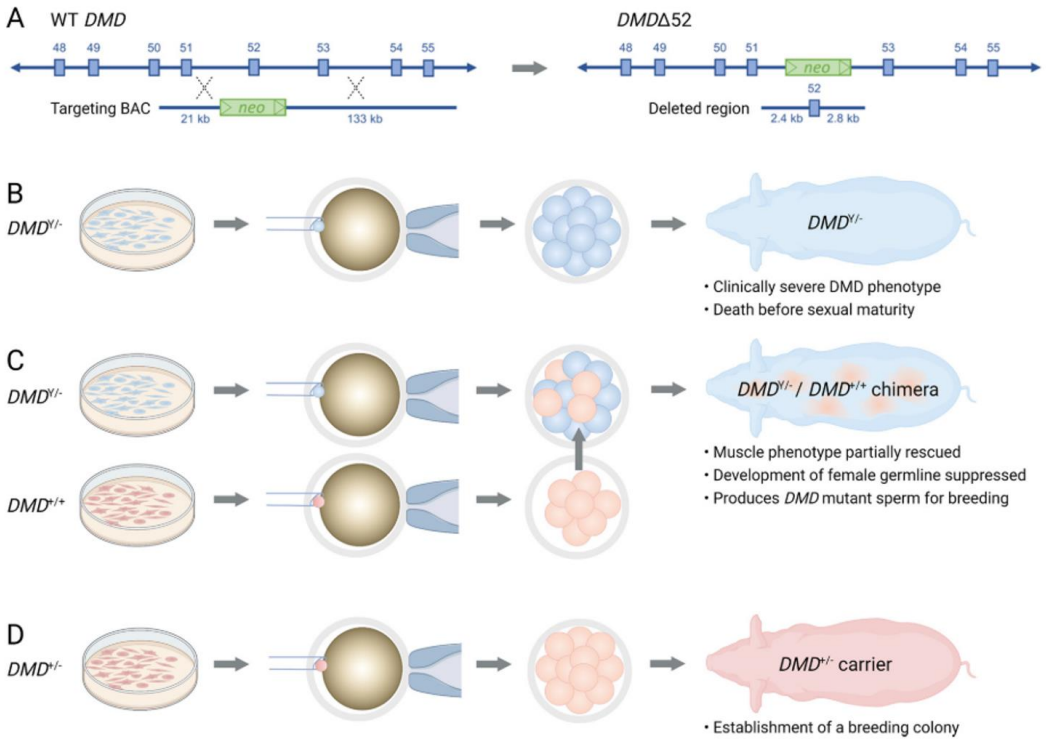

Figure 4: Strategies for the generation of transgenic DMDΔ52 pigs. (A) Generation of DMDΔ52 fibroblasts by homologous recombination with a bacterial artificial chromosome (BAC), carrying a neomycin resistant cassette instead of DMD exon 52. (B) The DMDΔ52 fibroblasts were used for somatic cell nuclear transfer (SCNT) and SCNT embryos were transferred to recipient sows, resulting in the birth of DMDΔ52 piglets. (C) Amelioration of the disease phenotype by generating chimeras ($DMD^{Y/-}$/$DMD^{+/+}$) to get boars for breeding. WT SCNT blastomeres were injected in DMDΔ52 zygotes from SCNT. The chimeric embryos were transferred to recipient sows and resulted in the birth of chimeric $DMD^{Y/-}$/$DMD^{+/+}$ piglets. (D) Heterozygous carrier sows ($DMD^{+/-}$) were produced by SCNT from a fibroblast cell line, carrying a heterozygous deletion of DMD exon 52 ($DMD^{+/-}$). Figure from (STIRM et al., 2022).

Consistently, all generated porcine DMD models showed severe symptoms with rapid disease progression and a significantly shortened life expectancy. Serum creatine kinase levels were increased and skeletal muscle morphology, namely the proportion of muscle fibers with central nuclei and the heterogeneous muscle fiber diameters, was pathological changed compared to WT pigs (**Figure 5**). The histology of skeletal muscle was dramatically affected, even in the young animals, dominated by fibrosis, inflammation and muscle fiber degeneration (KLYMIUK et al., 2013) (YU et al., 2016; ECHIGOYA et al., 2021; STIRM et al., 2021; ZOU et al., 2021). Further, proteomic analyses revealed dramatically altered expression

pattern in skeletal muscle and myocardium of cloned *DMD*Δ52 pigs (FROHLICH et al., 2016; TAMIYAKUL et al., 2020) and *DMD*Δ52 pigs, which were propagated by breeding (STIRM et al., 2021). The loss of dystrophin resulted in significantly reduced cardiac function and symptoms of dilated cardiomyopathy in the *DMD*Δ52 model. Additional cognitive impairments were found in this model (STIRM et al., 2021).

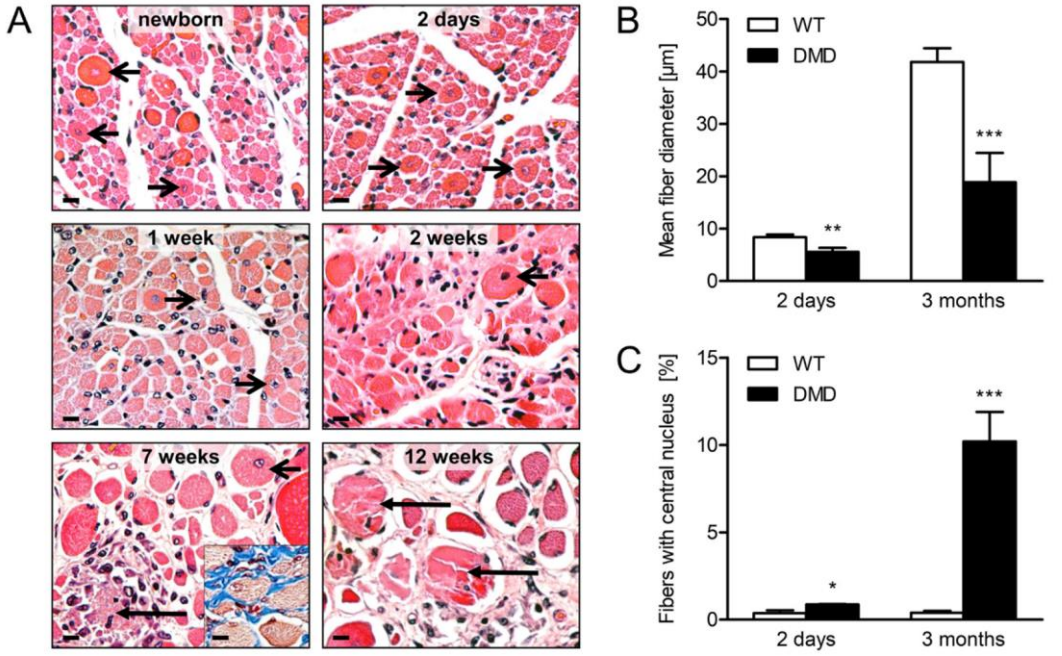

Figure 5: Pathological changes in the skeletal muscle of DMDΔ52 pigs. (A) Different ages of DMDΔ52 pigs presented muscle fibers with central nuclei in hematoxylin eosin (HE) stain. Increased fibrosis was identified by Masson's trichrome stain (insert). (B) Mean fiber diameters were reduced in DMDΔ52 pigs at 2 days and 3 months post partum, while the proportion of muscle fibers with central nuclei was increased. Figure from (STIRM et al., 2022).

The pig models for DMD perfectly combine the severe disease phenotype, with symptoms similar to human patients, an early progression with an easy reproduction for the generation of appropriate animal numbers for trials. Thus, the porcine models for DMD have become increasingly important in recent years, as they have already been used for preclinical therapeutic trials (MORETTI et al., 2020) and testing of new diagnostic tools (REGENSBURGER et al., 2019) and will continue to be positioned alongside the long-established murine and canine models in the future (STIRM et al., 2022).

4. Animal models for Becker muscular dystrophy

4.1. Murine models

The *mdx* mouse model has shaped preclinical research for Duchenne muscular dystrophy in recent decades like no other animal model. In addition to the original *mdx* mouse, with a premature stop codon in exon 23 in the *Dmd* gene, a large number of different mouse models for DMD were generated (VAN PUTTEN et al., 2020). In contrast, hardly any mouse model with an in-frame mutation corresponding to human Becker muscular dystrophy has been developed. One of the few exceptions is the X-linked Becker muscular dystrophy (*bmx*) mouse model which carries a deletion of exons 45 to 47 in the *Dmd* gene, which does not disrupt the reading frame. Consequently, a shortened dystrophin protein is formed, even though the dystrophin level in the skeletal muscle is significantly reduced (20-50%) compared to WT. The shortened dystrophin seems to be partially functional, since it ameliorates some of the pathological findings of the *mdx*52 mouse model for DMD (forelimb grip, hindlimb grip, wire hang, box hang), while other changes were not significantly improved in the bmx versus the *mdx*52 groups (left ventricular ejection fraction, left ventricular fractional shortening). At the same time, *bmx* mice had also reduced muscle strength and heart function, as well as histopathological changes in skeletal and cardiac muscle compared to healthy mice (HEIER et al., 2023).

A different strategy was followed by Olson's group. They tried to correct the point mutation in *Dmd* exon 23 in *mdx* mice using CRISPR/Cas9. They co-injected Cas9-RNA, sgRNA that cuts in the region of the nonsense mutation and ssODN to *mdx* zygotes. After embryonic development of the zygotes, mosaic mice with a different proportion of reading frame-corrected cells (2-100%) by homology-directed repair (HDR) or non-homologous end joining (NHEJ) were born. They detected not only a restored dystrophin expression in skeletal and heart muscle, but also improved muscle strength and a reduction of the diagnostic serum marker CK activity (LONG et al., 2014). Three years later, the same group showed that comparable results are also possible with a CRISPR/Cpf1 approach using LbCpf1 from Lachnospiraceae bacterium as RNA-guided endonuclease instead of the most widespread Cas9. In line with previous reports, they described a correlation between the proportion of corrected cells and a reduction in the disease related phenotype (ZHANG et al., 2017).

4.2. Rat models

In addition to the mouse, the rat is another rodent species used as a model organism for Becker muscular dystrophy. Teramoto et al. generated a rat model, carrying an in-frame mutation in the *Dmd* gene. In particular, this rat model has a deletion of exons 3 to 16, which corresponds to a loss of 324,981 bp. These rats had a reduced expression of the shortened dystrophin, compared with WT rats. Serum CK levels were increased already one month after birth and affected animals presented dystrophic changes in skeletal muscle morphology, but muscle strength remained unaffected. Corresponding to the skeletal muscles, the myocardial histology was altered, not only by an increase in fibrosis, but also by infiltration of lymphocytes. Remarkably, even at 16 months of age, these changes did not significantly affect cardiac function as assessed by echocardiography (TERAMOTO et al., 2020). In contrast to the functional findings in the BMD rat model, DMD rats had reduced left ventricular ejection fraction (LVEF) (SZABO et al., 2021) and reduced muscle strength (NAKAMURA et al., 2014).

4.3. Canine models

Before the generation of the first porcine models for Duchenne muscular dystrophy (KLYMIUK et al., 2013; ECHIGOYA et al., 2021), various spontaneously generated canine models were the most widely used large animal models for DMD research. Despite the increasing use of pigs, canine model organisms continue to be of great importance for preclinical research (KORNEGAY et al., 2012; KORNEGAY, 2017), so it is surprising that no canine model for Becker muscular dystrophy has yet been established. Although several case reports of dogs with a comparable phenotype and genotype to BMD have been described, none of these dogs have been used to set up a laboratory breeding colony (JONES et al., 2004; BARONCELLI et al., 2014; JEANDEL et al., 2019). In 2022, Oh et al. published the generation of a new dystrophin mutant dog, using CRISPR Cas9 and SCNT. The only pup born carried a mutation in exon 6, specifically a 57 bp deletion, which represents an in-frame mutation and therefore reflects human BMD. The clinical findings supported this. However, it remains unclear, whether this animal will be used for breeding and for experiments in the future, or whether this publication represents a proof of principle study (OH et al., 2022).

4.4. Feline Becker-Type muscular dystrophy

In a case report two male Maine Coon crossbred cats, from the same litter, were identified as Becker-Type muscular dystrophy affected. Both cats presented mild disease symptoms, like abnormal gait, hypertrophy of the skeletal musculature and hyperglossia. CK levels were also increased in both animals, supporting the clinical findings of muscle involvement. The causal mutation, a point mutation, a single nucleotide change from C to T (position 4186), was identified by whole genome sequencing and resulted in the exchange of one amino acid (histidine to tyrosine) at position 1396. Immunohistochemistry against dystrophin, performed on skeletal muscle from biopsy, resulted in reduced dystrophin expression in the musculature of the affected individuals. Further, the muscle presented for muscular dystrophies typical findings like atrophy, hypertrophy and necrosis of fibers. The cats showed a milder clinical course and milder progression compared with cats, carrying a mutation correlating to the human Duchenne muscular dystrophy. Even at an advanced age of 3.5 years, echocardiography found no cardiac involvement in these cats (HILTON et al., 2023).

4.5. Becker and Becker-like porcine models

Globally millions of pigs are produced and slaughtered every year. Therefore, it is not surprising that different research groups identified animals with a Becker-like phenotype (NONNEMAN et al., 2012; HORIUCHI et al., 2014; SCHWARZ et al., 2021; AIHARA et al., 2022). After all, due to the length of the *DMD* gene, BMD occurs in about 8 of 100,000 male newborns in humans (DUAN et al., 2021) and a comparable frequency in pigs can be assumed, due to similar size of the dystrophin gene.

In 2012, Nonneman et al. became aware of a pig line that exhibited stress intolerance. They screened genes, connected to human malignant hyperthermia (*RYR1*, *CACNA1S*, *CPT2*, *RYR2*), but found no causing mutation. Afterwards, they identified by genome-wide association analyses the responsible mutation in exon 41 of the *DMD* gene, a single nucleotide polymorphism, the change from arginine to tryptophan (R1958W), by sequencing of 250 related pigs, of which about one fifth was affected. Dystrophin expression levels in skeletal and heart muscle were decreased in the affected pigs, suggesting a pathology comparable to BMD in

humans. This hypothesis was supported by histopathological findings in the myocardium (NONNEMAN et al., 2012). Additionally, various skeletal muscles presented an increase in fibrosis and, with exception of the psoas muscle, fatty infiltration. The CK levels were significantly higher in the BMD pigs compared to their WT littermates (HOLLINGER et al., 2014). The reduced dystrophin led to an altered electrocardiogram (ECG), reduced stride length and sudden death (SELSBY et al., 2015).

Independently of the mentioned BMD model, another "Becker muscular dystrophy-like" pig was identified in a Japanese slaughterhouse in 2014. Prominent was the fat infiltration in the musculature of this pig. Histological examinations of the skeletal muscles revealed not only significant fatty infiltration, but also heterogonous muscle fiber cross sections, central nuclei and degenerating fibers. A reduced dystrophin expression was detected by immunofluorescence. The sex of the pig was determined as male by PCR against the *SRY* gene, coding for the sex determining region of Y-protein. However, the causal mutation could not be detected by the researchers (HORIUCHI et al., 2014).

Schwarz et al. presented another case of fatty muscular dystrophy from an Austrian slaughterhouse. The authors speculated whether this could be a dystrophinopathy. However, one of the two affected pigs was female, which would require both parents to be carriers, because of the X-linked location of the *DMD* gene. A non-genetic cause could not be ruled out either (SCHWARZ et al., 2021).

The latest case report was also discovered in a meat inspection center. The only clinical alteration of the pig was its enlarged tongue, which presented a histology, typical for dystrophic striated muscle. Replacement of myocytes by fibrosis and fat cells could be found, as well as heterogonous cross section, central nuclei, lymphocyte infiltration, regenerating fibers and necrosis. Immunofluorescence, using a primary antibody against dystrophin, detected only a weak dystrophin expression in the myocytes. Sequencing of cDNA, synthesized from mRNA from skeletal muscle, delivered the causing mutation. An insertion of 62 bp between exon 26 and 27 resulted in the reduced dystrophin levels (AIHARA et al., 2022).

To date, no other research group has generated and published a tailored, genetically engineered pig model for BMD.

III. MATERIALS AND METHODS

1. Animals

1.1. Generation and breeding of *DMD*Δ52 animals

The Duchenne muscular dystrophy pig model was initially generated by BAC targeting. The porcine *DMD* exon 52 was replaced by a neomycin resistance cassette (neo®) on a BAC clone. The modified BAC was linearized and nucleofected into a male porcine kidney cell line. Cells were afterwards screened for neomycin resistance and the identified cell clones with the integrated resistance cassette and thus a deletion of exon 52, where used for somatic cell nuclear transfer (SCNT). SCNT was performed as described elsewhere (KUROME et al., 2006). SCNT embryos were transferred to recipient sows and resulted in the birth of the first *DMD*Δ52 piglets (KLYMIUK et al., 2013). However, none of the animals reached sexual maturity, which meant that the model could only be produced by SCNT. To solve this problem, a heterozygous female cell line was generated in the same way as the male previously and resulted in the birth of the founder sow #3040 after SCNT. From then on, the model could be propagated by mating heterozygous carrier sows with WT boars, resulting in an average of 25% affected animals (*DMD*Δ52), 25% WT males, 25% WT females and 25% heterozygous females (*DMD*Δ52_het), which could be used for breeding (STIRM et al., 2021). Whenever possible, the natural cycle of the sows was used. In some cases, estrus synchronization of several breeding females was performed to obtain larger experimental groups. The estrus synchronization protocol is described in the table below.

Day 1-18	4 ml Regumate® (4 mg/ml), MSD Tiergesundheit
Day 20	2 ml Maprelin® (75 µg/ml), Veyx
Day 23	1,7 ml Ovogest® (300 I.E./ml), MSD Tiergesundheit
Day 24-25	Mating/ artificial insemination

1.2. Generation of *DMD*Δ51-52 animals

For the generation of the *DMD*Δ51-52 pig model, a primary kidney cell line (fibroblasts) of a *DMD*Δ52 pig (#6790) (STIRM et al., 2021) was used. Exon 51 of the *DMD* gene was deleted by co-transfection of the cells with two plasmids, carrying an intein-split Cas9 and two guide RNAs (AGAGTTCCTAAGGT AGAGAG**AGG** and ATAAAGATAAGAGCTGGCAG**AGG**, PAM underlined), flanking exon 51. The membrane of the fibroblasts was made permeable for the plasmids by electroporation (EPO)(Nucleofector®II, Amaxa Biosystems). Correctly modified cells were identified by PCR and Sanger sequencing and used for SCNT. A total of 259 SCNT embryos were transferred to three estrus-synchronized recipient sows by endoscopic embryo transfer (ET) to the oviduct at day one or two after SCNT. ET resulted in two pregnancies and the birth of nine live-born and one stillborn piglet, of which seven could be raised to weaning. All seven were used for echocardiography studies. Four were used for necropsy and for tissue collection at an age of four months and one at an age of nine months, age-matched to the cell donor (#6790). The remaining two *DMD*Δ51-52 are still used for breeding purposes to establish a *DMD*Δ51-52 breeding herd.

1.3. Healthy control animals

The healthy control group (WT group) was recruited from the unaffected, male littermates from the *DMD*Δ52 litters, born by heterozygous *DMD*Δ52 carrier sows, which have been mated with WT boars.

1.4. Housing

All *DMD*Δ51-52 animals were kept in a specific-pathogen-free environment (SPF) in the Center for Innovative Medical Models (CiMM) at the Ludwig-Maximilians-University Munich. To enlarge the WT and *DMD*Δ52 groups, animals from a second facility at the Lehr- und Versuchsgut Oberschleißheim (LVG) of the LMU were used. Food and water were available to the animals ad libitum. On the third day after birth, all animals got a single intramuscular injection of 1 ml of Eisen20 (bela-pharm) for iron supplementation. In the third week of life, piglets were vaccinated against porcine circovirus type 2 (PCV2) (Ingelvac CircoFLEX®, Boehringer Ingelheim, Ingelheim am Rhein, Germany). Animals from the LVG were additional vaccinated against Mycoplasma hyopneumoniae (Ingelvac MycoFLEX®, Boehringer Ingelheim, Ingelheim am Rhein, Germany), due to the

lower microbiological status of this facility. Experiments were performed according to German Animal Welfare Act and Directive 2010/63/EU (Protection of animals used for scientific purposes) and the Government of Upper Bavaria approved all experiments (ROB-55.2-2532.Vet_02-17-136).

2. Materials

2.1. Apparatuses

Centrifuge 1	RotinaA 380 R	Hettich, Tuttlingen, Germany
Centrifuge 2	Centrifuge 5804 R	Eppendorf, Hamburg, Germany
Centrifuge 3	Centrifuge 5424	Eppendorf, Hamburg, Germany
Incubator	Class 3.1	Binder, Tuttlingen, Germany
Electroporator	Nucleofector®II	Amaxa Biosystems, Lonza, Köln, Germany
Imaging system for multi-well plates	Cellavista®	Innovatis, SYNENTEC GmbH, Elmshorn, Germany
Gel photo chamber	UVP GelStudio Plus	Analytik Jena, Jena, Germany
Spectrophotometer	SimpliNano™	General Electric Company, Boston, USA
PCR Cycler	labcycler	SensoQuest, Göttingen, Germany
Heating Thermoshaker	HTM	HTA-Bio Tec, Bovenden, Germany
Shaker	RS-VA10	Phoenix Instrument, Garbsen, Germany

Electrophoresis power supply	PowerPac™ 300	BioRad, Feldkirchen, Germany
Gel chamber	Owl™ EasyCast™ B2	Thermo Scientific, Waltham, USA
Precision scale	Precision balance Chyo MK-2000B	YMC CO. Ltd., Kyoto, Japan
Laminar flow hood	LaminAir® HB2448 K	Heraeus Instruments
Water purification system	Easypure® II ultrapure water system	Werner, Leverkusen, Germany
Tissue processor	Excelsior AS	Thermo Scientific, Waltham, USA
Paraffin embedding system	TES 99 modular paraffin embedding system	MEDITE Medical GmbH, Burgdorf, Germany
Microtome	Microm HM 325	Thermo Scientific, Waltham, USA
Microwave	Daewoo KOC-154K	Daewoo, Seoul, South-Korea
Water bath	Grant JB Nova water bath	Grant Instruments, Shepreth, UK
Microscope	Leitz DMRBE microscope	Leica Microsystems, Mannheim, Germany
Digital camera	DMC4500 camera	Leica Microsystems, Mannheim, Germany
Ultrasound system	MyLab X8 system	Esaote, Genua, Italy
Tissue homogenizer	Art-Miccra D-8	ART Labortechnik, Müllheim, Germany

2.2. Software

Software	Version
FinchTV	1.4.0
BioEdit	7.0.5.3
ImageJ	1.53k
Sperm Vision® Therio, Minitube	1.0.2
GraphPad Prism	5.04
PathoZoom® LiveView	1.0
LAS software, Leica Microsystems	4.13.0

2.3. Consumables

PCR Stripes/tubes of 8 caps	Brand GmbH + Co. KG, Wertheim, Germany
Pipette tips	Kisker, Steinfurth, germany
Safe-Lock Tubes Eppendorf 1.5 ml and 2.0 ml	Eppendorf, Hamburg, Germany
Erlenmeyer flask Simax®	Schott AG, Mainz, Germany
Latex Examination Gloves – Powder free	Brightway®, Klang, Malaysia
Cell culture dish 100x20mm	Eppendorf, Hamburg, Germany
TC plate 6 well Standard F	Sarstedt AG, Nümbrecht, Germany
Corning™ Costar™ 96 well cell culture plate	Corning Incorporated - Life Sciences, Kennebunk, USA

Cryo tube 1.5 ml	TPP Techno Plastic Products AG, Trasadingen, Switzerland
Electroporation cuvette	Carl Roth, Karlsruhe, Germany
Cellstar® tubes 15ml and 50ml (Falcon)	Greiner bio-one, Frickenhausen, Germany
Uni-Link Einbettkassetten	Engelbrecht Medizin- Labortechnik GmbH, Edermünde, Germany
Sarstedt Monovettes® (Serum: S-Monovette)	Sarstedt AG, Nümbrecht, Germany
Monovette® 9 ml LH (Lithium-Heparin)	Sarstedt AG, Nümbrecht, Germany
Monovette® 9 ml K3E (EDTA)	Sarstedt AG, Nümbrecht, Germany

2.4. Chemicals and reagents

GeneRuler 1 kb DNA Ladder	Thermo Scientific, Waltham, USA
GeneRuler 100 bp DNA Ladder	Thermo Scientific, Waltham, USA
Dry ice	TKD Trockeneis und Kohlensäure Distribution GmbH, Fraunberg-Tittenkofen, Germany
100 mM dNTP set, PCR grade	Invitrogen, Karlsruhe, Germany
GELRED 10000x in water	Biotium, Fremont, USA
Agarose, universal, poqGOLD, Electran®, DNA-pure	VWR Life Science, Radnor, USA
Bromophenol blue sodium salt for	Carl Roth, Karlsruhe, Germany

electrophoresis	
Iron(III)chloride	Sigma-Aldrich, St. Louis, USA
Hydrochloric acid 25 %	Carl Roth, Karlsruhe, Germany
Acid fuchsin (Rubin S)	Sigma-Aldrich, St. Louis, USA
Glacial acetic acid	VWR Chemicals, Radnor, USA
Xylidine Ponceau	RAL Diagnostics, Martillac, France
Azophloxin for microscopy	Schmid GmbH, Köngen, Germany
Phosphotungstic acid hydrate	Sigma-Aldrich, St. Louis, USA
Orange G	Sigma-Aldrich, St. Louis, USA
Aniline blue	Sigma-Aldrich, St. Louis, USA
Ethanol 99.5 % denaturated with 1 % MEK (Histology)	VWR Chemicals, Radnor, USA
Ethanol, BioUltra, for molecular biology, ≥99.8 % (absolute alcohol, without additive) (molecular biology)	Sigma-Aldrich, St. Louis, Germany
Ethanol ROTIPURAN® ≥99.8 %, p.a.	Carl Roth, Karlsruhe, Germany
Chloroform, 99.0-99.4 %	Sigma-Aldrich, St. Louis, USA
TRIzol® Reagent	ambion® by life technologies™, Carlsbad, USA
Formaldehydlösung 37 %, ≥37 %	Carl Roth, Karlsruhe, Germany
Mayer's hemalum solution for microscopy	Sigma-Aldrich, St. Louis, USA
Eosin 2 %, wässrig	Engelbrecht Medizin- Labortechnik GmbH, Edermünde, Germany
Xylene for histology	CHEMSOLUTE®, TH Geyer GmbH & Co. KG, Renningen, Germany
Hematoxylin for microscopy	Sigma-Aldrich, St. Louis, USA

Goat serum	MP Biomedicals, Santa Ana, USA
PCR buffer 10x	Qiagen, Hilden, Germany

2.5. Drugs and vaccines

Regumate® (4 mg/ml)	MSD Tiergesundheit, Unterschleißheim, Germany
Maprelin® (75 µg/ml)	Veyx Pharma, Schwarzenborn, Germany
Ovogest®	MSD Tiergesundheit, Unterschleißheim, Germany
Ursotamin®	Serumwerke Bernburg, Bernburg, Germany
Azaporc®	Serumwerke Bernburg, Bernburg, Germany
Propofol 2%	Fresenius Kabi, Bad Homburg, Germany
Eisen20	bela-pharm GmbH & CO. KG, Vechta, Germany
Ingelvac CircoFLEX®	Boehringer Ingelheim, Ingelheim am Rhein, Germany
Ingelvac MycoFLEX®	Boehringer Ingelheim, Ingelheim am Rhein, Germany

2.6. Enzymes and oligonucleotides

Enzyme	Enzyme type	Manufacturer
Acc65I (Recognition site: 3'…CCATGG…5')	Restriction enzyme	Thermo Scientific, Waltham, USA

HotStarTaq Plus DNA Polymerase	DNA Polymerase	Qiagen, Hilden, Germany
SMART MMLV Reverse Transcriptase	Reverse transcriptase	TaKaRa Bio Inc., Mountain View, USA

2.7. Buffers, media and solutions

2.7.1. Cell culture media

Culture medium for porcine fibroblasts (15% solution)	DMEM 15% FCS 1% non-essential amino acid 1% HEPES-buffer 0.1 mM mercaptoethanol
Stop medium (STOP solution)	DMEM 10% FCS
Phosphate-buffered saline (PBS) without Calcium and Magnesium for cell culture	8 g NaCl 0.2 g KCl 0.2 g KH_2PO_4 2.14 g Na_2HPO_4 1000 ml aqua dest. (pH 7.2-7.4)
Trypsin	Trypsin, Thermo Fisher Scientific, USA
Freeze solution	90% FCS 10% DMSO
Nucleofection solution	Amaxa™ Basic Nucleofector™ Kit

2.8. Kits

Kit	Manufacturer
nexttec™ 1-step DNA Isolation Kit for Tissue and Cells	nexttec™ Biotechnologie GmbH, Hilgertshausen, Germany

Picro-Sirius Red Stain Kit (For Collagen)	ScyTek Laboratories, Logan, USA
Exo-CIP™ Rapid PCR Cleanup Kit	New England Biolabs GmbH, Ipswich, USA
RNA to cDNA EcoDry™ Premix (Double Primed)	TaKaRa Bio Inc., Mountain View, USA
ImmPACT™ DAB Peroxidase (HRP) Substrate	Vetor Laboratories, Biozol, Eching, Germany
Vectastain® Elite ABC-Peroxidase Kit	Vetor Laboratories, Biozol, Eching, Germany

2.9. Antibodies

Target	Antibody
Dystrophin (Rod domain)	monoclonal mouse anti-DYS1 (rod domain; NCL-DYS1, clone Dy4/6D3, Leica Biosystems)
Dystrophin (C-terminus)	monoclonal mouse anti-DYS2 (C-terminus; NCL-DYS2, clone DY8/6C5, Leica Biosystems)
Embryonic myosin/Myosin heavy chain 3 (MYH3)	polyclonal rabbit anti-Myosin 3 (Myosin 3 antibody, RB934, orb385438, Biorbyt)
Mouse IgG	biotinylated goat anti-mouse IgG (no. 115-065-146, lot 118375, Jackson ImmunoResearch
Rabbit IgG	biotinylated goat anti-rabbit IgG antibody (BA-1000-1.5, ZH0818, Vector Laboratories)

3. Methods

3.1. Genotyping of single cell clones

Cells were dissolved in Stop-solution and transferred to a 1.5 ml Eppendorf-tube, after trypsin digestion and centrifuged for 5 min at 2000 × *g*. Supernatant was removed and cell pellet was frozen at -80°C until further processing.

After thawing, cell pellet was dissolved in 100 µl PK buffer (200 mM Tris + 1 M NaCl + 40 mM EDTA). Then 10 µl SDS (10%) and 4.4 µl DTT (1 M) were added and the whole suspension was incubated for 1h at 60°C. After the hour, 2 µl of of Proteinase K (20 mg/ml) were added and Eppendorf tubes were put back on the thermos shaker and were incubated for another hour. After adding 30 µl NaCl (4.5 M), the tubes were placed on ice for 10 min, followed by centrifugation at room temperature for 20 min at full speed. Supernatant was transferred to a new tube and 0.7 volumes of pure isopropanol were added and the liquids were mixed carefully, followed from centrifugation at room temperature for 20 min at full speed. Supernatant was discarded and 500 µl of 70% ethanol were added and mixed carefully. The suspension was incubated at 4°C over night. The following day, tubes were centrifuged at room temperature for 20 min at full speed and supernatant was discarded. DNA pellets were dried for 5 min in the tubes. Dried DNA pellets were dissolved in 35 µl of T buffer and incubated for 1 h at 55°C.

To detect the deletion of *DMD* exon 51, a PCR flanking exon 51 was performed. The forward primer (dex51f1) was located upstream of exon 51 in intron 50, while the reverse primer (dex51r3) bound downstream in intron 51. Deletion of exon 51, resulted in a shortened PCR product length and thus PCR products were screened by gel electrophoresis in the Owl™ EasyCast™ B2 gel chamber (electrophoresis power supply: PowerPac™ 300). Single cell clones with shortened band lengths were checked for the absence of exon 51 by restriction enzyme digestion (Acc65I (Recognition site: 3'…CCATGG…5')) and by Sanger sequencing.

3.2. Genotyping of piglets

To ensure unambiguous genotyping of the piglets, small tissue samples were taken from the tails of the animals after they had received their ear tag. For the DNA isolation, the nexttec™ 1-step DNA Isolation Kit for Tissue and Cells was used,

according to manufacturer instructions. For the genotyping of piglets from heterozygous *DMD*Δ52 sows, a PCR against *DMD* exon 52 was performed and a second against the neomycin resistance cassette, which is inserted instead of the exon 52 in the affected X-chromosome. For the genotyping of the *DMD*Δ51-52 pigs, a PCR, using a primer pair flanking *DMD* exon 51(dex51f1/ dex51r3), was done and resulted in different band lengths. After PCR, PCR products were mixed with bromophenol blue and a gel electrophoresis, using 1.5% agarose gel (Agarose universal, peqGOLD, Electran®-DNA pure grade, VWR Life Science), was performed in the Owl™ EasyCast™ B2 gel chamber (Thermo Scientific). Gel electrophoresis was stopped after 30 min and a picture, illuminated with ultraviolet light, was taken in the UVP GelStudio Plus gel photo chamber. To confirm the correct deletion, the PCR products of the *DMD*Δ51-52 were sequenced by Sanger sequencing.

3.2.1. PCR

PCR *DMD* exon 52:

The PCR against *DMD* exon 52 was performed, to detect unmutated alleles. Only male WT piglets or heterozygous carrier sows, carrying both, the mutated and WT allele, presented a band in the gel electrophoresis. For this PCR the foreword primer DMDqf1 and the reverse primer DMDqr1 were used. The sequences of all primers used can be found in the table below.

	1 reaction
H_20	14 µl
dNTPs (2 µM)	2 µl
10xbuffer	2 µl
DMDqf1 (10 µM)	0.4 µl
DMDqr1 (10 µM)	0.4 µl
Hot Start Taq Polymerase	0.2 µl
	19 µl

Denaturation	5 min	95°C	
Denaturation	30 sec	95°C	35x
Annealing	30 sec	62°C	
Elongation	30 sec	72°C	
Final elongation	5 min	72°C	
Termination	∞	4°C	

PCR neomycin resistance cassette:

All piglets which carried a mutated *DMD* gene and thus a neomycin resistance cassette instead of the *DMD* exon 52, were identified by a PCR against the neomycin resistance cassette. The primers used for this purpose were neoPf and neoSr. Not only the *DMD*Δ52, but also *DMD*Δ52_het and *DMD*Δ51-52 showed a proving band in the gel electrophoresis.

	1 reaction
H_20	14 µl
dNTPs (2µM)	2 µl
10xbuffer	2 µl
neoPf (10µM)	0.4 µl
neoSr (10µM)	0.4 µl
Hot Start Taq Polymerase	0.2 µl
	19 µl

Denaturation	5 min	95°C	
Denaturation	30 sec	95°C	35x
Annealing	30 sec	62°C	

Elongation	30 sec	72°C	
Final elongation	5 min	72°C	
Termination	∞	4°C	

PCR *DMD* exon 51:

The deletion of *DMD* exon 51 was detected by a primer pair, which bound the DNA upstream (dex51f1) and downstream (dex51r3) of both cutting sites of the sgRNAs. Thus, the deletion resulted in a shorter band (~1150 bp or ~710 bp) than the WT allele (~2175 bp) in the gel electrophoresis after PCR. All animals, excluding the *DMD*Δ51-52, presented the longer band of ~2175 bp.

	1 reaction
H_20	14 µl
dNTPs (2 µM)	2 µl
10xbuffer	2 µl
dex51f1 (10 µM)	0.4 µl
dex51r3 (10 µM)	0.4 µl
Hot Start Taq Polymerase	0.2 µl
	19µl

Denaturation	5 min	95°C	
Denaturation	30 sec	95°C	
Annealing	30 sec	62°C	35x
Elongation	3 min	72°C	
Final elongation	5 min	72°C	
Termination	∞	4°C	

PCR deletion of *DMD* exon 51 and exon52 in the cDNA:

RNA was isolated from triceps brachii muscle and cDNA was synthesized. The exact protocols can be found below. The forward primer (DMDex50f2) was designed to bind to the *DMD* exon 50, while the reverse primer (DMDex53r4) was specific for exon 53.

	1 reaction
H_20	14 µl
dNTPs (2 µM)	2 µl
10xbuffer	2 µl
DMDex50f2 (10 µM)	0.4 µl
DMDex53r4 (10 µM)	0.4 µl
Hot Start Taq Polymerase	0.2 µl
	19 µl

Denaturation	5 min	95°C	
Denaturation	30 sec	95°C	35-38x
Annealing	30 sec	51°C	
Elongation	60 sec	72°C	
Final elongation	5 min	72°C	
Termination	∞	4°C	

Due to the different amount of dystrophin mRNA and thus also of cDNA, different numbers of cycles were carried out in the PCR (WT=35; *DMD*Δ51-52=35; *DMD*Δ52=38). The results are non-quantitative.

All primers were designed, using the *Sus scrofa* reference sequence from ensemble.org and the primer-BLAST tool from NCBI. All oligonucleotides were synthesized by biomers.net GmbH (Ulm, Germany).

Primer	Sequence
DMDqf1	5´-TGC ACA ATG CTG GAG AAC CTC A-3´
DMDqfr1	5´-GTT CTG GCT TCT TGA TTG CTG G-3´
neoPf	5‘-CAG CTG TGC TCG ACG TTG TC-3‘
neoSr	5‘-GAA GAA CTC GTC AAG AAG GCG ATA G-3‘
dex51f1	5'- GTA ATG TCA GGA ACT GTG CTA CT-3'
dex51r3	5'-ATT CTT CGG GCC TGT TAT CC-3'
DMDex50f2	5'-AAC CCC TGG ACT GAC CAC TA-3'
DMDex53r4	5'-TTG TGT AGG GAC CCT CCT TCC ATG-3'

3.2.2. Sanger sequencing

Sanger sequencing was performed by the sequencing service of the Faculty of Biology of the LMU Munich, using BigDye. Afterwards, the sequences were analyzed with FinchTV version 1.4.0 and BioEdit version 7.0.5.3.

For the genotyping of single-cell clones and piglets, forward and reverse sequences were sequenced, using dex51f1 as forward primer and dex51r3 as reverse.

To detect the deletions of *DMD* exon 51 and/or 52 from the cDNA, the primer pair DMDex50f2/DMDdex53r4 was used.

Prior providing the DNA to the sequencing service, the PCR was cleaned up with the Exo-CIP^{TM} Rapid PCR Cleanup Kit, according to manufacturer’s instructions. 3 µl of the Exo-CIP^{TM} cleaned up PCR product was mixed with 2 µl primer solution (2 pmol/µl) and filled up to a total volume of 7 µl with 10 mM Tris/HCl.

3.2.3. Restriction enzyme digestion

To find out whether the single-cell clones selected on the basis of band length still contain *DMD* exon 51, a restriction enzyme digestion of the PCR product (dex51f1/dex51r3) was performed, followed by gel electrophoresis. A restriction enzyme was chosen, which has its recognition site within exon 51 of the *DMD* gene (Acc65I – 3’…CCATGG…5’). Consequently, this enzyme can only cut in PCR

products from single cell clones that still have an intact *DMD* exon 51. The reaction mix that was used is shown in the table below. The amplification was done on the thermoshaker for 3 h at 37°C, followed by the inactivation at 65°C for 20 min.

Reagents	Volume
PCR product	20 µl
H_2O	36 µl
10x Buffer O	4 µl
Acc65I	2 µl

3.3. Cell culture

3.3.1. Thawing of the cells

Frozen kidney fibroblasts from a *DMD*Δ52 pig, which were previously stored in freeze solution in liquid nitrogen, were thawed in the water bath (37°C) and dissolved in 2 ml of warm (37°C) STOP-medium. Afterwards, the whole liquid was transferred to a 15-ml Falcon tube with 8 ml warm (37°C) STOP-solution. The 15-ml Falcon was then centrifuged for 5 min at 170 rcf. The supernatant was discarded and the cell pellet dissolved in 2 ml of warm (37°C) culture medium (15%-solution). The 2 ml cell suspension was seeded in a 10-cm plate, which was previously coated with collagen, and already contained 3 ml of warm culture medium. 600,000 cells were seeded. The plate was stored for 24 h in the incubator (37°C; 5% CO_2).

3.3.2. Electroporation (#EPO201111) and gene editing

After 24 h, the cells grew adherent and had already divided, filling approximately 70% of the plate. After removing the culture medium, cells were washed with 5 ml warm (37°C) PBS solution. PBS was removed and 750 µl of trypsin solution was added to the fibroblasts to remove the connection of the cells with the plate. After incubation for 5 min, 4.25 ml of STOP-solution was added to suspend the cells and the whole volume was pipetted into 15-ml Falcon and centrifuged (5 min; 170 rcf). Supernatant was removed and discarded. The cell pellet was suspended in 5 ml of warm culture medium. After calculation of cell number ($4.625x10^5$cells/ml), 1.08

ml (~500,000 cells) were transferred to an Eppendorf tube and centrifuged (5 min; 170 rcf). Cell pellet was dissolved in 100 µl of nucleofection solution (Amaxa™ Basic Nucleofector™ Kit) (room temperature) and transferred to an Eppendorf tube with 5 µl of plasmid solution. The whole volume was then transferred to an electroporation cuvette. Cell suspension, containing the two plasmids (intein-split Cas9 + 2 gRNAs) was then electroporated (ID: EPO201111) in the Nucleofector®II (Amaxa Biosystems). Afterwards the cell suspension was immediately seeded in a six-well plate, containing 2 ml of warm (37°C) culture medium and transferred to the incubator.

3.3.3. Clonal separation

After 24 h, the adherent fibroblasts reached ~90% confluence. They were washed two times with 5 ml of PBS, followed by 5 min trypsin (400 µl) digestion for removal of the cells in the incubator. Digestion was stopped with 1.4 ml of STOP-solution and the concentration was calculated ($2.05x10^5$ cells/ml). 100 µl of cell suspension was diluted with 900 µl 15%-solution and 47 µl of this suspension was suspended in 50 ml of warm culture medium in a 50-ml Falcon. Cells were then seeded to ten 96-well half-area plates (50 µl per well). Plates were labeled and transferred to the incubator. After two days, the medium was exchanged (50 µl culture medium per well). On day four after clonal separation, 50 µl culture medium was added to each well. In the afternoon of the same day, the first images from the wells, with the imaging system for 96-well plates (Cellavista®) were made, to check growth of the single-cell clones. Cellavista® images were made every two days, followed by full medium changes (100 µl). As soon as single-cell clones reached ~65% confluence, they were washed (PBS) and then removed (trypsin digest), dissolved in 100 µl of culture medium and split between two wells of a 96-well full-area plate. One well of each single-cell clone from the 96-well full-area plate was frozen and stored in liquid nitrogen, as soon as it reached ~65% confluence, while the other was used to harvest DNA for the genotyping. Until the cells were detached, the medium was changed every other day and the plates were stored in the incubator throughout, except during manipulation. In total, 120 single-cell clones (bck1-bck120) were harvested and frozen in liquid nitrogen for long-term storage.

3.4. Somatic cell nuclear transfer and embryo transfer

Two of the identified, correctly mutated single-cell clones were thawed and used for somatic cell nuclear transfer (SCNT). 259 SCNT embryos were laparoscopically transferred to the oviducts of three estrus-synchronized recipient sows. Sow #11054 got 63 embryos from single-cell clones bck101 and bck 107, #11112 100 embryos from bck27 and #11106 96 embryos (bck101 and bck107). The SCNT and embryo transfer (ET) procedures were described elsewhere (KUROME et al., 2006; KUROME et al., 2015). Pregnancies were routinely checked at day 21 after ET, using a handheld ultrasound system.

Recipient #11054 gave birth to three *DMD*Δ51-52 piglets and #11106 to seven. In #11112, no implantation of embryos took place.

3.5. Tissue collection and fixation

3.5.1. Blood sampling and clinical chemistry

Blood was taken from the right jugular vein, while pigs were under general anesthesia for the heart ultrasound, using a needle (1.2 x 38 mm; AGANI NEEDLE™, TERUMO®) and Sarstedt Monovettes® (Serum: S-Monovette, Sarstedt AG & Co. KG; Lithium-Heparin: Monovette® 9 ml LH, Sarstedt AG & Co. KG; EDTA: Monovette® 9 ml K3E, Sarstedt AG & Co. KG). EDTA and lithium-heparin blood was centrifuged immediately after blood sampling, while serum Monovettes® were kept at room temperature for clotting, prior centrifugation for 20 min. Centrifugation protocol for all anticoagulants and serum was 20 min at 1800 × *g* at 4°C. Creatine kinase and aspartate aminotransferase serum levels were measured by the laboratory of the Clinic for Ruminants of the LMU Munich. Creatinine was measured in the laboratory of the Clinic of Small Animal Medicine of the LMU Munich. The troponin I was detected by SYNLAB.vet Augsburg.

3.5.2. Necropsy

Pigs were sedated with 20 mg/kg ketamine (Ursotamin®, Serumwerke Bernburg, Bernburg, Germany) and 2 mg/kg azaperone (Azaporc®, Serumwerke Bernburg) and anesthesia was maintained by 4 mg/kg/h of propofol (Propofol 2%, Fresenius Kabi, Bad Homburg, Germany). Prior to euthanasia, pigs received a bolus of propofol and were euthanized by overdosing potassium chloride until heart arrest (Kaliumchlorid 7.45% Braun, Braun), followed by immediate blood extraction.

To ensure tissue sample quality, especially with respect to RNA and protein degradation, sampling was performed rapidly after death occurred. This ensured that all frozen samples were at -80°C within half an hour to prevent protease and RNase activity.

From the heart, two localizations each from the left ventricle, right ventricle and intraventricular septum were taken. Skeletal muscle was taken from triceps brachii muscle, biceps femoris muscle, diaphragm and the tongue. Additionally, liver, kidney, lungs and spleen were included to the sampling protocol, as well as urine, for further research on biomarkers.

3.5.3. Formalin fixed paraffin embedded (FFPE) samples

Tissue was cut into slices no more than 5 mm thick to ensure quick fixation, placed in embedding cassettes and stored in 4% buffered formaldehyde solution for 48 h. After formalin fixation, tissue was automatically dehydrated and transferred to paraffin by the Thermo Scientific Excelsior. The 16-h protocol included the following steps, which are shown in the table below.

70% Ethanol	70% Ethanol	90% Ethanol	90% Ethanol	100% Ethanol	100% Ethanol	100% Xylene	100% Xylene	100% Xylene	100% Paraffin	100% Paraffin	100% Paraffin
1.5h	1.5h	1.5h	1h	1h	1h	1h	1h	1h	1.75h	1.75h	2h

Tissue samples were afterwards embedded in paraffin using the TES 99 modular paraffin embedding system (MEDITE Medical GmbH) and histological slices (nominal thickness: 3 µm) were cut with the microtome Microm HM 325 (Thermo Scientific) and mounted to Star Frost® microscope slides. The mounted slides were stored at 37°C in the incubator until staining or immunohistochemistry were performed.

3.5.4. Cryopreservation

Tissue samples for RNA and proteomic studies, as well as for cryo histology, were snap frozen. Cryo samples were cut to small pieces of about 10 x 10 x 4 mm and embedded by O.C.T. compound (TissueTek®, Sakura Finetek, Torrance, USA), a water-soluble solution of glycols and resins and placed in Cryomold® cassettes

(TissueTek®, Sakura Finetek, Torrance, USA), followed by snap freezing on dry ice. For molecular analyses, smaller cubes of about 3 x 3 x 3 mm were cut and immediately placed on dry ice. As soon as the whole pieces were frozen, they were placed into precooled Eppendorf tubes and stored on -80°C within a freezer for later use.

3.6. Histological staining protocols

All histological stains were done on FFPE samples. Slides were deparaffinized and rehydrated prior staining. The slides were processed as followed:

100%	100%	100%	100%	96%	96%	70%	100%
Xylene	**Xylene**	**Ethanol**	**Ethanol**	**Ethanol**	**Ethanol**	**Ethanol**	**H_2O dest.**
20 min	20 min	2 min	2 min	2 min	2 min	2 min	2 min

Hematoxylin and eosin stain (HE):

5 min	5 min	1-2 times	5 min	2 min	2-3 times
Hematoxylin	**Tap water** (warm)	**0.5% HCl-Ethanol**	**Tap water** (warm)	**Eosin**	**H_2O dest.**

Sirius red stain:

For collagen detection, the Picro-Sirius Red Stain Kit (For Collagen) (ScyTek Laboratories, Logan, USA) was used. After sections were deparaffinized and rehydrated, the tissue sections were covered with the Picro-Sirius-Red solution, provided by the kit. Picro-Sirius-Red solution was removed after 60 min (RT) by rinsing the sections in two changes of 0.5% acetic acid solution, followed by standard dehydration protocol.

Masson's trichrome stain:

5 min	5 min	2 times	5 min	5 min	3 times	3min	3 times	30 sec	3 times
Weigert's Iron hematoxylin	**Tap water** (warm)	**0.5% HCl-Ethanol**	**Tap water** (warm)	**Biebrich scarlet-acid fuchsin**	**0.5% Acetic acid**	**Phosphor-molybdic-phospho-tungstic acid–Orange G**	**0.5% Acetic acid**	**Aniline blue**	**0.5% Acetic acid**

After staining, all tissue slides were again dehydrated and mounted with Roti® Histokitt (Carl Roth GmbH + Co. KG, Karlsruhe, Germany) and microscope slide coverslips (Carl Roth GmbH + Co. KG, Karlsruhe, Germany). For the dehydration step, following procedure was performed:

100%	70%	96%	96%	100%	100%	100%
H_2O dest.	**Ethanol**	**Ethanol**	**Ethanol**	**Ethanol**	**Ethanol**	**Xylene**
2 min	2 min	2 min	2 min	2 min	2 min	5 min

3.7. Immunohistochemistry

Immunohistochemistry was done on formalin-fixated tissue (FFPE), after deparaffinization and rehydration, according to protocol above.

10 mM citrate buffer pH 6.0 + 0.05% Tween (abcam)	15 min (Sub boiling temperature in the microwave)
Cooling	30 min RT
TBS	10 min RT
Blocking with 1% H_2O_2 in TBS	15 min RT
2x TBS	10 min RT

5% goat serum	1 h RT
Primary antibody	Overnight at 4°C
3x TBS	10 min
Secondary antibody	1 h RT
3x TBS	10 min RT
Avidin-biotin complex (1:100) in TBS	30 min RT
3x TBS	10 min RT
ImmPACT™ DAB Peroxidase (HRP) (Vectastain. Biozol, Eching, Germany) (3.3'-diaminobenzidine tetrahydrochloride dehydrate)	Up to 15 min RT
Tap water	5 min
Meyer's hemalum	Up to 5 min RT
Tap water	5 min

Dystrophin IHC (Rod domain):

	Antibody	Dilution
Primary antibody	monoclonal mouse anti-DYS1 (rod domain; NCL-DYS1, clone Dy4/6D3, Leica Biosystems)	1:20
Secondary antibody	biotinylated goat anti-mouse IgG (no. 115-065-146, lot 118375, Jackson ImmunoResearch	1:250

Dystrophin IHC (C-terminus):

	Antibody	Dilution
Primary antibody	monoclonal mouse anti-DYS2 (C-terminus; NCL-DYS2, clone DY8/6C5, Leica Biosystems)	1:50
Secondary antibody	biotinylated goat anti-mouse IgG (no. 115-065-146, lot 118375, Jackson ImmunoResearch	1:250

Embryonic myosin/Myosin heavy chain 3 (Myh3) IHC:

	Antibody	Dilution
Primary antibody	polyclonal rabbit anti-Myosin 3 (Myosin 3 antibody, RB934, orb385438, Biorbyt	1:375
Secondary antibody	biotinylated goat anti-rabbit IgG antibody (BA-1000-1.5, ZH0818, Vector Laboratories	1:200

3.8. Morphological analysis

For morphological analysis, stained sections (hematoxylin) were photographed using the Leitz DMRBE microscope (Leica Microsystems) and the installed digital camera system (DMC4500 camera, Leica Microsystems). For the camera, the adapted software (LAS software, Version 4.13.0, Leica Microsystems) was used. The minimal Feret's diameter of muscle fiber cross sections was analyzed with the ImageJ software (version 1.53k). For each group, four animals were included. Per animal, 10 systematically randomly sampled fields of view of triceps brachii muscle were analyzed. To obtain an accurate result, all muscle fiber cross sections were analyzed in the field of view (analyzed pictures: n_{WT}=40; $n_{DMD\Delta52}$=40; $n_{DMD\Delta51\text{-}52}$=40) (analyzed muscle fiber sections: n_{WT}=2364; $n_{DMD\Delta52}$=3313; $n_{DMD\Delta51\text{-}$

$_{52}$=1701). For the calculation of the proportion of muscle fiber section with central nuclei, all muscle fiber cross section of an image were counted, followed by all cross sections with central nuclei. Counting was performed, using the ImageJ software (version 1.53k). Four animals were analyzed per group. For each animal, 15 systematically randomly sampled fields of view of triceps brachii muscle were analyzed (analyzed pictures: n_{WT}=60; $n_{DMD\Delta 52}$=60; $n_{DMD\Delta 51\text{-}52}$=60).

3.9. RNA isolation and cDNA synthesis

Total RNA was extracted from snap-frozen triceps brachii muscle samples with the TRIzol™ method, according to manufactures instruction. Tissue was stored, until use, at -80°C to avoid RNase activity. Tissue were taken from dry ice and immediately transferred to a Eppendorf tube with 1 ml TRIzol™ reagent and homogenized with the tissue homogenizer Art-Miccra D-8. After incubation for 5 min at room temperature, 0.2 ml of chloroform were added and mixed carefully, followed by 3 min incubation. After incubation, the tubes were centrifuged for 15 min at 12,000 × *g* at 4°C. The upper aqueous phase was transferred to a new Eppendorf tube and 0.5 ml isopropanol were added, followed by an incubation step for 10 min. After centrifugation for 10 min at 12,000 × *g* at 4°C, supernatant was discarded and the formed RNA pellet was resuspended in 1 ml of 75% ethanol. After vortexing, samples were centrifuged for 5 min at 7500 × *g* at 4°C and supernatant removed. RNA pellet was air dried for 6 min at room temperature in the Eppendorf tube. After drying, the RNA pellet was solved in 51.5 µl of RNase-free water and incubated for 20 min at 37°C on the thermo-shaker. RNA concentration was measured with the Nanodrop.

Prior cDNA synthesis, DNA digestion was performed, using the dsDNase (Thermo Scientific) according to manufactures instructions. The cDNA was synthesized by RNA to cDNA EcoDry™ Premix (Double Primed) Kit. Due to template length, the double primed kit was used, including not only oligo (dT)-primer, but also random hexamers primers.

3.10. Echocardiography

Echocardiography was performed with an Esaote MyLab X8 system, according to (STIRM et al., 2021). Pigs were investigated with a transthoracic 2D echo view. Left ventricular ejection fraction and left ventricular fractional shortening were measured in the M-mode. All echocardiographic investigations were performed by

Andreas Lange. Pigs were sedated prior to the investigation with 20 mg/kg ketamine (Ursotamin®, Serumwerke Bernburg, Bernburg, Germany) and 2 mg/kg azaperone (Azaporc®, Serumwerke Bernburg). During the heart ultrasound, they received 4 mg/kg/h of propofol (Propofol 2%, Fresenius Kabi, Bad Homburg, Germany).

3.11. Semen analysis

Sperm motility of the *DMD*Δ52 (#6790) and *DMD*Δ51-52 (#11914) boars was analyzed with the Computer Assisted Semen analysis (CASA) software Sperm Vision® Therio (Minitube, Tiefenbach, Germany) by Dr. Mayuko Kurome.

3.12. Statistics

GraphPad Prism version 5.04 and SAS (Statistical Analysis System) were used for the statistical evaluation.

For the evaluation of measurements that considered only one age group, a one-way analysis of variance (one-way ANOVA), followed by a Bonferroni correction as post hoc analysis, was performed.

Statistical analyses of results, containing more than one time point (CK and AST), were performed by a two-way ANOVA, followed by Bonferroni correction.

The survival of the *DMD*Δ52 and *DMD*Δ51-52 was compared with a Mantel-Cox Test and with a Gehan-Breslow-Wilcoxon Test.

Level of significance was set to $P < 0.05$. *P*-values were presented as: * = $p < 0.05$; ** = $p < 0.01$; *** = $p < 0.001$; **** = $p < 0.0001$; n.s. = $p \geq 0.05$ (not significant).

IV. RESULTS

1. Generation of *DMD*Δ51-52 fibroblasts for SCNT

Clonal separation of the fibroblasts, after electroporation, resulted in 120 single-cell clones (**Figure 6 A**), which could be cryopreserved in liquid nitrogen for long-term storage. The PCR, spanning the deletion site from intron 50 to intron 51 (dex51f1/dex51r3), identified five single-cell clones, carrying a deletion of the correct size (bck1, bck20, bck27, bck101 and bck107). After restriction enzyme digestion (Acc65I), one of these single-cell clones was excluded (bck20), because the restriction enzyme, which had its recognition site within exon 51, cut the PCR product of bck20 (**Figure 6 B**). Sanger sequencing confirmed the presence of exon 51 in bck20 and identified a deletion in intron 51 which led to the shortened PCR band. The remaining single-cell clones were selected and two were used for SCNT (bck101 and bck107). Deletions in the two chosen single cell clones had different sizes. The deletion of bck101 had a length of about 1000 bp, while in bck107 about 1470 bp were missing.

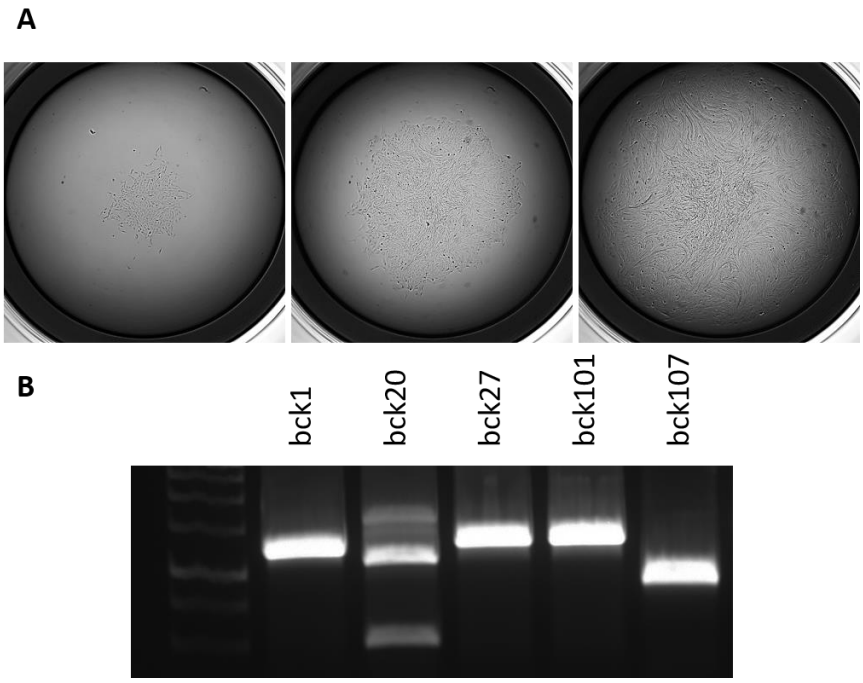

Figure 6: (A) Development of a single cell clone in cell culture medium in a 96-well plate at day 4, 6 and 8 after clonal separation. Images were taken with the Cellavista®. (B) The five single cell clones, with the correct band lengths, were screen for DMD exon 51 by restriction enzyme digest, using the enzyme Acc65I from Acinetobacter aceti. In single cell clone bck20, the DMD exon 51 could be detected.

2. Generation of the *DMD*Δ51-52 pig model

Embryo transfer of 63 SCNT embryos, at age one and two days, resulted in a pregnancy in sow #11054, which gave birth to two live-born and one still-born piglet. Another 196 SCNT embryos were transferred to two other sows (#11112 got 100 embryos and #11106 got 96) and resulted in one pregnancy and the birth of seven piglets. One piglet was crushed by the recipient sow at day 1 p.p. and another one died at day 21 p.p. in anesthesia, due to unknown reasons. The remaining seven piglets could be raised. The genotype was proofed by PCR **(Figure 7)** and Sanger sequencing **(Figure 8)**, showing the correct mutation. All piglets carried the deletion of *DMD* exon 51, additional to exon 52.

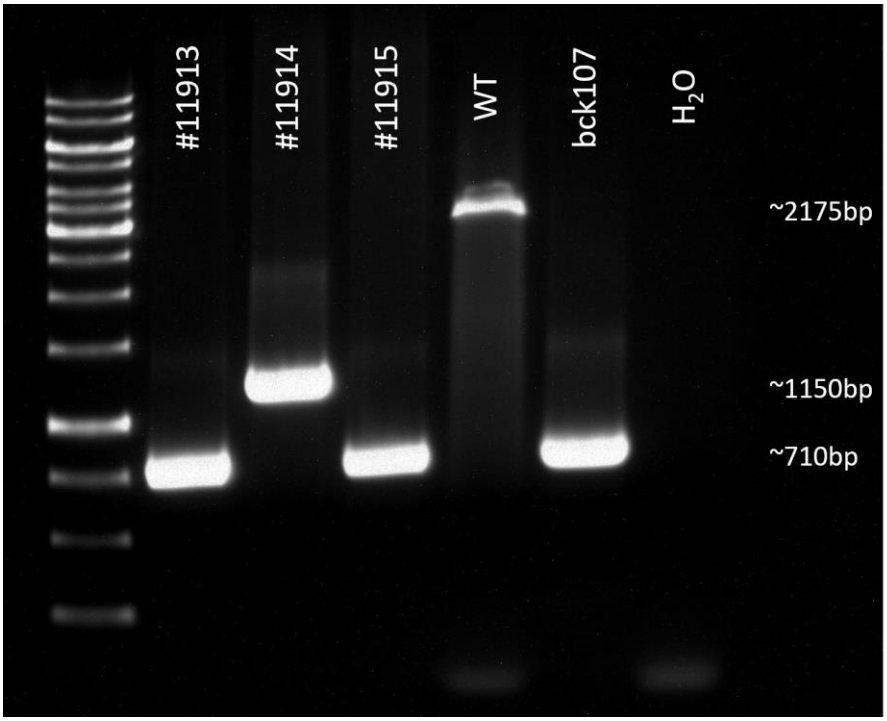

Figure 7: Detection of the deletion of DMD exon 51 in the first DMDΔ51-52 litter from SCNT by PCR, followed by gel electrophoresis. The PCR primers were placed outside the two gRNA cutting sites (dex51f1/dex51r3). While the PCR product in the WT animal, with the intact exon 51, had a length of ~2175bp, the piglets had band lengths of ~710bp (#11913 and #11915) respectively ~1150bp (#11914). Different band lengths resulted from the origin from different single cell clones. #11914 resulted from SCNT from single cell clone bck101 and #11913 and #11915 from bck 107.

At an age of four months, four of the *DMD*Δ51-52 pigs were euthanized and tissue samples were added to a biobank, which has already contained samples of age matched WT and *DMD*Δ52 animals. The generation of the DMD biobank was published elsewhere (STIRM et al., 2021). *DMD*Δ51-52 was used for the same

purposes at an age of 9 months, age matched to the original *DMD*Δ52 animal (#6790), which were used as cell donor for the fibroblast cell line, which has been used to generate the *DMD*Δ51-52 single cell clones. The last two remaining animals were kept for breeding and establishment of a breeding herd for the new Becker muscular dystrophy model.

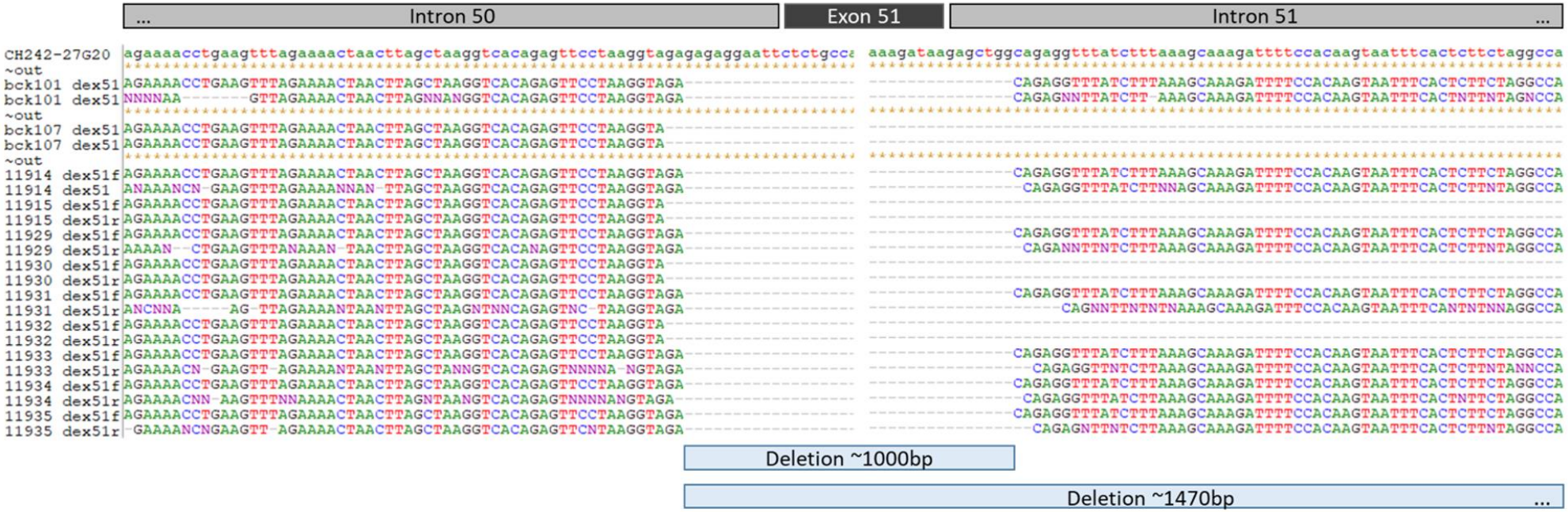

Figure 8: Sequences from Sanger sequencing proofed the deletion of DMD exon 51. In the first line, the Sus scrofa reference sequence from ensemble.org is added for comparison. For each piglet, sequences were sequenced in both direction, forward and reverse. Piglets, origin from bck107 had a longer deletion of ~1470bp, while the piglets from bck101 had a deletion of ~1000bp. Both deletions included exon 51.

To check the restoration of the reading frame in the dystrophin gene, which was achieved by the additional deletion of exon 51, RNA was isolated from triceps brachii muscle of the four animals after necropsy and from triceps brachii muscle of four age-matched WT and *DMD*Δ52 animals. The isolated mRNA was reverse transcribed and a PCR, using a primer pair, spanning *DMD* exons 50 to 53, was performed. Gel electrophoresis of the PCR product proofed the shortened band length of the *DMD*Δ51-52 compared to *DMD*Δ52, while the WT had an even longer PCR product (**Figure 9B**). Sanger sequencing of the PCR product confirmed the deletion. **Figure 9A** presents the sequence from Sanger sequencing. Due to the length of the deletion of 351 bp in the *DMD*Δ51-52 model and 118 bp in the *DMD*Δ52 model, the sequence is shortened illustrated.

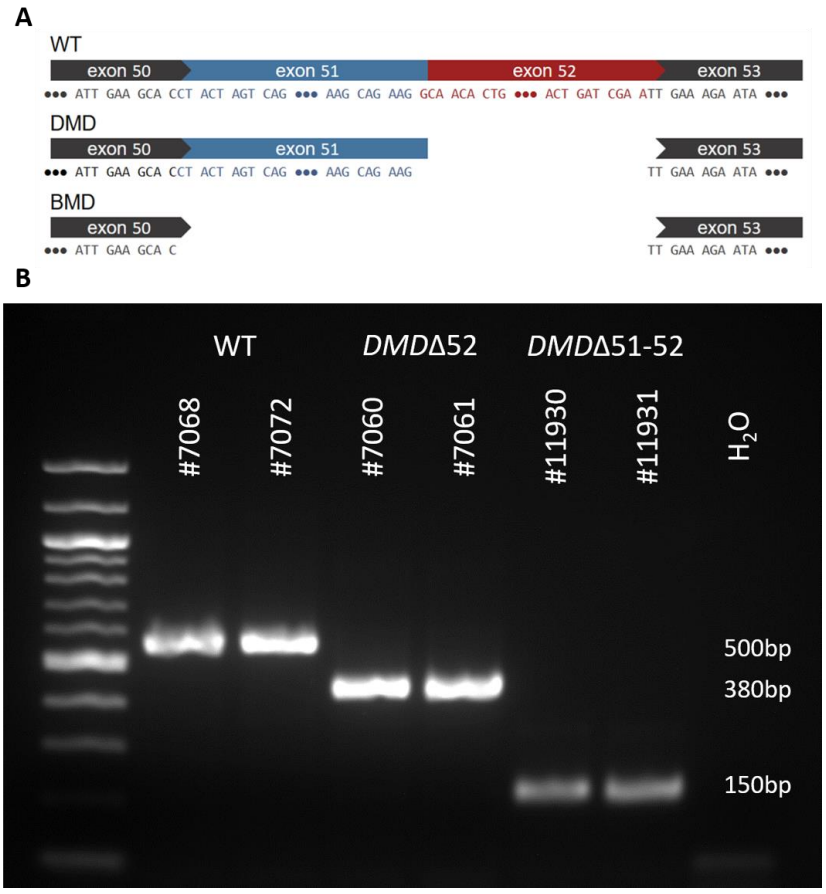

Figure 9: Deletion of DMD exon 51 and exon 52 in the cDNA. (A) Clearly shortened representation of the sequences from Sanger sequencing. Forward primer was located in exon 50, while reverse primer was in exon 53 (DMDex50f2/DMDex53r4). The length of the deletion in DMDΔ52 animals was 118bp, corresponding to exon 52 and in the DMDΔ51-52 pigs 351bp (exons 51 and 52). The mutation in DMDΔ52 represents a frame-shift mutation, while the mutation in DMDΔ51-52 restores the correct reading frame and thus a shortened dystrophin is produced. (B) Gel electrophoresis of PCR products performed with cDNA, using primers from exons 50 to 53 (DMDex50f2/DMDex53r4) resulted in different band lengths for WT, DMDΔ52 and DMDΔ51-52.

Animal #11914 (*DMD*Δ51-52) was raised to an age of nine months, age-matched to #6790 *(DMD*Δ52). In contrast to its clone animal with the frame-shift deletion, #11914 presented no clinical symptoms, while #6790 had a reduced respiratory function and presented stenosis of the airway (STIRM et al., 2021). Body weight was increased in the animals with the corrected reading-frame to an average weight of 168.7 kg (n=3) compared to 76.5 kg in the original pig. **Figure 10** shows both animals before necropsy at an age of 9 months.

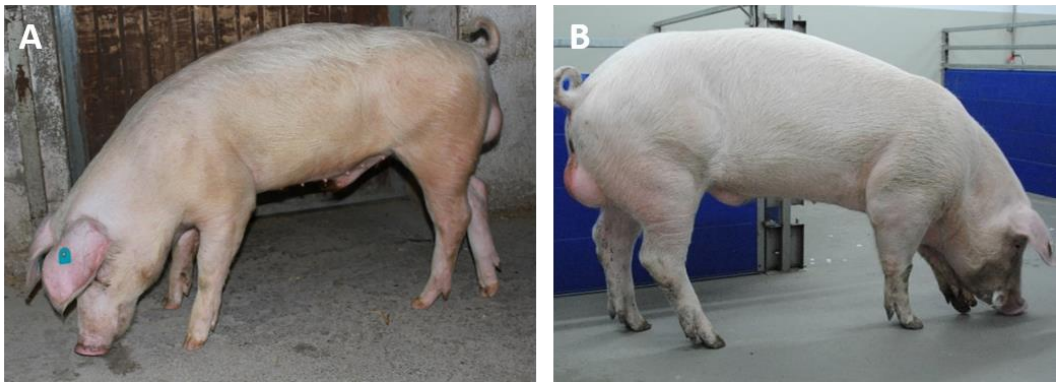

Figure 10: Comparison of the DMDΔ52 donor of the fibroblast cell line, which was used for the generation of the DMDΔ51-52 model, with one of the F0 DMDΔ51-52 animals after somatic cell nuclear transfer (SCNT). Both pictures were made at an age of ~9 months. (A) #6790 (DMDΔ52) and (B) his identical clone (#11914, DMDΔ51-52) with the corrected reading frame in the DMD gene.

#6790 was housed until necropsy with a female littermate (*DMD*Δ52_het, #6794) without performing naturale mating. At an age of 9 months, *DMD*Δ52 #6790 presented growth retardation compared with the female littermate (**Figure 11**).

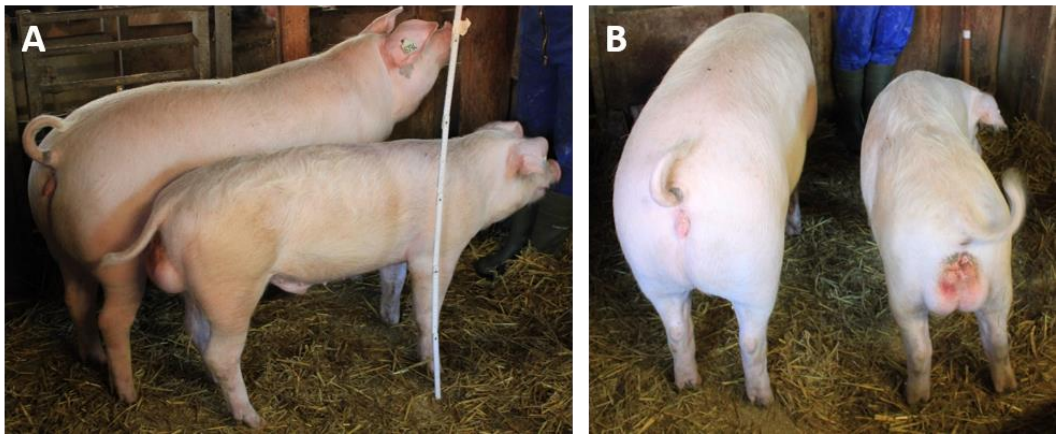

Figure 11: Comparison of DMDΔ52 animal (#6790) with a female littermate (DMDΔ52_het, #6794) at an age of 9 months (A) + (B).

3. Characterization of the new Becker muscular dystrophy pig model

3.1. Dystrophin detection

The restored dystrophin expression was proofed by immunohistochemistry on sections of formalin-fixed skeletal muscle and myocardium, using a monoclonal antibody against human dystrophin, which also detects porcine dystrophin protein (DYS1. Leica). DYS1 IHC presented a high expression of dystrophin in the *DMD*Δ51-52 animals and the WT animals, in myocardium and skeletal muscle, but a total absence in the *DMD*Δ52 animals (**Figure 12**). In order to detect not only the Rod domain but also the C-terminus of the truncated protein, an additional IHC was performed with DYS2 (Leica), a specific antibody against the C-terminus of dystrophin (**Figure 13**).

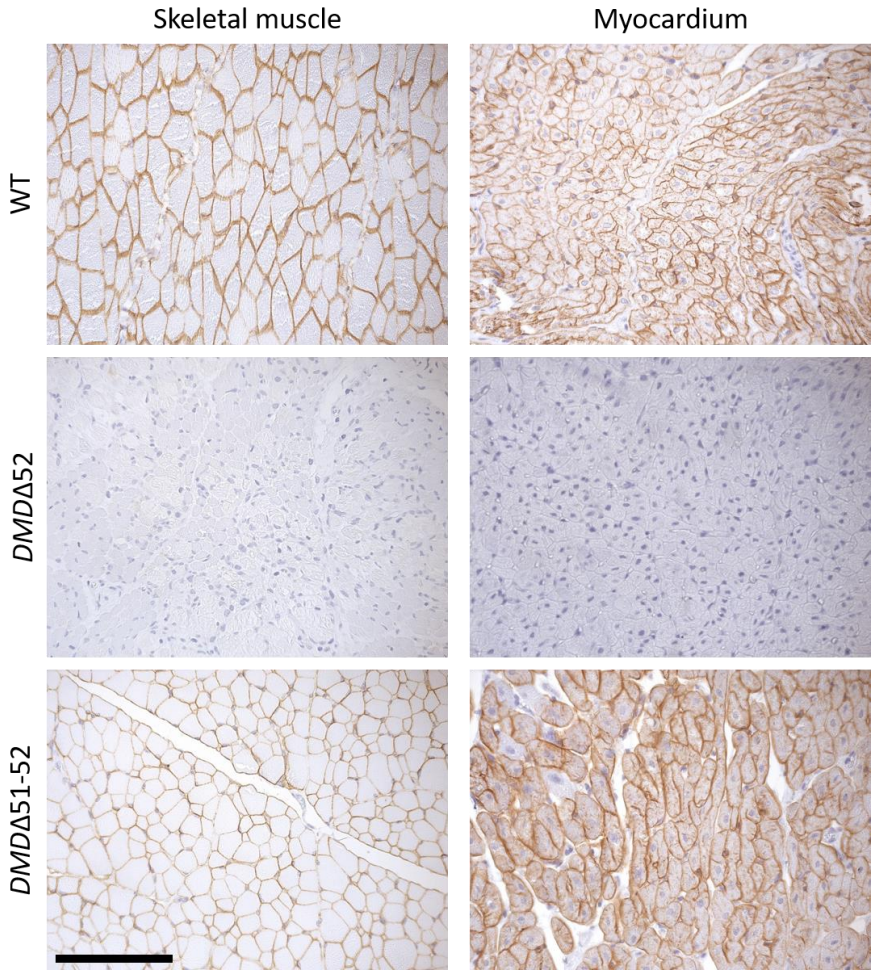

Figure 12: Dystrophin protein detection by immunohistochemistry (IHC) using a monoclonal antibody (DYS1, Leica) against Dystrophin (Rod Domain). IHC detected a high expression of dystrophin in skeletal muscle (Triceps brachii muscle) and myocardium of WT and DMDΔ51-52 animals. No dystrophin expression was found in skeletal muscle and myocardium of DMDΔ52 animals (Scale bar=100 µm).

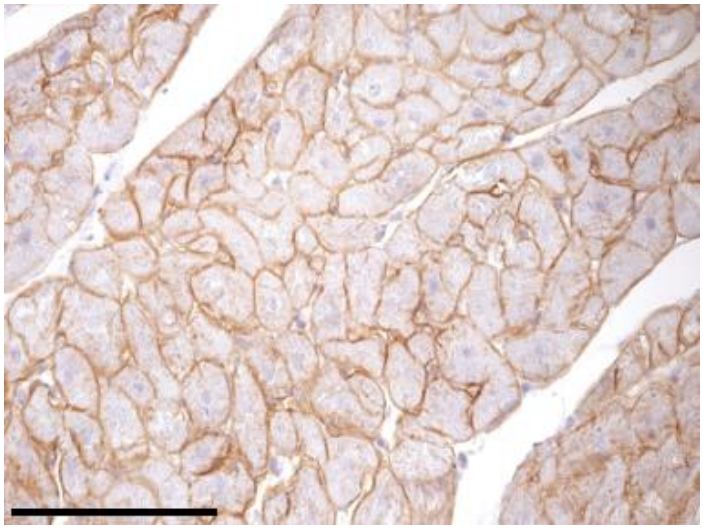

Figure 13: Detection of the C-terminus of the dystrophin protein in the myocardium of a DMDΔ51-52 pig by immunohistochemistry (IHC). IHC was performed with a monoclonal primary antibody against the C-terminus of the dystrophin protein (DYS2, Leica) (Scale bar =100 µm).

3.2. Growth and survival

The *DMD*Δ51-52 animals had a similar body weight as WT animals at an age of 3 months. The mean weight of the *DMD*Δ52 animals was significantly reduced, compared to the other two groups. Results are shown in **Figure 14**. Only animals which were housed in the Center for Innovative Medical Models (CiMM) were included in this analysis, which explains the small group sizes of WT and *DMD*Δ52 groups.

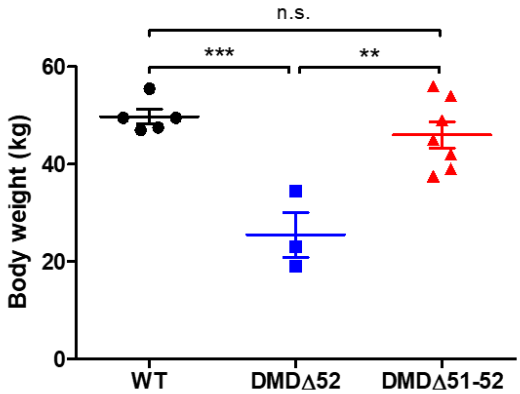

*Figure 14: Body weight of WT, DMDΔ52 and DMDΔ51-52 animals at an age of 3 months. Significant differences were indicated: * = p < 0.05; ** = p < 0.01; *** = p < 0.001; **** = p < 0.0001; n.s. = p ≥ 0.05 (not significant).*

One *DMD*Δ51-52 piglet was crushed by the sow at day 1 p.p. and another died spontaneously during anesthesia at day 21 p.p.. All remaining animals showed no clinical symptoms until they were euthanized for tissue harvesting. **Figure 15** shows the Kaplan-Meier curves of survival for the *DMD*Δ52 and for the *DMD*Δ51-52 models. Only the first 90 days are included, because most of the animals were used for tissue collection at an age of 100-120 days. In total, nine *DMD*Δ51-52 and 52 *DMD*Δ52 are included in the analyses. ~78% of *DMD*Δ51-52 and ~55% of *DMD*Δ52 animals survived the first 90 days. Differences were not significant.

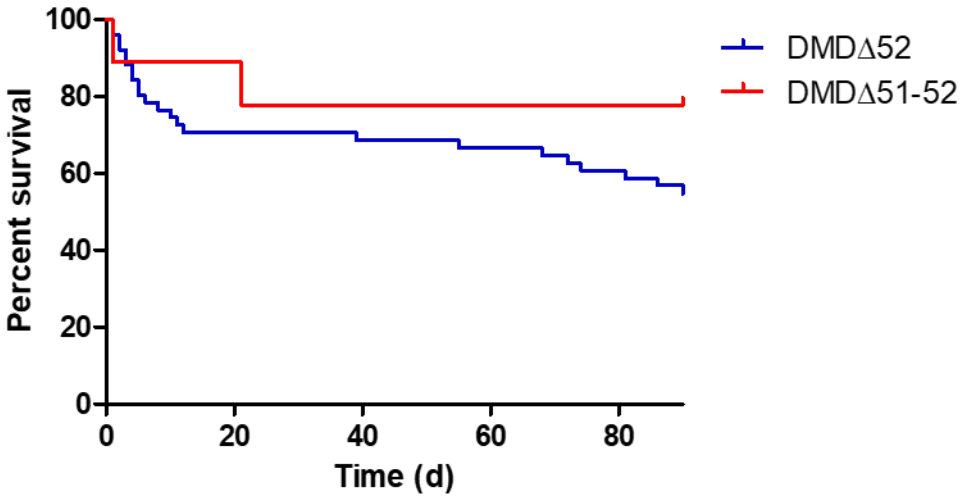

Figure 15: Kaplan-Meier curve of survival of the DMDΔ52 group (blue, n=52) and the DMDΔ51-52 group (red, n=9). Only spontanous deaths, within the first 90 days post partum were included. 2 of 9 DMDΔ51-52 died during the thirst 90 day, while 23 of 52 DMDΔ52 died. Differences were not significant.

3.3. Serum parameters

Different serum parameters are changed in *DMD*Δ52 pigs compared to WT. Creatine kinase is widely used serum marker for the diagnosis of neuromuscular disease (DUAN et al., 2021). As in human patients, CK activity is dramatically increased in our Duchenne pig model, at all three investigated time points (2 months (WT = 622.8 U/l; *DMD*Δ52 = 49523.3 U/l; *DMD*Δ51-52 = 2099.3 U/l) – 4 months (WT = 918.3 U/l; *DMD*Δ52 = 61915.7 U/l; *DMD*Δ51-52 = 1899.4 U/l) – 6 months (WT = 1241 U/l; *DMD*Δ52 = 97815 U/l; *DMD*Δ51-52 = 1742 U/l)). In the Becker muscular dystrophy model, the mean CK level is slightly, but not significantly, increased at all three time points. The levels increased with the age of the animals

in the WT and in the *DMD*Δ52 groups. CK levels are presented in **Figure 16 A**. Note the logarithmic scale, which was chosen because of the variation of CK serum levels between the groups.

Aspartate aminotransferase (AST), a further diagnostic marker for dystrophinopathies, was significantly increased in our *DMD*Δ52 pigs at all three time points, too. The *DMD*Δ51-52 had in contrast only mildly increased serum levels, which were not significantly changed to WT levels (**Figure 16 B**) (2 months (WT = 43.6 U/l; *DMD*Δ52 = 655.5 U/l; *DMD*Δ51-52 = 60.5 U/l) – 4 months (WT = 33.2 U/l; *DMD*Δ52 = 238.6 U/l; *DMD*Δ51-52 = 48.8 U/l) – 6 months (WT = 28.7 U/l; *DMD*Δ52 = 765 U/l; *DMD*Δ51-52 = 41.2 U/l)).

Troponin I, a specific serum marker for myocardial damage, was also increased in the *DMD*Δ52, but not in the *DMD*Δ51-52 model (WT = 0.04 ng/ml; *DMD*Δ52 = 0.12 ng/ml; *DMD*Δ51-52 = 0.02 ng/ml). Differences between *DMD*Δ52 and *DMD*Δ51-52 were significant, but not between WT and *DMD*Δ52. One animal of the WT control group had also an increased level, due to unknown reason (**Figure 16 C**).

In human dystrophinopathy patients, creatinine levels correlate well with disease severity and could even be used to distinguish between Duchenne and Becker muscular dystrophy (WANG et al., 2017). These findings are in line with the results from our models. The mean creatinine serum level in *DMD*Δ52 is significantly reduced compared to WT and *DMD*Δ51-52, while *DMD*Δ51-52 mean levels are only mildly, not significantly decreased compared to the control animals (**Figure 16 D**) (WT = 85.6µmol/l; *DMD*Δ52 = 27.4 µmol/l; *DMD*Δ51-52 = 74.0 µmol/l).

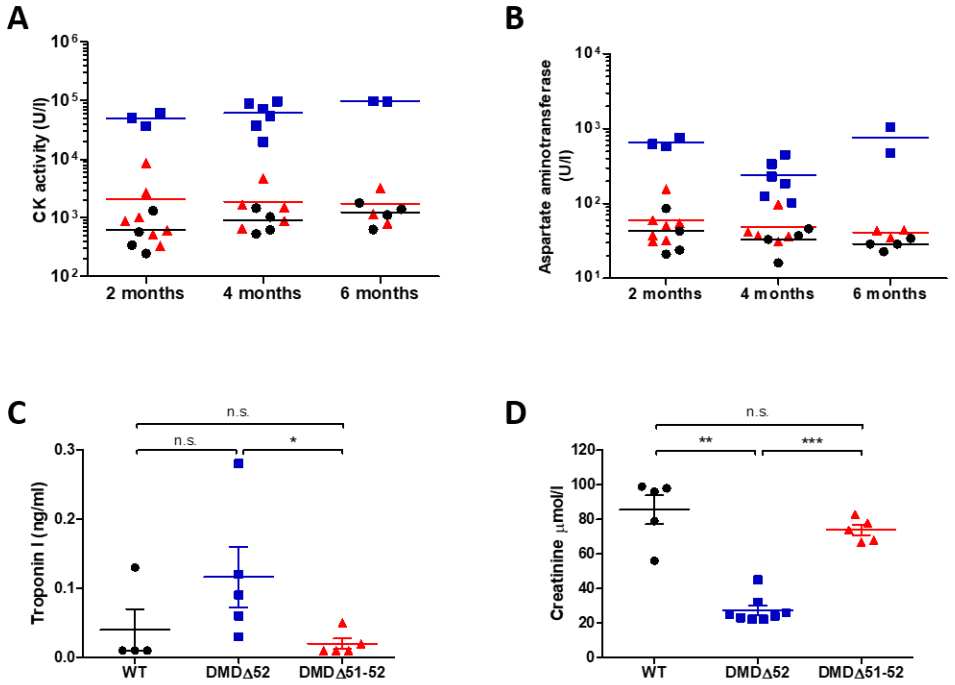

*Figure 16: Changes in serum parameters. (A) CK activity in serum samples at 2, 4 and 6 months p.p. of WT, DMDΔ52 and DMDΔ51-52. At all three time points, CK levels were significantly increased in the DMDΔ52 group compared with the other groups. (B) Aspartate aminotransferase serum levels were significantly increased in DMDΔ52 at 2, 4 and 6 months p.p. compared with DMDΔ51-52 and WT. (C) Troponin I was significantly elevated in serum of DMDΔ52 compared with DMDΔ51-52. The differences between DMDΔ51-52 and WT respectively DMDΔ52 and WT were not significant. (D) Creatinine levels were significantly reduced in DMDΔ52 animals, compared with the other groups. Significant differences were indicated: * = p < 0.05; ** = p < 0.01; *** = p < 0.001; **** = p < 0.0001; n.s. = p ≥ 0.05 (not significant).*

Statistical analysis of serum CK (Two-way ANOVA, Bonferroni multiple comparisons)

	WT vs. *DMD*Δ52	***DMD*Δ52 vs. *DMD*Δ51-52**	**WT vs. *DMD*Δ51-52**
2 months	*** (P < 0.001)	*** (P < 0.001)	n.s. (P > 0.05)
4 months	**** (P < 0.0001)	**** (P < 0.0001)	n.s. (P > 0.05)
6 months	**** (P < 0.0001)	**** (P < 0.0001)	n.s. (P > 0.05)

Statistical analysis of serum AST (Two-way ANOVA, Bonferroni multiple comparisons)

	WT vs. *DMD*Δ52	***DMD*Δ52 vs. *DMD*Δ51-52**	**WT vs. *DMD*Δ51-52**
2 months	**** (P < 0.0001)	**** (P < 0.0001)	n.s. (P > 0.05)
4 months	* (P < 0.05)	* (P < 0.05)	n.s. (P > 0.05)
6 months	**** (P < 0.0001)	**** (P < 0.0001)	n.s. (P > 0.05)

3.4. Histology

3.4.1. Skeletal muscle

3.4.1.1. Skeletal muscle morphology and histopathology

The *DMD*Δ51-52 animals presented an almost restored morphology of the skeletal muscle. The proportion of triceps brachii muscle fiber profiles with central nuclei was significantly increased in *DMD*Δ51-52 compared with the WT control group. *DMD*Δ51-52 presented 2.48% of fiber cross sections with central nuclei, compared to 0.91% in WT. In contrast, the proportion was highly significantly increased in the dystrophic *DMD*Δ52 pigs (13.77%) compared with both other groups (**Figure 17 A**).

A typical histopathological finding in neuromuscular diseases is the heterogeneity in muscle fiber diameters. We measured the minimal Feret's diameter of ten randomly taken images at 40x magnification per animal. In total four animals per group were analyzed. The variation in minimal Feret's diameter of muscle fibers was highly increased in the *DMD*Δ52 group (51.9%) compared to the WT (26.8%) and *DMD*Δ51-52 group (26.4%). The differences between the WT and *DMD*Δ51-52 groups were not significant (**Figure 17 B**).

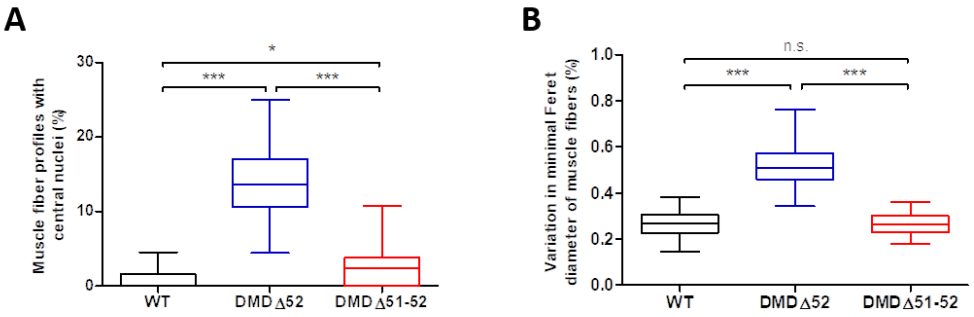

*Figure 17: Alterations in muscle fiber morphology. (A) Proportion of muscle fiber cross sections in triceps brachii muscle with central nuclei. (B) Variation of minimal Feret diameter of muscle fibers of the triceps brachii muscle was significantly increased in the DMDΔ52 group. Significant differences were indicated: * = $p < 0.05$; ** = $p < 0.01$; *** = $p < 0.001$; **** = $p < 0.0001$; n.s. = $p \geq 0.05$ (not significant).*

Hematoxylin eosin (HE) stain of triceps brachii muscle of four animals per group, presented a restored morphology in the skeletal muscle of the *DMD*Δ51-52 animals, while the *DMD*Δ52 had a dramatically changed histomorphology. The musculature of the *DMD*Δ52 animals presented a high proportion of central nuclei in the muscle

fiber cross section as well as varying diameters. Further, focal accumulation of inflammatory cells were omnipresent, just like fibrosis and necrotic muscle fibers (**Figure 18**).

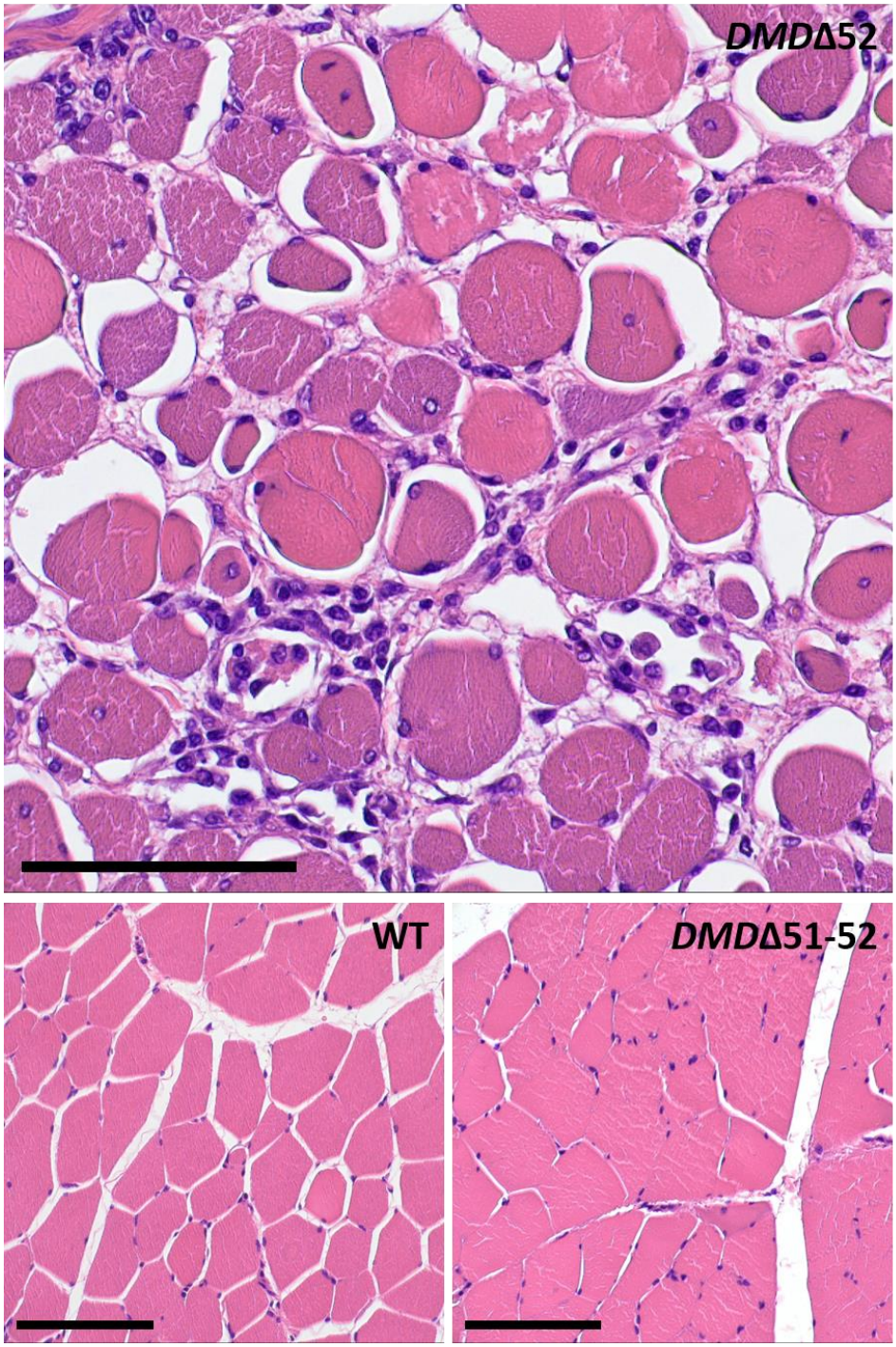

Figure 18: Hematoxylin eosin (HE) stain of skeletal muscle (triceps brachii muscle) at an age of 4 months. DMDΔ52 muscle presented various diseases typical, pathological changes, like a high proportion of muscle fiber cross section with central nuclei, heterogeneous minimal Feret's diameters of cross section, accumulations of inflammatory cells, connective tissue and necrotic fibers. Skeletal muscle morphology was comparable in the DMDΔ51-52 animals to WT in HE stain (scale bar=100 µm).

While the fibrosis of the skeletal muscle of the *DMD*Δ52 group was dramatically increased, the *DMD*Δ51-52 group presented no increase in fibrosis compared to the WT group. For this analysis we performed Masson's trichrome stain on triceps brachii muscle sections of four WT, four *DMD*Δ51-52 and four *DMD*Δ52 animals. The Masson's trichrome protocol stains selectively the connective tissue blue. In **Figure 19** representative images for each group are presented.

Embryonic myosin (myosin heavy chain 3, MYH3) is only expressed during fetal development and in regenerating muscle fibers in skeletal muscle. IHC using an antibody, specific against MYH3, presented a high proportion of regenerating fibers in triceps brachii muscle of *DMD*Δ52 animals at an age of 4 months, while no muscle fibers of WT and *DMD*Δ51-52, both expressing at least a shortened dystrophin, were stained. MYH3 IHC resulted in cytoplasmic staining pattern in the muscles of the *DMD*Δ52 group. Staining intensity varied between muscle fibers **(Figure 19)**. Appropriate tissue (porcine fetal skeletal muscle) was used as positive control.

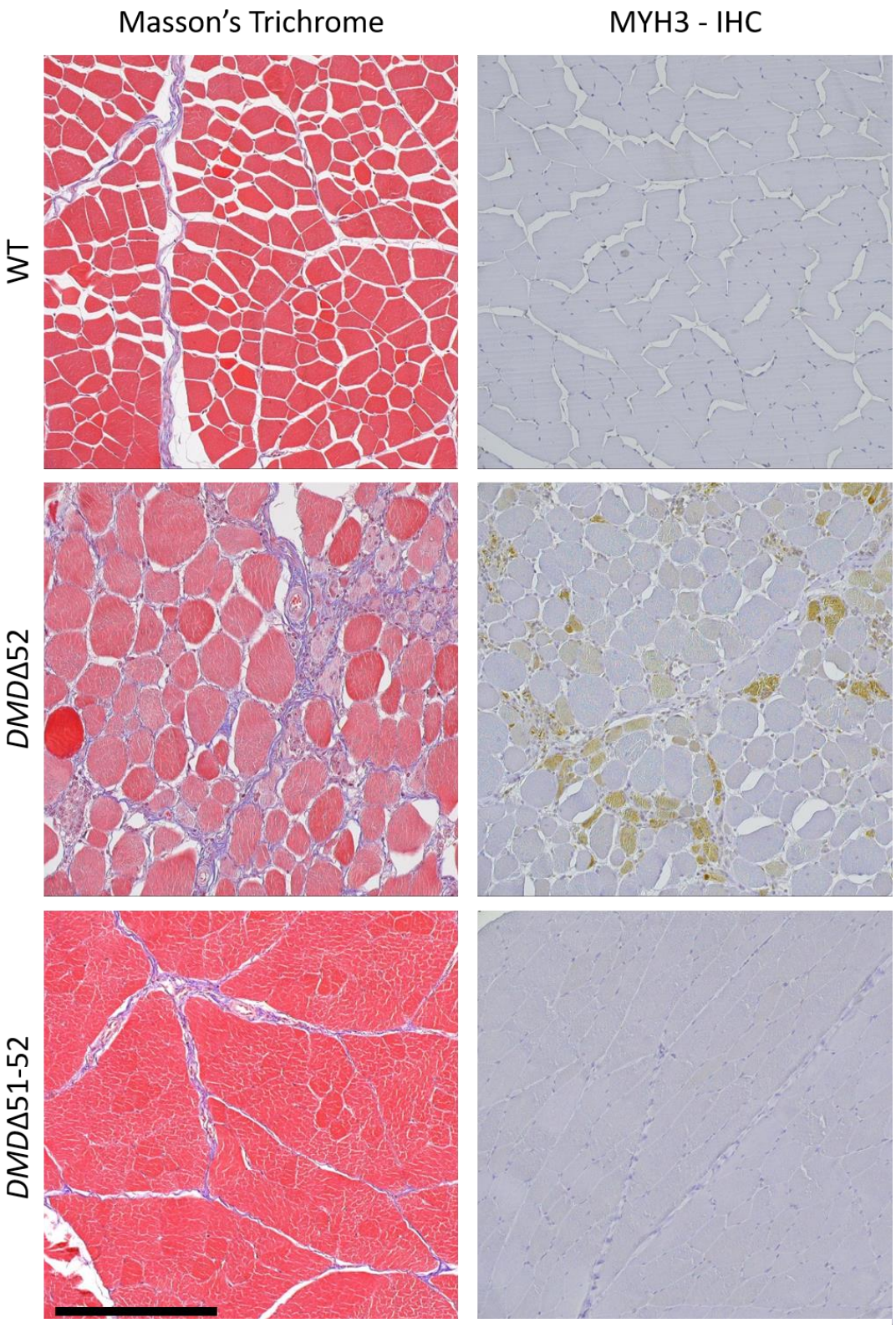

Figure 19: Fibrosis and regenerating fibers in the skeletal muscle at an age of 4 months. Masson's trichrome stain presented an increase in muscle fibrosis in the DMDΔ52 group, but not in the DMDΔ51-52 group in triceps brachii muscle. Immunohistochemistry (anti-MYH3) revealed a high proportion of positive stained, regenerating muscle fibers in the skeletal muscle (Triceps brachii muscle) of the DMDΔ52 animals, while no fibers were stained in the DMDΔ51-52 and WT pigs (scale bar=250 µm).

3.4.2. Myocardium

3.4.2.1. Myocardial histopathology

Fibrosis was not increased in 4 months old *DMD*Δ52 or *DMD*Δ51-52 compared with the WT control group. However, in the 9 months old animals, the *DMD*Δ52 boar (#6790) presented an increase in myocardial fibrosis, detected by Masson's Trichrome stain. #11914 (*DMD*Δ51-52) in contrast, showed no change in heart fibrosis. All investigated myocardial samples were taken from the basal left ventricle (**Figure 20**).

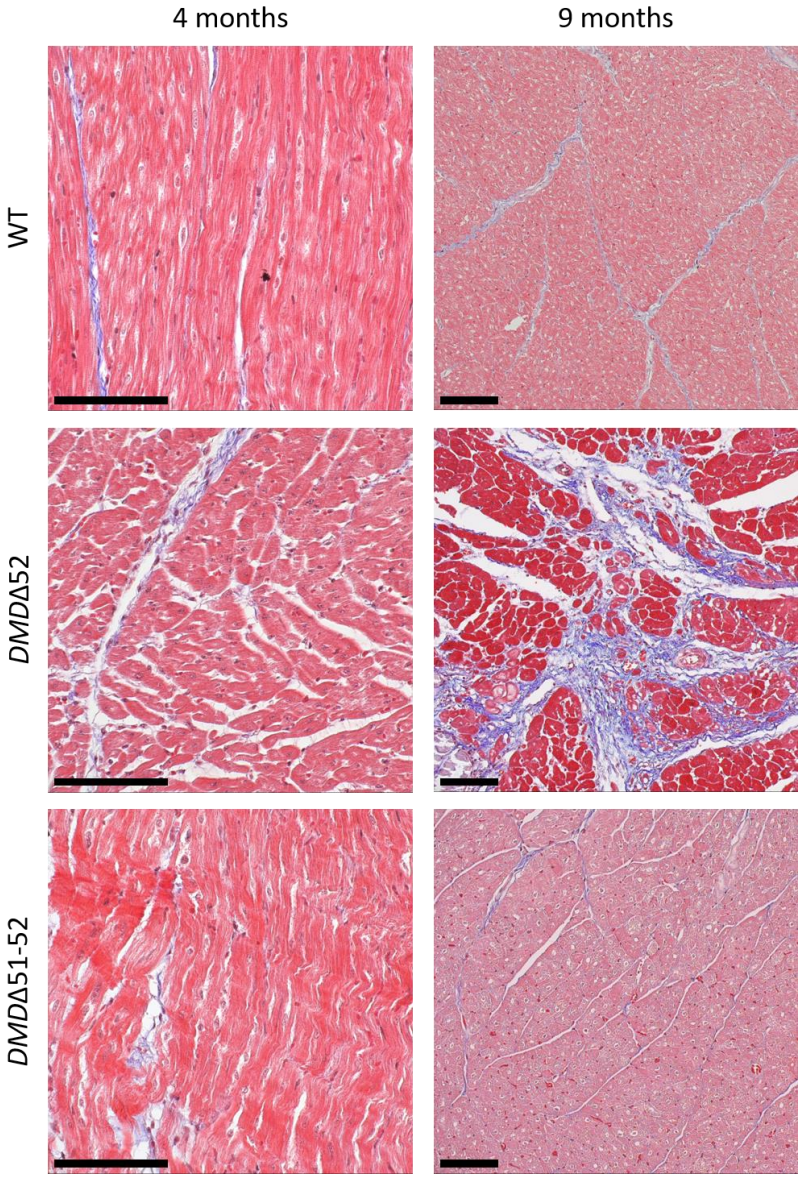

Figure 20: Masson's trichrome stain for the detection of connective tissue in the basal left ventricle of 4 months and 9 months old pigs. At an age of 4 months, no significant differences in myocardial fibrosis were found between DMDΔ52, DMDΔ51-52 and WT animals. Five months later, the DMDΔ52 pig presented a severe myocardial fibrosis, while no differences between WT and the DMDΔ51-52 could be detected (scale bar =100 µm).

Neither in HE stain nor in the MYH3 IHC significant differences in the myocardium between the three groups were detected at an age of 4 months (data not shown). In contrast, at an age of 9 months, the myocardium of the *DMD*Δ52 animals had various areas with a high proportion of regenerating cardiomyocytes, identified by MYH3-IHC and infiltrations of inflammatory cells could be seen in HE stain (**Figure 21**).

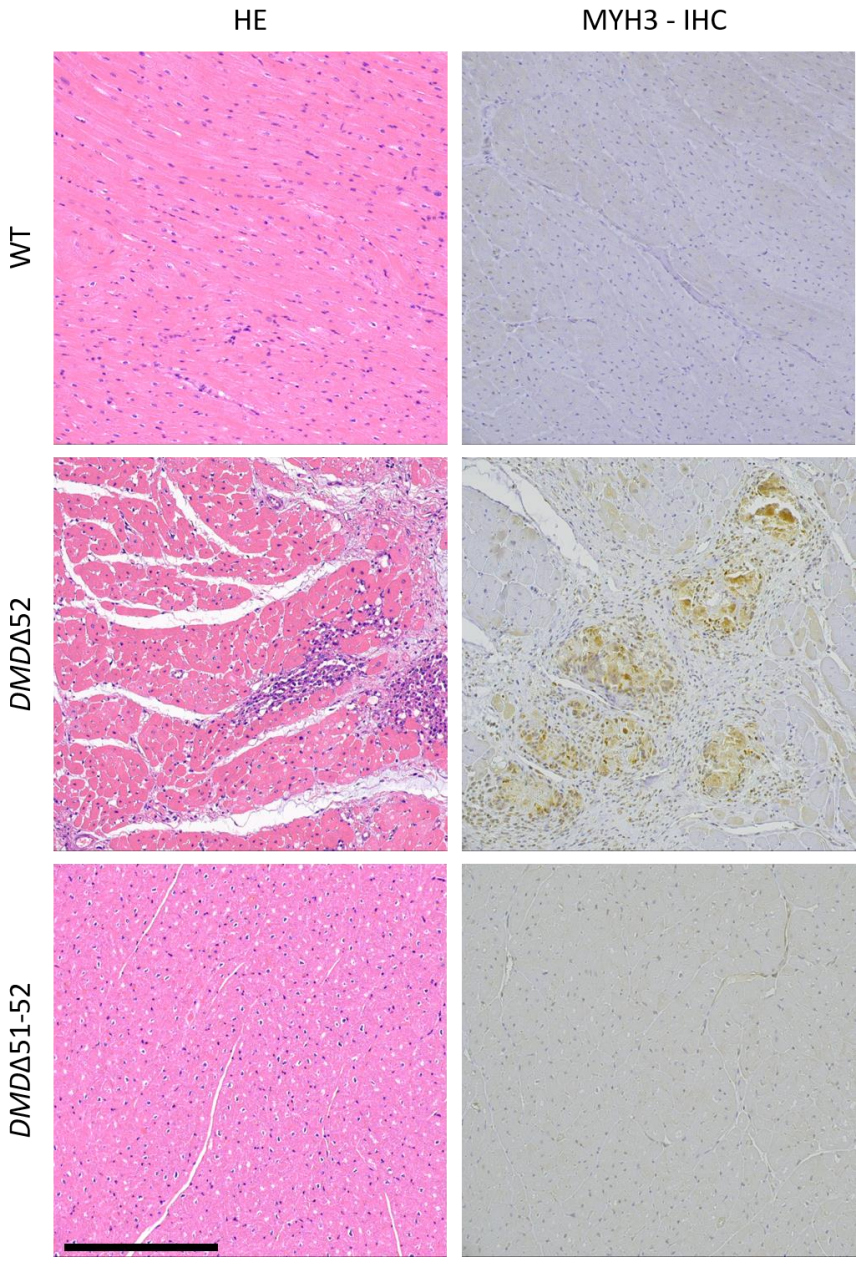

Figure 21: Pathological alterations in the myocardium of the left ventricle at an age of 9 months. Hematoxylin eosin stain presented focal accumulations of lymphocytes in the myocardium of the DMDΔ52 pig. In the WT and DMDΔ51-52 only single, isolated lymphocytes were found. IHC against embryonic myosin (anti-MYH3) detected regenerating fibers in the myocardium of the DMDΔ52, but not in DMDΔ51-52 and WT. Scale bar =250 µm.

3.4.3. Tongue

Since significant pathological changes in the tongue of a pig, suspected to suffer from Becker muscular dystrophy, were described (AIHARA et al., 2022), we analyzed the tongues of 4 WT, 4 *DMD*Δ52 and 4 *DMD*Δ51-52 pigs. Regardless of genotype, all pigs presented a high proportion of fatty infiltrations in hematoxylin eosin (HE) stain and the tissue was dominated by connective tissue in the Sirius red stain (**Figure 22**).

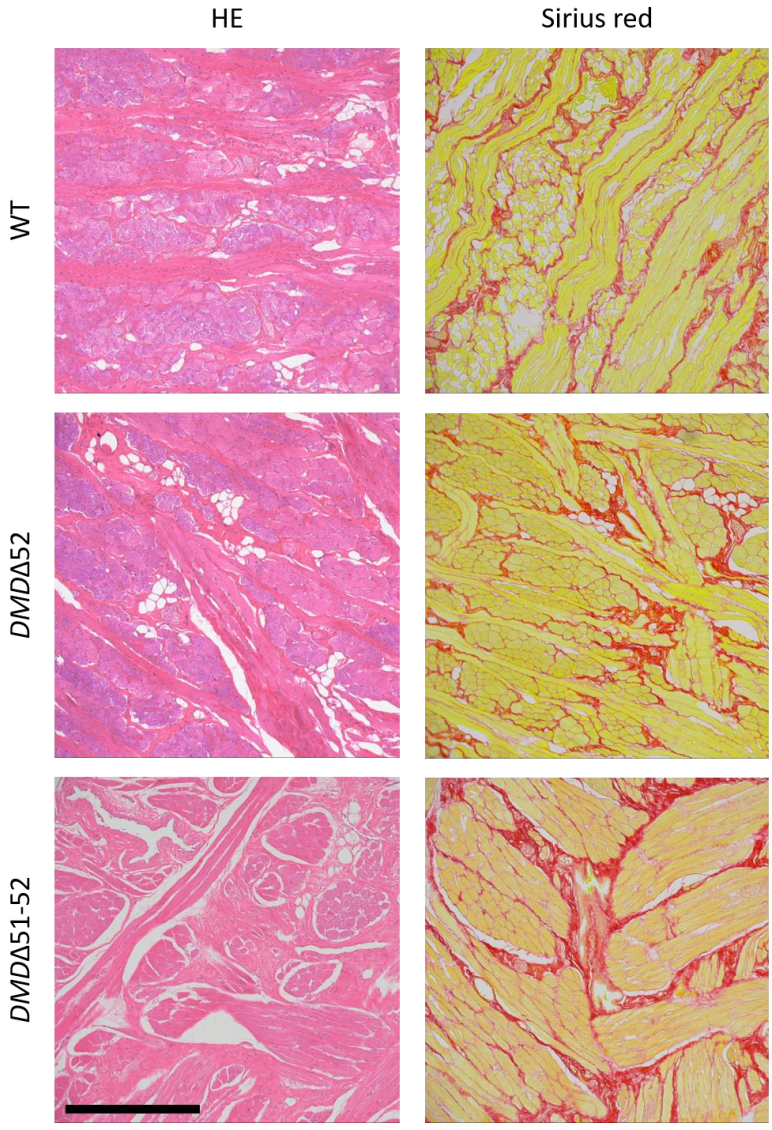

Figure 22: Histological comparison of the tongue of 4 months old DMDΔ52, DMDΔ51-52 and WT pigs. Hematoxylin eosin stain revealed fatty infiltrations in all investigated genotypes. Sirius red stain presented a high proportion of connective tissue not only in affected pig (DMDΔ52 and DMDΔ51-52) but also in healthy controls (WT). Scale bar = 500 µm.

3.5. Heart function

The restoration of the dystrophin expression resulted in the total restoration of the heart function. Left ventricular ejection fraction (LVEF) and left ventricular fractional shortening (LVFS) were measured by echocardiography. All animals were age-matched at ~100 days. 12 WT, 12 *DMD*Δ52 and 7 *DMD*Δ51-52 animals were investigated. In the dystrophic pigs, LVEF was highly significantly reduced (58.8%) compared to WT (70.3%) and *DMD*Δ51-52 (72.3%). The differences between WT and *DMD*Δ51-52 were not significant (**Figure 23 A**). As for the LVEF, the reduction of LVFS was highly significant in the *DMD*Δ52 model (30.6%), but not in the *DMD*Δ51-52 model (40.9%), compared to the unaffected control group (39.9%) (**Figure 23 B**).

The heart weight to body weight ratio was 0.35% in the 9 months old *DMD*Δ51-52 vs. 0.43% in the age-matched *DMD*Δ52 animal (heart weight: *DMD*Δ52=327.1g, *DMD*Δ51-52=570g; body weight: *DMD*Δ52=76.5kg, *DMD*Δ51-52=164kg). The heart weight to body weight ratio of the *DMD*Δ51-52 is thus in line with the findings published by Zurbrigg et al., who found a mean ratio of 0.309% in 23 pigs without lesions in the heart in a Canadian slaughterhouse (ZURBRIGG et al., 2018). The increased ratio of the *DMD*Δ52 animal indicates a cardiac hypertrophy.

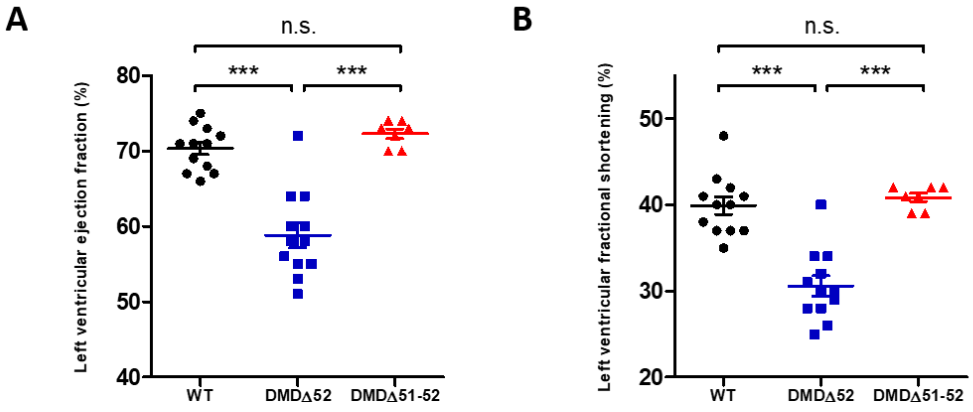

*Figure 23: Restoration of cardiac function. Echocardiography revealed a restored (A) Left ventricular ejection fraction and (B) fractional shortening in the DMDΔ51-52 group compared with the DMDΔ52. Differences between WT and DMDΔ51-52 were not significant. Significant differences were indicated: * = p < 0.05; ** = p < 0.01; *** = p < 0.001; **** = p < 0.0001; n.s. = p ≥ 0.05 (not significant).*

4. Establishment of a breeding herd

Heterozygous carrier sows (*DMD*Δ51-52_het) were generated by breeding the *DMD*Δ51-52 boars, when they reached fertility at an age of 7 months, to several breeding sows. Two types of carrier sows (*DMD*Δ51-52_het and *DMD*Δ51-52/52) were born in the F1 (**Figure 24 A**). In total 81 piglets resulted from these litters, of which 22 were *DMD*Δ52, 16 *DMD*Δ51-52/52, 20 *DMD*Δ51-52_het and 23 male WT (**Figure 24 B**). After raising to fertility, two of these sows are currently used for breeding. The sows are inseminated with WT boars and according to Mendelian rules, 25% of the resulting animals will be *DMD*Δ51-52 piglets in the F2. If double transgenic sows are used, sows which carries the mutation for *DMD*Δ51-52 on one X-chromosome and *DMD*Δ52 on the second, 25% of the offspring will be *DMD*Δ51-52 and another 25% *DMD*Δ52, reducing the number of piglets with incorrect genotype (**Figure 24 C**). In addition, epididymal sperm was collected from #6790 and #11914, after necropsy and frozen to liquid nitrogen for long-term conservation. **Figure 24 D** shows the testis of #11914 at an age of 9 months. The Computer Assisted Semen Analysis (CASA) of both boars revealed a high proportion of motile sperm (#6790: Motility = 77.59%, Progressive motility = 73.93%, Local motility = 3.75%, Immotile = 22.4%; #11914: Motility = 84.97%, Progressive motility = 81.84%, Local motility = 3.12%, Immotile = 15.04%) (**Figure 24 E)**.

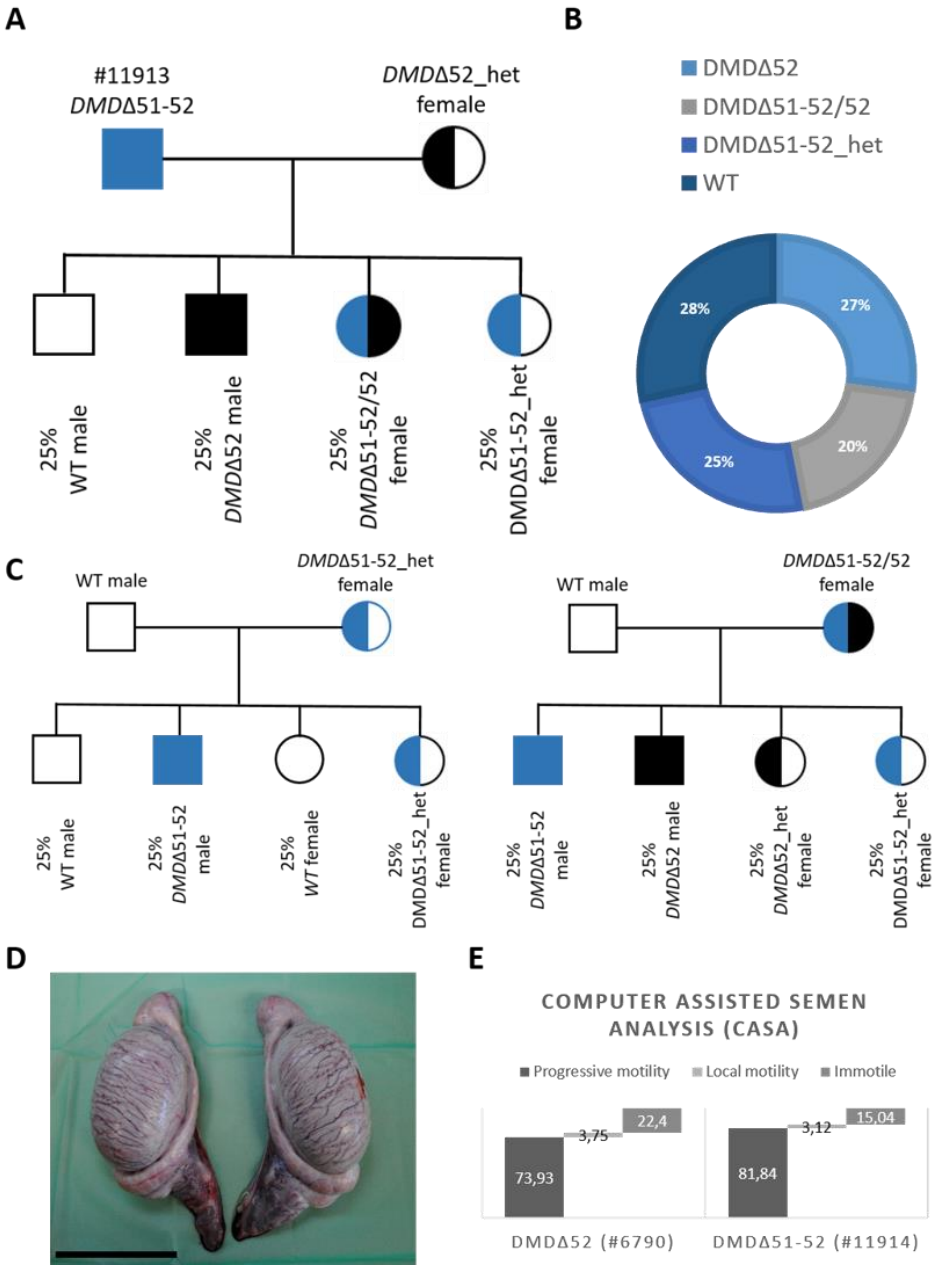

Figure 24: Establishment of a DMDΔ51-52 breeding herd. (A) Breeding of one of the founder animals (#11913, F0, DMDΔ51-52) with carrier sows (DMDΔ52_het) resulted in the births of carrier sows for DMDΔ51-52 (DMDΔ51-52/52 and DMDΔ51-52_het). (B) Offspring from F0 DMDΔ51-52 boars. (C) The DMDΔ51-52 carrier sows will be used for the production of DMDΔ51-52 piglets. Breeding the carrier sows with WT boars will result in 25% DMDΔ51-52 piglets. (D) Testes of DMDΔ51-52 (#11914) at an age of 9 months. (Scale bar=10 cm) (E) Computer Assisted Semen analysis (CASA) of both boars revealed a high proportion of motil sperm (#6790: Motility = 77.59%, Progressive motility = 73.93%, Local motility = 3.75%, Immotile = 22.4%; #11914: Motility = 84.97%, Progressive motility = 81.84%, Local motility = 3.12%, Immotile = 15.04%).

V. DISCUSSION

In the last years and decades, the therapy of Duchenne and Becker muscular dystrophy has been improved and life expectancy could be increased, due to optimal care, especially thanks to longtime glucocorticoid treatment and artificial respiration. However, both diseases are still not curable, limit the quality of life and life expectancy. Consequently, further research on the disease pathophysiology and drug trials are needed (DUAN et al., 2021). It is therefore essential to have good animal models, which not only mimic the disease symptoms seen in human patients well, but also are comparable in size and physiology and are available in sufficient numbers (MCGREEVY et al., 2015). In most of these respects, the pig is superior to other animal models (STIRM et al., 2022). The *mdx* mouse and other murine models for dystrophinopathies are easy to breed, cheap, available in large numbers and could even easily modified for the specific researchers needs. On the other hand, most murine models present only a mild disease phenotype and thus for example the life expectancy is just mildly reduced. Furthermore, the body physiology between a murine model and a human is hardly to compare, if one only considers the different body weights (30 g vs 60-90 kg) (PARTRIDGE, 2013) and the significantly different heart rates (~500-700 bpm in mice vs 50-90 bpm in resting human) (JANSSEN et al., 2016; NANCHEN, 2018). Nevertheless, the *mdx* mouse model contributed much to our understanding of neuromuscular diseases and will play a major role in the future. The CXMD dog models and the GRMD dog model in specific, benefit from their more severe phenotype, simulating the pathological findings in humans well. Even the reduced cardiac function is seen in affected dogs, however at a progressed stage. This late onset of the dilated cardiomyopathy, which reflects the most frequent reason for death in Becker and Duchenne patients, together with the difficulties in breeding and housing, as well as the ethical aspect of using classical pet animals as laboratory animals, are the main disadvantages of the canine models. The porcine models thus combine well the advantages of the murine and canine models. The dilated cardiomyopathy, for example is already present at an age of 4 months (STIRM et al., 2021) and thus the suitability for drug trials of the porcine model is superior to the canine. Its main disadvantage, the early mortality, could be solved by excessive neonatal care (STIRM et al., 2021).

Among various different approaches to treat Duchenne muscular dystrophy, the most prominent one is exon skipping. The frame-shift mutation is thereby transformed to an in-frame mutation, e.g., by deleting adjacent exons within the *DMD* gene. Thus, the severe Duchenne muscular dystrophy is changed to the milder Becker muscular dystrophy by the restoration of dystrophin expression, in specific, the expression of a shortened, truncated dystrophin (TAKEDA et al., 2021). However, the success of this strategy is mainly influenced by two factors, the efficiency of the gene editing and the functionality of the truncated dystrophin. In 2020, an AAV-mediated exon 51 skipping study in our *DMD*Δ52 was published. The treated pigs presented an amelioration of the disease symptoms, like reduced CK levels, improved activity and cardiac function, even though the efficiency of the therapy was relatively low, reaching up to 32% of muscle cells and the efficiency was even worse in myocardium (MORETTI et al., 2020). To simulate the best possible outcome of such a therapy, with an efficacy of 100% corrected myocytes, we generated the new *DMD*Δ51-52 pig model with a 117 amino acids shortened dystrophin protein. For the clinical classification and the characterization of the new model, we compared the *DMD*Δ51-52 pigs with age-matched animals from the original DMD model (*DMD*Δ52) and unaffected WT. To match the slower progressivity and the later onset of Becker muscular dystrophy, we added, to the 4 months old groups, a comparison of single animals at the higher age of 9 months, corresponding to young adults. Particularly interesting is this comparison, although no statistical relevant group size was used, since the both affected boars, #6790 for the *DMD*Δ52 model and #11914 for the *DMD*Δ51-52, are identical clones, except of the missing exon 51, which restores the reading-frame of the *DMD* gene, in #11914. We could detect a good expression of dystrophin in the skeletal muscle and myocardium of the animals with the restored reading frame (*DMD*Δ51-52), while in the original *DMD*Δ52 model, dystrophin protein could not be detected by immunohistochemistry. To confirm the presence of the whole dystrophin protein, of course except the amino acid sequence corresponding exon 51 and 52, we used two different antibodies (DYS1 and DYS2), of which one was specific for the C-terminus and the other for the Rod-domain of the protein. The neonatal mortality of the nine *DMD*Δ51-52 piglets, born from SCNT, was reduced compared to the *DMD*Δ52 model. For this analysis, only the first 90 days were included, because most of the involved animals were used for tissue collection after this period. The body weight after 3 months was comparable between the WT and the *DMD*Δ51-52

groups, while the mean weight of the *DMD*Δ52 group was reduced. To exclude environmental influences, only animals housed in the new facility (Center for Innovative Medical Models (CiMM)) were included. Creatine kinase activity, the most important diagnostic serum marker for dytrophinopathies, aspartate aminotransferase, troponin I and creatinine were significantly changed in the *DMD*Δ52 model, but normalized in the *DMD*Δ51-52 pigs. The small deviation within the groups for the creatinine serum levels, predestinate this parameter to be used for measuring the therapeutic outcome of future drug trials in the DMD model. In human patients, creatinine could be used to distinguish between Duchenne and Becker and is discussed as potential biomarker for drug trials (WANG et al., 2017). Further the histopathological findings in the skeletal muscle of the 4 months old *DMD*Δ52 pigs were ameliorated in *DMD*Δ51-52, were almost no differences, compared with the WT pigs, were found. Consistently, the pathological alterations of the myocardium of the 9 months old *DMD*Δ52 boar were absent in the age-matched clone of this animal, with the corrected *DMD* reading frame. Consequently, it can be stated that the truncated dystrophin (*DMD*Δ51-52) has a high functionality, despite missing 117 amino acids and thus the exon 51-skipping therapy is a promising approach for treating DMD and could ameliorate the disease symptoms in the patients. However, the patients must be identified and treated early before secondary lesions such as fibrosis or scoliosis of the spine occur. Further the efficacy of the therapy has to be improved, to reach a sufficient number of myocytes. Then about 14% of patients' mutations could be treated with this single exon skipping approach. Especially patients, carrying and out-of-frame deletion of exon 50 or 52 could benefit from this drug, restoring the reading-frame by additional deleting exon 51. However, Young et al. proofed, that even larger deletions, in this case the deletion of exons 45 to 55, are possible, resulting in a still partially functional dystrophin protein, due to absence of only repetitive sequences, the spectrin-like repeats. This approach would be available for about 60% of all DMD patients (YOUNG et al., 2016). However, it has so far only been tested in the murine model and trials in the large animal model are still pending. Our pig model would be ideally suited for this purpose, as it carries the exon 52 deletion, in contrast to the classical GRMD dog model, a mutation that can be treated by this therapy. In addition, we could generate a tailored *DMD*Δ45-55 model that simulates the therapy in order to estimate the success of the therapy.

One limitation of the study is the use of pigs from SCNT, since cloning artifacts could not be excluded. However, the phenotype seen in the cloned *DMD*Δ52 pigs from the first publication (KLYMIUK et al., 2013) could be confirmed by the latest publication (STIRM et al., 2021), where only *DMD*Δ52 pigs were included, which were produced by breeding. Further, at the time of completion of this work, heterozygous *DMD*Δ51-52_het breeding sows are already available to breed future *DMD*Δ51-52 pigs by natural mating or artificial insemination without cloning.

Macroglossia and severe histopathological alterations of the tongue, as they were seen in a spontaneously mutated pig at a Japanese slaughterhouse (AIHARA et al., 2022), but also in various cats with mutations similar to Becker or Duchenne muscular dystrophy (CARPENTER et al., 1989; GASCHEN et al., 1992; HILTON et al., 2023), could not be found, neither in the *DMD*Δ51-52 model, nor in the more severe *DMD*Δ52 model. The investigated tongues had no significant increase in fibrosis or fatty replacements. Further, signs of inflammation were absent. In contrast, all three groups, the two affected and the unaffected WT control group, presented a high proportion of connective tissue in Sirius red stain of tongue tissue and, compared with other skeletal muscles, a high proportion of fat cells within the musculature. A possible explanation for the severe changes in the tongue of the Japanese Case report could be the higher age of the described case report. The affected Japanese pig was 6 months old, compared with the 4 months old *DMD*Δ51-52 and *DMD*Δ52 pigs, which were investigated by us.

In a previous publication, Giemsa staining of *DMD*Δ52 myocardium and skeletal muscle proofed lymphocyte infiltrations in the tissue (STIRM et al., 2021). This inflammation could drive the muscle wasting and thus could be a promising target for experimental drugs. Since our institute has established an efficient pipeline for the generation of tailored genetically modified pig models for preclinical research (KUROME et al., 2006; KUROME et al., 2015), it would be conceivable to generate multiple modified Duchenne pigs in the future to simulate potential therapies. One possibility would be the generation of a double mutant *DMD*Δ52/*NLRP3*$^{-/-}$ pig since the downregulation of the *NLRP3* inflammasome had resulted in *mdx* mice in a significantly improved muscle force and reduced inflammation in the skeletal muscle (DUBUISSON et al., 2022). For this purpose, more research is necessary for the characterization of the inflammation of dystrophic musculature in the future. Additionally, various modifier genes known

from humans and other experimental animals would be suitable for this purpose, such as *LTBP4*, *SPP1* (PASCUAL-MORENA et al., 2021) or *JAG1* (VIEIRA et al., 2015). Both, gene knockouts or overexpression, using tissue specific or ubiquitous promoters, like the CAG promoter (MIYAZAKI et al., 1989), would be feasible.

The new porcine model for BMD showed an unexpectedly mild symptomatology. On the one hand, of course, this illustrates the chances that an exon 51 skipping therapy would have for DMD patients, but on the other hand, it naturally mitigates its areas of application as a model organism for BMD. One explanation for the mild symptoms is the young age of the animals examined. 4-month-old pigs are still in the middle of growth (KUSEC et al., 2008) and thus correspond to subadult human patients. However, many Becker patients show their first symptoms much later, as young adults (BUSHBY & GARDNER-MEDWIN, 1993). Therefore, the 9-month-old animal is of particular interest, as it is already fertile at this age and has already reached about half of its final weight. However, this animal did not show any clear symptoms yet. The young age alone could no longer be held responsible for this. Rather, it could also be due to the location of the mutation in the *DMD* gene, because not all BMD is the same. It is known from human BMD patients that the severity of the symptoms can vary considerably and that there is definitely a connection between the specific mutation and the severity of the disease. The deletion of *DMD* exon 51 and exon 52 are located in the part of the gene, coding for the Rod domain of the dystrophin protein, specific the twentieth spectrin-like repeat (DUAN et al., 2021). Deletion of these two exons results in the loss of 117 amino acids and thus a truncated dystrophin protein. Gao et al. (2015) stated that the dystrophin Rod domain is remarkably tolerant to larger deletions, as long as the deletions do not affect the correct reading-frame (GAO & MCNALLY, 2015), what could be confirmed by our findings in the new *DMD*Δ51-52 porcine model. Furthermore, in our new model, not only the twentieth spectrin-like repeat of the dystrophin protein is influenced by the mutation, but the interspersed hinge 3, too. Carsana et al. (2005) identified the involvement of hinge 3 as crucial for disease severity. In a study, which included 61 BMD patients, the patients without the hinge 3 regions had milder symptoms, compared with these, in which the hinge 3 were intact, even when the deletions were larger, than in the control group with the hinge 3 (CARSANA et al., 2005). The onset of the cardiac involvement is significantly delayed in BMD patients without hinge 3 (median age 43 years), compared with

BMD patients, with deletions of *DMD* exons 45 to 49, which do not affect hinge 3 (mean age 29.5 years), by 13.5 years (KASPAR et al., 2009b). These findings in human patients could explain why the contractility of the hearts were not reduced in our *DMD*Δ51-52 pigs and in general the mild symptomatology. In contrast, the murine and rat models for BMD, in which the mutations do not affect hinge 3, present more severe symptoms (TERAMOTO et al., 2020; HEIER et al., 2023).While Waldrop et al. (2020) described a variating severity of the disease in patients, which carried the same mutation as our porcine model (*DMD*Δ51-52). Some patients presented severe, almost DMD symptoms, while other had only mild or even no symptoms (WALDROP et al., 2020). In contrast, another publication reported only mild symptom in a cohort of BMD patients, which had in-frame deletions, which included exon 51 of the *DMD* gene, comparable to our *DMD*Δ51-52 model (HELDERMAN-VAN DEN ENDEN et al., 2010).

For further analysis of the functionality of the truncated dystrophin protein, it would be enlightening to compare older, adult *DMD*Δ51-52 pigs with WT. However, this takes away the possibility of having a *DMD*Δ52 control group, since many *DMD*Δ52 animals die spontaneously at an age older than four months (STIRM et al., 2021). However, this would show whether the animals at a later time, analogous to the human patients, still develop symptoms, like dilated cardiomyopathy or show signs of muscle wasting in histology.

In a previous publication, we were able to detect cognitive impairments in the DMD piglets, compared with their littermates in the ‘Novel object recognition test’ and the ‘Black and white discrimination test’ (STIRM et al., 2021). This is consistent with the findings in many muscular dystrophy patients (DOORENWEERD et al., 2017). Since the porcine brain morphology has a high correlation to human (SAULEAU et al., 2009), our porcine models are predestinated for further research on histological and molecular levels in the brain phenotype of Duchenne muscular dystrophy and additional of Becker muscular dystrophy.

This work shows, that both the now well-established porcine model for Duchenne muscular dystrophy but also the new generated model for Becker muscular dystrophy are well suited for preclinical research and tissue delivery. Both are easy to produce by breeding of heterozygous carrier sows, presenting only mild disease symptoms, with WT boars. Using estrus synchronization protocols and artificial insemination (AI) with sperm from the same boar, gives us the additional possibility

to work with age-matched, homogeneous groups with a sufficient group size.

VI. ZUSAMMENFASSUNG

Generierung und Charakterisierung eines Schweinemodells für die Becker-Muskeldystrophie

Die Duchenne-Muskeldystrophie (DMD) ist eine neuromuskuläre Erkrankung, die mit einer Frequenz von ungefähr einem aus 5000-6000 neugeborenen Jungen auftritt. Verursacht wird diese Erkrankung durch unterschiedlichste Mutationen im Dystrophin-Gen (*DMD*), die fast ausnahmelos zu einer Leserasterverschiebung und dadurch zu verfrühten STOP-Codons führen, die die Translation des Dystrophinproteins verfrüht beenden. Dies führt zur Abwesenheit des Dystrophins in den Betroffenen. Da dieses jedoch essenziell für die Membranstabilität von Skelettmuskelzellen (Myozyten) und Herzmuskelzellen (Kardiomyozyten) ist, kommt es dadurch folglich zu progressiver Skelettmuskelschwäche und Muskelschäden, ebenso wie zu einem fortschreitenden Versagen der respiratorischen Muskulatur und des Herzens. Neben der DMD ist eine mildere Erkrankung, die Becker-Muskeldystrophie (BMD) bekannt, die deutlich seltener auftritt, mit einer Häufigkeit von ungefähr acht aus 100 000 männlichen Neugeborenen und durch eine, verglichen mit DMD, mildere Symptomatik und langsamere Progressivität charakterisiert ist. Verursacht wird diese mildere Erkrankung gewöhnlich durch Mutationen im *DMD*-Gen, bei denen ein intaktes Leseraster erhalten bleibt, wodurch ein verkürztes und teilweise funktionelles Dystrophin exprimiert wird. Jedoch sind beide Erkrankungen unheilbar und Betroffene können bisher ausschließlich symptomatisch behandelt werden. State-of-the-Art ist weiterhin die Langzeitgabe von Glukokortikoiden, mit sämtlichen Nebenwirkungen. Folglich haben sich in den letzten Jahren viele Forschungsgruppen weltweit mit der Suche nach neuen Behandlungsstrategien, vor allem für die schwerverlaufende DMD, befasst. Der wohl am weitesten verbreitete Ansatz ist das „Exon-skipping“, bei dem meist durch zusätzliche Deletion eines oder mehrerer weiteren Exons des *DMD*-Genes ein intaktes Leseraster hergestellt wird. Im Jahr 2020 wurde von unserer Forschungsgruppe die erfolgreiche *in vivo* Deletion von Exon 51 in unserem *DMD*Δ52-Schweinemodel für DMD veröffentlicht. Dabei wurden, durch virale Vektoren, die Information für das Cas9-Protein, sowie zweier guide RNAs, deren Zielregionen flankierend zu Exon 51 waren, systemisch bzw. lokal in die *DMD*Δ52-Schweine übertragen, wodurch es zu

einer Korrektur des Leserasters in manchen Muskelzellen bzw. Herzmuskelzellen kam und ein verkürztes Dystrophinprotein (*DMD*Δ51-52) exprimiert wurde. Die therapierten Tiere zeigten eine Verbesserung der Symptomatik, obwohl nur ein gewisser Prozentsatz der Zellen erreicht wurde. Um den bestmöglichen Therapieerfolg zu simulieren, haben wir nun ein *DMD*Δ51-52-Schweinemodell generiert, bei dem ausschließlich dieses verkürzte Dystrophinprotein (*DMD*Δ51-52) exprimiert wird, wodurch dieses neue Schweinemodel gleichzeitig auch ein Modell für Becker-Muskeldystrophie darstellt.

Um dieses *DMD*Δ51-52-Schweinemodel zu generieren, wurde eine Nierenzelllinie (Fibroblasten) eines *DMD*Δ52-Schweines verwendet und *DMD* Exon 51, durch einen CRISPR-Cas9-Ansatz, deletiert. Fibroblasten, bei denen Exon 51 korrekt entfernt wurde, wurden anschließend für den Kerntransfer verwendet und die resultierenden Embryonen wurden auf drei Empfängersauen übertragen, wovon zwei Tiere trächtig wurden und insgesamt neun lebende *DMD*Δ51-52-Ferkel geboren wurden. Diese Ferkel zeigten eine reduzierte Sterberate und eine höhere Gewichtszunahme, verglichen mit den Schweinen mit einer Leserastermutation im *DMD*-Gen (*DMD*Δ52). Die korrekte Deletion der beiden Exons 51 und 52 wurde in der cDNA durch PCR und anschließender Gelelektrophorese, sowie Sanger-Sequenzierung, bestätigt. Die Expression des Dystrophinproteins wurde mittels Immunhistochemie nachgewiesen. Anschließend wurde eine Verbesserung der Serumparameter Kreatinkinase, Aspartataminotransferase, Troponin I und Kreatinine festgestellt, die sich bei den *DMD*Δ51-52-Schweinen nicht signifikant von den unveränderten Wildtyp-Schweinen unterschieden. In der histologischen Untersuchung von Skelettmuskel, Herzmuskel und Zunge konnte nur ein signifikanter Anstieg der Muskelfaserquerschnitte mit einem zentralen Zellkern, verglichen mit den WT-Tieren, festgestellt werden. Die *DMD*Δ52-Tiere zeigten dagegen erheblich Abweichungen in der Skelettmuskelmorphologie, bereits mit 4 Monaten. Auffallend waren dabei, neben den heterogenen Muskelfaser-durchmessern, dem hohen Anteil an Muskelfaserzellen mit zentralem Kern und einer Zunahme der Fibrose, auch ein hoher Anteil an sich regenerierenden und untergehenden Muskelzellen. Im Myokardium waren im Alter von 4 Monaten noch keine deutlichen Veränderungen zu sehen, jedoch war das Myokard beim 9 Monate alten *DMD*Δ52-Schwein erheblich verändert, im Vergleich zum *DMD*Δ51-52- und WT-Schwein. Allerdings zeigten die jüngeren *DMD*Δ52-Tiere bereits eine

erheblich eingeschränkte Herzfunktion, namentlich eine reduzierte Auswurfleistung (left ventricular ejection fraction) und eine reduzierte Kontraktilität (left ventricular fractional shortening), während beide Parameter bei den altersgleichen *DMD*Δ51-52-Schweinen unverändert waren. Die histologischen Veränderungen, die in der Skelettmuskulatur des Triceps brachii gefunden wurden und ebenfalls für die Zungenmuskulatur beschrieben sind, konnten in vier Monate alten *DMD*Δ51-52- und *DMD*Δ52-Schweinen nicht betätigt werden.

Zwei der generierten *DMD*Δ51-52-Tiere wurden bis zur Geschlechtsreife aufgezogen und für die Zucht verwendet. Die Nachkommen der F0-Tiere werden in Zukunft für die Produktion weiterer *DMD*Δ51-52-Ferkel verwendet werden.

Mit dieser Arbeit konnte gezeigt werden, dass das verkürzte *DMD*Δ51-52-Dystrophin hochfunktional ist und den klinischen Phänotyp, den man in altersgleichen *DMD*Δ52-Schweinen findet, deutlich abmildern kann. Somit stellt die „Exon skipping-Therapie“ einen vielversprechenden Ansatz für die DMD dar, da dadurch die DMD in den Patienten in eine mildere BMD umgewandelt werden kann, die eine Verbesserung der Symptomatik verspricht.

VII. SUMMARY

Generation and characterization of a porcine model for Becker muscular dystrophy

Duchenne muscular dystrophy (DMD) is a neuromuscular disease that occurs with a frequency of approximately one in 5000-6000 newborn boys. This disease is caused by a wide variety of mutations in the dystrophin gene (*DMD*), which almost invariably lead to a reading frame shift and thus to premature STOP codons that prematurely terminate translation of the dystrophin protein. This leads to the absence of the dystrophin protein in affected individuals and consequently to progressive skeletal muscle weakness and muscle damage, as well as progressive respiratory and cardiac failure, as the dystrophin protein is essential for the membrane stability of skeletal muscle cells (myocytes) and cardiac muscle cells (cardiomyocytes). In addition to DMD, there is a milder disease known as Becker muscular dystrophy (BMD), which is less common, occurring in about eight out of every 100,000 newborn males, and is characterized by milder symptoms and slower progression compared to DMD. This milder disease is usually caused by mutations in the *DMD* gene that do not affect the correct reading frame, resulting in the expression of a shortened and thus partially functional dystrophin protein. Both diseases are incurable and those affected can so far only be treated symptomatically. The state-of-the-art treatment is still the long-term administration of glucocorticoids, with all the side effects. Consequently, in recent years, many research groups worldwide have been engaged in the search for a drug, especially for severe DMD. Probably the most widely used approach is "exon-skipping", which restores the correct reading frame by deleting one or more additional exons of the *DMD* gene. In 2020, our research group published the successful in vivo deletion of exon 51 in our porcine *DMD*Δ52 model for DMD. The information for the Cas9 protein, as well as two guide RNAs whose target regions were flanking exon 51, were transferred systemically or locally into the *DMD*Δ52 pigs by viral vectors, resulting in a correction of the reading frame in some muscle cells and cardiac muscle cells, respectively, and the expression of a shortened dystrophin protein (*DMD*Δ51-52). The treated animals showed an amelioration of the symptoms, although only a certain percentage of cells were reached. In order to simulate the best possible therapeutic success, we have now generated a *DMD*Δ51-

52 pig model in which only this truncated dystrophin protein (*DMD*Δ51-52) is expressed, making this new pig model also a model for Becker muscular dystrophy.

To generate this *DMD*Δ51-52 pig model, a kidney cell line (fibroblasts) from a *DMD*Δ52 pig was used and *DMD* exon 51was selective deleted through a CRISPR-Cas9 approach. Fibroblasts in which exon 51 was correctly deleted were then used for nuclear transfer and the resulting embryos were transferred to three recipient sows, two of which became pregnant and gave birth to a total of nine live *DMD*Δ51-52 piglets. These piglets showed a reduced mortality rate and higher weight gain compared to the pigs with a reading frame mutation in the *DMD* gene (*DMD*Δ52). The correct deletion of both exons 51 and 52 was confirmed in the cDNA by PCR followed by gel electrophoresis, and Sanger sequencing. Expression of the dystrophin protein was detected by immunohistochemistry. Subsequently, serum parameters creatine kinase, aspartate aminotransferase, troponin I and creatinine were found to be improved and not significantly different in the *DMD*Δ51-52 pigs compared to the unaffected wild-type pigs (WT). In the histological examination of skeletal muscle, cardiac muscle and tongue, only a significant increase in muscle fiber cross-sections with a central nuclei, compared to the WT animals, was detected. The *DMD*Δ52 animals, on the other hand, showed considerable deviations in skeletal muscle morphology, already at 4 months of age. In addition to the heterogeneous muscle fiber diameters, the high proportion of muscle fiber cells with a central nuclei, an increase in fibrosis and a high proportion of regenerating and necrotic muscle cells were noticeable. No distinct changes were yet seen in the myocardium at 4 months of age, but the myocardium was significantly altered in the 9-month-old *DMD*Δ52 pig, compared to the *DMD*Δ51-52 and WT pigs. However, the younger *DMD*Δ52 animals already showed significantly impaired cardiac function, namely reduced ejection fraction (left ventricular ejection fraction) and reduced contractility (left ventricular fractional shortening), whereas both parameters were unchanged in the age-matched *DMD*Δ51-52 pigs. The histological changes found in the skeletal muscles of the triceps brachii and also described for the tongue musculature could not be confirmed in four-month-old *DMD*Δ51-52 and *DMD*Δ52 pigs.

Two of the generated *DMD*Δ51-52 animals were reared to sexual maturity and used for breeding. The offspring of the F0 animals will be used for the production of further *DMD*Δ51-52 piglets in the future by breeding.

This work has demonstrated that the truncated *DMD*Δ51-52 dystrophin is highly functional and can significantly attenuate the clinical phenotype found in age-matched *DMD*Δ52 pigs. Thus, exon-skipping therapy represents a promising approach to DMD, as it can convert DMD in patients to a milder BMD that promises to attenuate symptoms.

VIII. INDEX OF FIGURES

IX. REFERENCES

Aartsma-Rus A, Van Deutekom JC, Fokkema IF, Van Ommen GJ, Den Dunnen JT. Entries in the Leiden Duchenne muscular dystrophy mutation database: an overview of mutation types and paradoxical cases that confirm the reading-frame rule. Muscle Nerve 2006; 34: 135-44.

Aartsma-Rus A, Ginjaar IB, Bushby K. The importance of genetic diagnosis for Duchenne muscular dystrophy. J Med Genet 2016; 53: 145-51.

Aartsma-Rus A, Arechavala-Gomeza V. Why dystrophin quantification is key in the eteplirsen saga. Nat Rev Neurol 2018; 14: 454-6.

Aihara N, Kuroki S, Inamuro R, Kamiya Y, Shiga T, Kikuchihara Y, Ohmori E, Noguchi M, Kamiie J. Macroglossia in a pig diagnosed as Becker muscular dystrophy due to dystrophin pseudoexon insertion derived from intron 26. Vet Pathol 2022: 3009858221079669.

Amoasii L, Hildyard JCW, Li H, Sanchez-Ortiz E, Mireault A, Caballero D, Harron R, Stathopoulou TR, Massey C, Shelton JM, Bassel-Duby R, Piercy RJ, Olson EN. Gene editing restores dystrophin expression in a canine model of Duchenne muscular dystrophy. Science 2018; 362: 86-91.

Angelini C, Marozzo R, Pegoraro V. Current and emerging therapies in Becker muscular dystrophy (BMD). Acta Myol 2019; 38: 172-9.

Anthony K, Cirak S, Torelli S, Tasca G, Feng L, Arechavala-Gomeza V, Armaroli A, Guglieri M, Straathof CS, Verschuuren JJ, Aartsma-Rus A, Helderman-van den Enden P, Bushby K, Straub V, Sewry C, Ferlini A, Ricci E, Morgan JE, Muntoni F. Dystrophin quantification and clinical correlations in Becker muscular dystrophy: implications for clinical trials. Brain 2011; 134: 3547-59.

Araki E, Nakamura K, Nakao K, Kameya S, Kobayashi O, Nonaka I, Kobayashi T, Katsuki M. Targeted disruption of exon 52 in the mouse dystrophin gene induced muscle degeneration similar to that observed in Duchenne muscular dystrophy. Biochem Biophys Res Commun 1997; 238: 492-7.

Archer JE, Gardner AC, Roper HP, Chikermane AA, Tatman AJ. Duchenne muscular dystrophy: the management of scoliosis. J Spine Surg 2016; 2: 185-94.

Atencia-Fernandez S, Shiel RE, Mooney CT, Nolan CM. Muscular dystrophy in the Japanese Spitz: an inversion disrupts the DMD and RPGR genes. Anim Genet 2015; 46: 175-84.

Baroncelli AB, Abellonio F, Pagano TB, Esposito I, Peirone B, Papparella S, Paciello O. Muscular dystrophy in a dog resembling human becker muscular dystrophy. J Comp Pathol 2014; 150: 429-33.

Barthelemy I, Calmels N, Weiss RB, Tiret L, Vulin A, Wein N, Peccate C, Drougard C, Beroud C, Deburgrave N, Thibaud JL, Escriou C, Punzon I, Garcia L, Kaplan JC, Flanigan KM, Leturcq F, Blot S. X-linked muscular dystrophy in a Labrador Retriever strain: phenotypic and molecular characterisation. Skelet Muscle 2020; 10: 23.

Beggs AH, Koenig M, Boyce FM, Kunkel LM. Detection of 98% of DMD/BMD gene deletions by polymerase chain reaction. Hum Genet 1990; 86: 45-8.

Birnkrant DJ, Bushby K, Bann CM, Apkon SD, Blackwell A, Brumbaugh D, Case LE, Clemens PR, Hadjiyannakis S, Pandya S, Street N, Tomezsko J, Wagner KR, Ward LM, Weber DR, Group DMDCCW. Diagnosis and management of Duchenne muscular dystrophy, part 1: diagnosis, and neuromuscular, rehabilitation, endocrine, and gastrointestinal and nutritional management. Lancet Neurol 2018; 17: 251-67.

Bladen CL, Salgado D, Monges S, Foncuberta ME, Kekou K, Kosma K, Dawkins H, Lamont L, Roy AJ, Chamova T, Guergueltcheva V, Chan S, Korngut L,

Campbell C, Dai Y, Wang J, Barisic N, Brabec P, Lahdetie J, Walter MC, Schreiber-Katz O, Karcagi V, Garami M, Viswanathan V, Bayat F, Buccella F, Kimura E, Koeks Z, van den Bergen JC, Rodrigues M, Roxburgh R, Lusakowska A, Kostera-Pruszczyk A, Zimowski J, Santos R, Neagu E, Artemieva S, Rasic VM, Vojinovic D, Posada M, Bloetzer C, Jeannet PY, Joncourt F, Diaz-Manera J, Gallardo E, Karaduman AA, Topaloglu H, El Sherif R, Stringer A, Shatillo AV, Martin AS, Peay HL, Bellgard MI, Kirschner J, Flanigan KM, Straub V, Bushby K, Verschuuren J, Aartsma-Rus A, Beroud C, Lochmuller H. The TREAT-NMD DMD Global Database: analysis of more than 7,000 Duchenne muscular dystrophy mutations. Hum Mutat 2015; 36: 395-402.

Bulfield G, Siller WG, Wight PA, Moore KJ. X chromosome-linked muscular dystrophy (mdx) in the mouse. Proc Natl Acad Sci U S A 1984; 81: 1189-92.

Bushby K, Muntoni F, Bourke JP. 107th ENMC international workshop: the management of cardiac involvement in muscular dystrophy and myotonic dystrophy. 7th-9th June 2002, Naarden, the Netherlands. Neuromuscul Disord 2003; 13: 166-72.

Bushby KM, Gardner-Medwin D. The clinical, genetic and dystrophin characteristics of Becker muscular dystrophy. I. Natural history. J Neurol 1993; 240: 98-104.

Carpenter JL, Hoffman EP, Romanul FC, Kunkel LM, Rosales RK, Ma NS, Dasbach JJ, Rae JF, Moore FM, McAfee MB, et al. Feline muscular dystrophy with dystrophin deficiency. Am J Pathol 1989; 135: 909-19.

Carsana A, Frisso G, Tremolaterra MR, Lanzillo R, Vitale DF, Santoro L, Salvatore F. Analysis of dystrophin gene deletions indicates that the hinge III region of the protein correlates with disease severity. Ann Hum Genet 2005; 69: 253-9.

Chen JJ, Cao BY, Su C, Liu M, Wu D, Li WJ, Gong CX. A Chinese girl with Turner syndrome and Duchenne muscular dystrophy: diagnosis and management of this "dual diagnosis". Chin Med J (Engl) 2020; 134: 743-5.

Ciafaloni E, Fox DJ, Pandya S, Westfield CP, Puzhankara S, Romitti PA, Mathews KD, Miller TM, Matthews DJ, Miller LA, Cunniff C, Druschel CM, Moxley RT. Delayed diagnosis in duchenne muscular dystrophy: data from the Muscular Dystrophy Surveillance, Tracking, and Research Network (MD STARnet). J Pediatr 2009; 155: 380-5.

Clemens PR, Niizawa G, Feng J, Florence J, D'Alessandro AS, Morgenroth LP, Gorni K, Guglieri M, Connolly A, Wicklund M, Bertorini T, Mah JK, Thangarajh M, Smith E, Kuntz N, McDonald CM, Henricson EK, Upadhyayula S, Byrne B, Manousakis G, Harper A, Bravver E, Iannaccone S, Spurney C, Cnaan A, Gordish-Dressman H, Investigators CB. The CINRG Becker Natural History Study: Baseline characteristics. Muscle Nerve 2020; 62: 369-76.

Clemens PR, Rao VK, Connolly AM, Harper AD, Mah JK, McDonald CM, Smith EC, Zaidman CM, Nakagawa T, Investigators CD, Hoffman EP. Long-Term Functional Efficacy and Safety of Viltolarsen in Patients with Duchenne Muscular Dystrophy. J Neuromuscul Dis 2022; 9: 493-501.

Cohen N, Muntoni F. Multiple pathogenetic mechanisms in X linked dilated cardiomyopathy. Heart 2004; 90: 835-41.

Connuck DM, Sleeper LA, Colan SD, Cox GF, Towbin JA, Lowe AM, Wilkinson JD, Orav EJ, Cuniberti L, Salbert BA, Lipshultz SE, Pediatric Cardiomyopathy Registry Study G. Characteristics and outcomes of cardiomyopathy in children with Duchenne or Becker muscular dystrophy: a comparative study from the Pediatric Cardiomyopathy Registry. Am Heart J 2008; 155: 998-1005.

Davis J, Samuels E, Mullins L. Nutrition Considerations in Duchenne Muscular Dystrophy. Nutr Clin Pract 2015; 30: 511-21.

De Wel B, Willaert S, Nadaj-Pakleza A, Aube-Nathier AC, Testelmans D, Buyse B, Claeys KG. Respiratory decline in adult patients with Becker muscular dystrophy: A longitudinal study. Neuromuscul Disord 2021; 31: 174-82.

Deconinck AE, Rafael JA, Skinner JA, Brown SC, Potter AC, Metzinger L, Watt DJ, Dickson JG, Tinsley JM, Davies KE. Utrophin-dystrophin-deficient mice as a model for Duchenne muscular dystrophy. Cell 1997; 90: 717-27.

Doorenweerd N, Mahfouz A, van Putten M, Kaliyaperumal R, PAC TH, Hendriksen JGM, Aartsma-Rus AM, Verschuuren J, Niks EH, Reinders MJT, Kan HE, Lelieveldt BPF. Timing and localization of human dystrophin isoform expression provide insights into the cognitive phenotype of Duchenne muscular dystrophy. Sci Rep 2017; 7: 12575.

Duan D. Duchenne muscular dystrophy gene therapy in the canine model. Hum Gene Ther Clin Dev 2015; 26: 57-69.

Duan D. Systemic AAV Micro-dystrophin Gene Therapy for Duchenne Muscular Dystrophy. Mol Ther 2018; 26: 2337-56.

Duan D, Goemans N, Takeda S, Mercuri E, Aartsma-Rus A. Duchenne muscular dystrophy. Nat Rev Dis Primers 2021; 7: 13.

Dubuisson N, Davis-López de Carrizosa MA, Versele R, Selvais CM, Noel L, Van den Bergh PYD, Brichard SM, Abou-Samra M. Inhibiting the inflammasome with MCC950 counteracts muscle pyroptosis and improves Duchenne muscular dystrophy. Frontiers in Immunology 2022; 13

Echigoya Y, Trieu N, Duddy W, Moulton HM, Yin H, Partridge TA, Hoffman EP, Kornegay JN, Rohret FA, Rogers CS, Yokota T. A Dystrophin Exon-52 Deleted Miniature Pig Model of Duchenne Muscular Dystrophy and Evaluation of Exon Skipping. International Journal of Molecular Sciences 2021; 22

Finder JD, Birnkrant D, Carl J, Farber HJ, Gozal D, Iannaccone ST, Kovesi T, Kravitz RM, Panitch H, Schramm C, Schroth M, Sharma G, Sievers L, Silvestri JM, Sterni L, American Thoracic S. Respiratory care of the patient with Duchenne muscular dystrophy: ATS consensus statement. Am J Respir Crit Care Med 2004; 170: 456-65.

Flanigan KM, Dunn DM, von Niederhausern A, Soltanzadeh P, Gappmaier E, Howard MT, Sampson JB, Mendell JR, Wall C, King WM, Pestronk A, Florence JM, Connolly AM, Mathews KD, Stephan CM, Laubenthal KS, Wong BL, Morehart PJ, Meyer A, Finkel RS, Bonnemann CG, Medne L, Day JW, Dalton JC, Margolis MK, Hinton VJ, United Dystrophinopathy Project C, Weiss RB. Mutational spectrum of DMD mutations in dystrophinopathy patients: application of modern diagnostic techniques to a large cohort. Hum Mutat 2009; 30: 1657-66.

Frank DE, Schnell FJ, Akana C, El-Husayni SH, Desjardins CA, Morgan J, Charleston JS, Sardone V, Domingos J, Dickson G, Straub V, Guglieri M, Mercuri E, Servais L, Muntoni F, Group S-NS. Increased dystrophin production with golodirsen in patients with Duchenne muscular dystrophy. Neurology 2020; 94: e2270-e82.

Frohlich T, Kemter E, Flenkenthaler F, Klymiuk N, Otte KA, Blutke A, Krause S, Walter MC, Wanke R, Wolf E, Arnold GJ. Progressive muscle proteome changes in a clinically relevant pig model of Duchenne muscular dystrophy. Sci Rep 2016; 6: 33362.

Fujii K, Minami N, Hayashi Y, Nishino I, Nonaka I, Tanabe Y, Takanashi J, Kohno Y. Homozygous female Becker muscular dystrophy. Am J Med Genet A 2009; 149A: 1052-5.

Gao QQ, McNally EM. The Dystrophin Complex: Structure, Function, and Implications for Therapy. Compr Physiol 2015; 5: 1223-39.

Gaschen FP, Hoffman EP, Gorospe JR, Uhl EW, Senior DF, Cardinet GH, 3rd, Pearce LK. Dystrophin deficiency causes lethal muscle hypertrophy in cats. J Neurol Sci 1992; 110: 149-59.

Gasiunas G, Barrangou R, Horvath P, Siksnys V. Cas9-crRNA ribonucleoprotein complex mediates specific DNA cleavage for adaptive immunity in bacteria. Proc Natl Acad Sci U S A 2012; 109: E2579-86.

Grain L, Cortina-Borja M, Forfar C, Hilton-Jones D, Hopkin J, Burch M. Cardiac abnormalities and skeletal muscle weakness in carriers of Duchenne and Becker muscular dystrophies and controls. Neuromuscul Disord 2001; 11: 186-91.

Hartnett MJ, Lloyd-Puryear MA, Tavakoli NP, Wynn J, Koval-Burt CL, Gruber D, Trotter T, Caggana M, Chung WK, Armstrong N, Brower AM. Newborn Screening for Duchenne Muscular Dystrophy: First Year Results of a Population-Based Pilot. Int J Neonatal Screen 2022; 8

Heier CR, McCormack NM, Tully CB, Novak JS, Newell-Stamper BL, Russell AJ, Fiorillo AA. The X-linked Becker muscular dystrophy (bmx) mouse models Becker muscular dystrophy via deletion of murine dystrophin exons 45-47. J Cachexia Sarcopenia Muscle 2023;

Helderman-van den Enden AT, Straathof CS, Aartsma-Rus A, den Dunnen JT, Verbist BM, Bakker E, Verschuuren JJ, Ginjaar HB. Becker muscular dystrophy patients with deletions around exon 51; a promising outlook for exon skipping therapy in Duchenne patients. Neuromuscul Disord 2010; 20: 251-4.

Hilton S, Christen M, Bilzer T, Jagannathan V, Leeb T, Giger U. Dystrophin (DMD) Missense Variant in Cats with Becker-Type Muscular Dystrophy. Int J Mol Sci 2023; 24

Hoffman EP, Brown RH, Jr., Kunkel LM. Dystrophin: the protein product of the Duchenne muscular dystrophy locus. Cell 1987; 51: 919-28.

Hollinger K, Yang CX, Montz RE, Nonneman D, Ross JW, Selsby JT. Dystrophin insufficiency causes selective muscle histopathology and loss of dystrophin-glycoprotein complex assembly in pig skeletal muscle. FASEB J 2014; 28: 1600-9.

Horiuchi N, Aihara N, Mizutani H, Kousaka S, Nagafuchi T, Ochiai M, Ochiai K, Kobayashi Y, Furuoka H, Asai T, Oishi K. Becker muscular dystrophy-like myopathy regarded as so-called "fatty muscular dystrophy" in a pig: a case report and its diagnostic method. J Vet Med Sci 2014; 76: 243-8.

Iff J, Gerrits C, Zhong Y, Tuttle E, Birk E, Zheng Y, Paul X, Henricson EK, McDonald CM, Investigators C-D. Delays in pulmonary decline in eteplirsen-treated patients with Duchenne muscular dystrophy. Muscle Nerve 2022; 66: 262-9.

Janssen PM, Biesiadecki BJ, Ziolo MT, Davis JP. The Need for Speed: Mice, Men, and Myocardial Kinetic Reserve. Circ Res 2016; 119: 418-21.

Jeandel A, Garosi LS, Davies L, Guo LT, Salguero R, Shelton GD. Late-onset Becker-type muscular dystrophy in a Border terrier dog. J Small Anim Pract 2019; 60: 514-7.

Jinek M, Chylinski K, Fonfara I, Hauer M, Doudna JA, Charpentier E. A programmable dual-RNA-guided DNA endonuclease in adaptive bacterial immunity. Science 2012; 337: 816-21.

Jones BR, Brennan S, Mooney CT, Callanan JJ, McAllister H, Guo LT, Martin PT, Engvall E, Shelton GD. Muscular dystrophy with truncated dystrophin in a family of Japanese Spitz dogs. J Neurol Sci 2004; 217: 143-9.

Kajimoto H, Ishigaki K, Okumura K, Tomimatsu H, Nakazawa M, Saito K, Osawa M, Nakanishi T. Beta-blocker therapy for cardiac dysfunction in patients with muscular dystrophy. Circ J 2006; 70: 991-4.

Kamdar F, Garry DJ. Dystrophin-Deficient Cardiomyopathy. J Am Coll Cardiol 2016; 67: 2533-46.

Kaspar RW, Allen HD, Montanaro F. Current understanding and management of dilated cardiomyopathy in Duchenne and Becker muscular dystrophy. J Am Acad Nurse Pract 2009a; 21: 241-9.

Kaspar RW, Allen HD, Ray WC, Alvarez CE, Kissel JT, Pestronk A, Weiss RB, Flanigan KM, Mendell JR, Montanaro F. Analysis of dystrophin deletion mutations predicts age of cardiomyopathy onset in becker muscular dystrophy. Circ Cardiovasc Genet 2009b; 2: 544-51.

Klymiuk N, Blutke A, Graf A, Krause S, Burkhardt K, Wuensch A, Krebs S, Kessler B, Zakhartchenko V, Kurome M, Kemter E, Nagashima H, Schoser B, Herbach N, Blum H, Wanke R, Aartsma-Rus A, Thirion C, Lochmuller H, Walter MC, Wolf E. Dystrophin-deficient pigs provide new insights into the hierarchy of physiological derangements of dystrophic muscle. Hum Mol Genet 2013; 22: 4368-82.

Kornegay JN, Bogan JR, Bogan DJ, Childers MK, Li J, Nghiem P, Detwiler DA, Larsen CA, Grange RW, Bhavaraju-Sanka RK, Tou S, Keene BP, Howard JF, Jr., Wang J, Fan Z, Schatzberg SJ, Styner MA, Flanigan KM, Xiao X, Hoffman EP. Canine models of Duchenne muscular dystrophy and their use in therapeutic strategies. Mamm Genome 2012; 23: 85-108.

Kornegay JN. The golden retriever model of Duchenne muscular dystrophy. Skelet Muscle 2017; 7: 9.

Kurome M, Ueda H, Tomii R, Naruse K, Nagashima H. Production of transgenic-clone pigs by the combination of ICSI-mediated gene transfer with somatic cell nuclear transfer. Transgenic Res 2006; 15: 229-40.

Kurome M, Kessler B, Wuensch A, Nagashima H, Wolf E. Nuclear transfer and transgenesis in the pig. Methods Mol Biol 2015; 1222: 37-59.

Kusec G, Kralik G, Djurkin I, Baulain U, Kallweit E. Optimal slaughter weight of pigs assessed by means of the asymmetric S-curve. Czech Journal of Animal Science 2008; 53: 98-105.

Landfeldt E, Thompson R, Sejersen T, McMillan HJ, Kirschner J, Lochmuller H. Life expectancy at birth in Duchenne muscular dystrophy: a systematic review and meta-analysis. Eur J Epidemiol 2020; 35: 643-53.

Larcher T, Lafoux A, Tesson L, Remy S, Thepenier V, Francois V, Le Guiner C, Goubin H, Dutilleul M, Guigand L, Toumaniantz G, De Cian A, Boix C, Renaud JB, Cherel Y, Giovannangeli C, Concordet JP, Anegon I, Huchet C. Characterization of dystrophin deficient rats: a new model for Duchenne muscular dystrophy. PLoS One 2014; 9: e110371.

Lebel DE, Corston JA, McAdam LC, Biggar WD, Alman BA. Glucocorticoid treatment for the prevention of scoliosis in children with Duchenne muscular dystrophy: long-term follow-up. J Bone Joint Surg Am 2013; 95: 1057-61.

Lee T, Takeshima Y, Kusunoki N, Awano H, Yagi M, Matsuo M, Iijima K. Differences in carrier frequency between mothers of Duchenne and Becker muscular dystrophy patients. J Hum Genet 2014; 59: 46-50.

Long C, McAnally JR, Shelton JM, Mireault AA, Bassel-Duby R, Olson EN. Prevention of muscular dystrophy in mice by CRISPR/Cas9-mediated editing of germline DNA. Science 2014; 345: 1184-8.

Long C, Amoasii L, Mireault AA, McAnally JR, Li H, Sanchez-Ortiz E, Bhattacharyya S, Shelton JM, Bassel-Duby R, Olson EN. Postnatal genome editing partially restores dystrophin expression in a mouse model of muscular dystrophy. Science 2016; 351: 400-3.

Lynch GS, Hinkle RT, Chamberlain JS, Brooks SV, Faulkner JA. Force and power output of fast and slow skeletal muscles from mdx mice 6-28 months old. J Physiol 2001; 535: 591-600.

Mah JK, Korngut L, Dykeman J, Day L, Pringsheim T, Jette N. A systematic review and meta-analysis on the epidemiology of Duchenne and Becker muscular dystrophy. Neuromuscul Disord 2014; 24: 482-91.

Matsunari H, Watanabe M, Nakano K, Enosawa S, Umeyama K, Uchikura A, Yashima S, Fukuda T, Klymiuk N, Kurome M, Kessler B, Wuensch A, Zakhartchenko V, Wolf E, Hanazono Y, Nagaya M, Umezawa A, Nakauchi H, Nagashima H. Modeling lethal X-linked genetic disorders in pigs with ensured fertility. Proc Natl Acad Sci U S A 2018; 115: 708-13.

McGreevy JW, Hakim CH, McIntosh MA, Duan D. Animal models of Duchenne muscular dystrophy: from basic mechanisms to gene therapy. Dis Model Mech 2015; 8: 195-213.

Melacini P, Fanin M, Danieli GA, Villanova C, Martinello F, Miorin M, Freda MP, Miorelli M, Mostacciuolo ML, Fasoli G, Angelini C, Dalla Volta S. Myocardial involvement is very frequent among patients affected with subclinical Becker's muscular dystrophy. Circulation 1996; 94: 3168-75.

Mercuri E, Bonnemann CG, Muntoni F. Muscular dystrophies. Lancet 2019; 394: 2025-38.

Miyazaki J, Takaki S, Araki K, Tashiro F, Tominaga A, Takatsu K, Yamamura K. Expression vector system based on the chicken beta-actin promoter directs efficient production of interleukin-5. Gene 1989; 79: 269-77.

Monaco AP, Bertelson CJ, Liechti-Gallati S, Moser H, Kunkel LM. An Explanation for the Phenotypic Differences between Patients Bearing Partial Deletions of the DMD Locus. Genomics 1988; 2: 90-5.

Moretti A, Fonteyne L, Giesert F, Hoppmann P, Meier AB, Bozoglu T, Baehr A, Schneider CM, Sinnecker D, Klett K, Frohlich T, Rahman FA, Haufe T, Sun S, Jurisch V, Kessler B, Hinkel R, Dirschinger R, Martens E, Jilek C, Graf A, Krebs S, Santamaria G, Kurome M, Zakhartchenko V, Campbell B, Voelse K, Wolf A,

Ziegler T, Reichert S, Lee S, Flenkenthaler F, Dorn T, Jeremias I, Blum H, Dendorfer A, Schnieke A, Krause S, Walter MC, Klymiuk N, Laugwitz KL, Wolf E, Wurst W, Kupatt C. Somatic gene editing ameliorates skeletal and cardiac muscle failure in pig and human models of Duchenne muscular dystrophy. Nat Med 2020; 26: 207-14.

Mostacciuolo ML, Miorin M, Pegoraro E, Fanin M, Schiavon F, Vitiello L, Saad FA, Angelini C, Danieli GA. Reappraisal of the incidence rate of Duchenne and Becker muscular dystrophies on the basis of molecular diagnosis. Neuroepidemiology 1993; 12: 326-30.

Moxley RT, 3rd, Pandya S, Ciafaloni E, Fox DJ, Campbell K. Change in natural history of Duchenne muscular dystrophy with long-term corticosteroid treatment: implications for management. J Child Neurol 2010; 25: 1116-29.

Muntoni F, Torelli S, Ferlini A. Dystrophin and mutations: one gene, several proteins, multiple phenotypes. Lancet Neurol 2003; 2: 731-40.

Naidoo M, Anthony K. Dystrophin Dp71 and the Neuropathophysiology of Duchenne Muscular Dystrophy. Mol Neurobiol 2020; 57: 1748-67.

Nakamura K, Fujii W, Tsuboi M, Tanihata J, Teramoto N, Takeuchi S, Naito K, Yamanouchi K, Nishihara M. Generation of muscular dystrophy model rats with a CRISPR/Cas system. Sci Rep 2014; 4: 5635.

Nanchen D. Resting heart rate: what is normal? Heart 2018; 104: 1048-9.

Nascimento Osorio A, Medina Cantillo J, Camacho Salas A, Madruga Garrido M, Vilchez Padilla JJ. Consensus on the diagnosis, treatment and follow-up of patients with Duchenne muscular dystrophy. Neurología (English Edition) 2019; 34: 469-81.

Nelson CE, Hakim CH, Ousterout DG, Thakore PI, Moreb EA, Castellanos Rivera RM, Madhavan S, Pan X, Ran FA, Yan WX, Asokan A, Zhang F, Duan D, Gersbach CA. In vivo genome editing improves muscle function in a mouse model of Duchenne muscular dystrophy. Science 2016; 351: 403-7.

Nonneman DJ, Brown-Brandl T, Jones SA, Wiedmann RT, Rohrer GA. A defect in dystrophin causes a novel porcine stress syndrome. BMC Genomics 2012; 13: 233.

Oh HJ, Chung E, Kim J, Kim MJ, Kim GA, Lee SH, Ra K, Eom K, Park S, Chae JH, Kim JS, Lee BC. Generation of a Dystrophin Mutant in Dog by Nuclear Transfer Using CRISPR/Cas9-Mediated Somatic Cells: A Preliminary Study. Int J Mol Sci 2022; 23

Okizuka Y, Takeshima Y, Awano H, Zhang Z, Yagi M, Matsuo M. Small mutations detected by multiplex ligation-dependent probe amplification of the dystrophin gene. Genet Test Mol Biomarkers 2009; 13: 427-31.

Partridge TA. The mdx mouse model as a surrogate for Duchenne muscular dystrophy. FEBS J 2013; 280: 4177-86.

Pascual-Morena C, Cavero-Redondo I, Saz-Lara A, Sequi-Dominguez I, Luceron-Lucas-Torres M, Martinez-Vizcaino V. Genetic Modifiers and Phenotype of Duchenne Muscular Dystrophy: A Systematic Review and Meta-Analysis. Pharmaceuticals (Basel) 2021; 14

Prigojin H, Brusel M, Fuchs O, Shomrat R, Legum C, Nudel U, Yaffe D. Detection of Duchenne muscular dystrophy gene products in amniotic fluid and chorionic villus sampling cells. FEBS Lett 1993; 335: 223-30.

Quan F, Janas J, Toth-Fejel S, Johnson DB, Wolford JK, Popovich BW. Uniparental disomy of the entire X chromosome in a female with Duchenne muscular dystrophy. Am J Hum Genet 1997; 60: 160-5.

Regensburger AP, Fonteyne LM, Jüngert J, Wagner AL, Gerhalter T, Nagel AM, Heiss R, Flenkenthaler F, Qurashi M, Neurath MF, Klymiuk N, Kemter E, Fröhlich T, Uder M, Woelfle J, Rascher W, Trollmann R, Wolf E, Waldner MJ, Knieling F. Detection of collagens by multispectral optoacoustic tomography as an imaging biomarker for Duchenne muscular dystrophy. Nature Medicine 2019; 25: 1905-15.

Ryder S, Leadley RM, Armstrong N, Westwood M, de Kock S, Butt T, Jain M, Kleijnen J. The burden, epidemiology, costs and treatment for Duchenne muscular dystrophy: an evidence review. Orphanet J Rare Dis 2017; 12: 79.

Sauleau P, Lapouble E, Val-Laillet D, Malbert CH. The pig model in brain imaging and neurosurgery. Animal 2009; 3: 1138-51.

Schwarz L, Schoner C, Brunthaler R, Weissenbock H, Bernreiter-Hofer T, Wallner B, Ladinig A. Investigations on the occurrence of a muscular disorder in Austrian slaughter pigs. Porcine Health Manag 2021; 7: 51.

Selsby JT, Ross JW, Nonneman D, Hollinger K. Porcine models of muscular dystrophy. ILAR J 2015; 56: 116-26.

Sicinski P, Geng Y, Ryder-Cook AS, Barnard EA, Darlison MG, Barnard PJ. The molecular basis of muscular dystrophy in the mdx mouse: a point mutation. Science 1989; 244: 1578-80.

Stalens C, Motte L, Behin A, Ben Yaou R, Leturcq F, Bassez G, Laforet P, Fontaine B, Ederhy S, Masingue M, Saadi M, Louis SL, Berber N, Stojkovic T, Duboc D, Wahbi K. Improved Cardiac Outcomes by Early Treatment with Angiotensin-Converting Enzyme Inhibitors in Becker Muscular Dystrophy. J Neuromuscul Dis 2021; 8: 495-502.

Stirm M, Fonteyne LM, Shashikadze B, Lindner M, Chirivi M, Lange A, Kaufhold C, Mayer C, Medugorac I, Kessler B, Kurome M, Zakhartchenko V, Hinrichs A, Kemter E, Krause S, Wanke R, Arnold GJ, Wess G, Nagashima H,

Hrabě de Angelis M, Flenkenthaler F, Kobelke LA, Bearzi C, Rizzi R, Bähr A, Reese S, Matiasek K, Walter MC, Kupatt C, Ziegler S, Bartenstein P, Fröhlich T, Klymiuk N, Blutke A, Wolf E. A scalable, clinically severe pig model for Duchenne muscular dystrophy. Dis Model Mech 2021; 14

Stirm M, Fonteyne LM, Shashikadze B, Stockl JB, Kurome M, Kessler B, Zakhartchenko V, Kemter E, Blum H, Arnold GJ, Matiasek K, Wanke R, Wurst W, Nagashima H, Knieling F, Walter MC, Kupatt C, Frohlich T, Klymiuk N, Blutke A, Wolf E. Pig models for Duchenne muscular dystrophy - from disease mechanisms to validation of new diagnostic and therapeutic concepts. Neuromuscul Disord 2022; 32: 543-56.

Sun C, Shen L, Zhang Z, Xie X. Therapeutic Strategies for Duchenne Muscular Dystrophy: An Update. Genes (Basel) 2020; 11

Sybert VP, McCauley E. Turner's syndrome. N Engl J Med 2004; 351: 1227-38.

Szabo PL, Ebner J, Koenig X, Hamza O, Watzinger S, Trojanek S, Abraham D, Todt H, Kubista H, Schicker K, Remy S, Anegon I, Kiss A, Podesser BK, Hilber K. Cardiovascular phenotype of the Dmd(mdx) rat - a suitable animal model for Duchenne muscular dystrophy. Dis Model Mech 2021; 14

t Hoen PA, de Meijer EJ, Boer JM, Vossen RH, Turk R, Maatman RG, Davies KE, van Ommen GJ, van Deutekom JC, den Dunnen JT. Generation and characterization of transgenic mice with the full-length human DMD gene. J Biol Chem 2008; 283: 5899-907.

Tabebordbar M, Zhu K, Cheng JKW, Chew WL, Widrick JJ, Yan WX, Maesner C, Wu EY, Xiao R, Ran FA, Cong L, Zhang F, Vandenberghe LH, Church GM, Wagers AJ. In vivo gene editing in dystrophic mouse muscle and muscle stem cells. Science 2016; 351: 407-11.

Takeda S, Clemens PR, Hoffman EP. Exon-Skipping in Duchenne Muscular Dystrophy. J Neuromuscul Dis 2021; 8: S343-S58.

Tamiyakul H, Kemter E, Kosters M, Ebner S, Blutke A, Klymiuk N, Flenkenthaler F, Wolf E, Arnold GJ, Frohlich T. Progressive Proteome Changes in the Myocardium of a Pig Model for Duchenne Muscular Dystrophy. iScience 2020; 23: 101516.

Tay SK, Ong HT, Low PS. Transaminitis in Duchenne's muscular dystrophy. Ann Acad Med Singap 2000; 29: 719-22.

Teramoto N, Sugihara H, Yamanouchi K, Nakamura K, Kimura K, Okano T, Shiga T, Shirakawa T, Matsuo M, Nagata T, Daimon M, Matsuwaki T, Nishihara M. Pathological evaluation of rats carrying in-frame mutations in the dystrophin gene: a new model of Becker muscular dystrophy. Dis Model Mech 2020; 13

Tinsley J, Deconinck N, Fisher R, Kahn D, Phelps S, Gillis JM, Davies K. Expression of full-length utrophin prevents muscular dystrophy in mdx mice. Nat Med 1998; 4: 1441-4.

Tozawa T, Itoh K, Yaoi T, Tando S, Umekage M, Dai H, Hosoi H, Fushiki S. The shortest isoform of dystrophin (Dp40) interacts with a group of presynaptic proteins to form a presumptive novel complex in the mouse brain. Mol Neurobiol 2012; 45: 287-97.

Valentine BA, Cooper BJ, Cummings JF, deLahunta A. Progressive muscular dystrophy in a golden retriever dog: light microscope and ultrastructural features at 4 and 8 months. Acta Neuropathol 1986; 71: 301-10.

Valentine BA, Cooper BJ, de Lahunta A, O'Quinn R, Blue JT. Canine X-linked muscular dystrophy. An animal model of Duchenne muscular dystrophy: clinical studies. J Neurol Sci 1988; 88: 69-81.

Valentine BA, Cummings JF, Cooper BJ. Development of Duchenne-type cardiomyopathy. Morphologic studies in a canine model. Am J Pathol 1989; 135: 671-8.

Valentine BA, Winand NJ, Pradhan D, Moise NS, de Lahunta A, Kornegay JN, Cooper BJ. Canine X-linked muscular dystrophy as an animal model of Duchenne muscular dystrophy: a review. Am J Med Genet 1992; 42: 352-6.

van Putten M, Lloyd EM, de Greef JC, Raz V, Willmann R, Grounds MD. Mouse models for muscular dystrophies: an overview. Dis Model Mech 2020; 13

Verma S, Goyal P, Beam C, Shah D. Turner syndrome and Duchenne muscular dystrophy. Muscle Nerve 2017; 56: E12-E5.

Vieira NM, Elvers I, Alexander MS, Moreira YB, Eran A, Gomes JP, Marshall JL, Karlsson EK, Verjovski-Almeida S, Lindblad-Toh K, Kunkel LM, Zatz M. Jagged 1 Rescues the Duchenne Muscular Dystrophy Phenotype. Cell 2015; 163: 1204-13.

Viggiano E, Ergoli M, Picillo E, Politano L. Determining the role of skewed X-chromosome inactivation in developing muscle symptoms in carriers of Duchenne muscular dystrophy. Human Genetics 2016; 135: 685-98.

Waldrop MA, Yaou RB, Lucas KK, Martin AS, O'Rourke E, Filnemus, Ferlini A, Muntoni F, Leturcq F, Tuffery-Giraud S, Weiss RB, Flanigan KM. Clinical Phenotypes of DMD Exon 51 Skip Equivalent Deletions: A Systematic Review. J Neuromuscul Dis 2020; 7: 217-29.

Walmsley GL, Arechavala-Gomeza V, Fernandez-Fuente M, Burke MM, Nagel N, Holder A, Stanley R, Chandler K, Marks SL, Muntoni F, Shelton GD, Piercy RJ. A duchenne muscular dystrophy gene hot spot mutation in dystrophin-deficient cavalier king charles spaniels is amenable to exon 51 skipping. PLoS One 2010; 5: e8647.

Wang L, Chen M, He R, Sun Y, Yang J, Xiao L, Cao J, Zhang H, Zhang C. Serum Creatinine Distinguishes Duchenne Muscular Dystrophy from Becker Muscular Dystrophy in Patients Aged </=3 Years: A Retrospective Study. Front Neurol 2017; 8: 196.

Wanke T, Toifl K, Merkle M, Formanek D, Lahrmann H, Zwick H. Inspiratory muscle training in patients with Duchenne muscular dystrophy. Chest 1994; 105: 475-82.

Willig TN, Carlier L, Legrand M, Riviere H, Navarro J. Nutritional assessment in Duchenne muscular dystrophy. Dev Med Child Neurol 1993; 35: 1074-82.

Wu RS, Gupta S, Brown RN, Yancy CW, Wald JW, Kaiser P, Kirklin NM, Patel PC, Markham DW, Drazner MH, Garry DJ, Mammen PP. Clinical outcomes after cardiac transplantation in muscular dystrophy patients. J Heart Lung Transplant 2010; 29: 432-8.

Yeldan I, Gurses HN, Yuksel H. Comparison study of chest physiotherapy home training programmes on respiratory functions in patients with muscular dystrophy. Clin Rehabil 2008; 22: 741-8.

Young CS, Hicks MR, Ermolova NV, Nakano H, Jan M, Younesi S, Karumbayaram S, Kumagai-Cresse C, Wang D, Zack JA, Kohn DB, Nakano A, Nelson SF, Miceli MC, Spencer MJ, Pyle AD. A Single CRISPR-Cas9 Deletion Strategy that Targets the Majority of DMD Patients Restores Dystrophin Function in hiPSC-Derived Muscle Cells. Cell Stem Cell 2016; 18: 533-40.

Young CS, Mokhonova E, Quinonez M, Pyle AD, Spencer MJ. Creation of a Novel Humanized Dystrophic Mouse Model of Duchenne Muscular Dystrophy and Application of a CRISPR/Cas9 Gene Editing Therapy. J Neuromuscul Dis 2017; 4: 139-45.

Young HK, Barton BA, Waisbren S, Portales Dale L, Ryan MM, Webster RI, North KN. Cognitive and psychological profile of males with Becker muscular dystrophy. J Child Neurol 2008; 23: 155-62.

Yu HH, Zhao H, Qing YB, Pan WR, Jia BY, Zhao HY, Huang XX, Wei HJ. Porcine Zygote Injection with Cas9/sgRNA Results in DMD-Modified Pig with Muscle Dystrophy. Int J Mol Sci 2016; 17

Yue Y, Pan X, Hakim CH, Kodippili K, Zhang K, Shin JH, Yang HT, McDonald T, Duan D. Safe and bodywide muscle transduction in young adult Duchenne muscular dystrophy dogs with adeno-associated virus. Hum Mol Genet 2015; 24: 5880-90.

Zalaudek I, Bonelli RM, Koltringer P, Reisecker F, Wagner K. Early diagnosis in Duchenne muscular dystrophy. Lancet 1999; 353: 1975.

Zhang Y, Long C, Li H, McAnally JR, Baskin KK, Shelton JM, Bassel-Duby R, Olson EN. CRISPR-Cpf1 correction of muscular dystrophy mutations in human cardiomyocytes and mice. Sci Adv 2017; 3: e1602814.

Zou X, Ouyang H, Pang D, Han R, Tang X. Pathological alterations in the gastrointestinal tract of a porcine model of DMD. Cell Biosci 2021; 11: 131.

Zurbrigg K, van Dreumel T, Rothschild MF, Alves D, Friendship R, O'Sullivan TL. Cardiac weights and weight ratios as indicators of cardiac lesions in pigs: A study of pig hearts from an Ontario abattoir. Canadian Journal of Veterinary Research-Revue Canadienne De Recherche Veterinaire 2018; 82: 198-202.

X. ACKNOWLEDGEMENTS

I am very grateful to Prof. Dr. Eckhard Wolf for giving me the opportunity to prepare my doctoral thesis at the Chair for Molecular Animal Breeding and Biotechnology of the Ludwig-Maximilians-University Munich, the excellent supervision and for reviewing this manuscript.

I also want to thank Prof. Dr. Andreas Parzefall from the Chair for Veterinary Pathology.

Furthermore, I would like to thank everyone at the Chair for Molecular Animal Breeding who has supported me over the past three years. I would especially like to thank Dr. Elisabeth Kemter, Dr. Lina Fonteyne, Dr. Mayuko Kurome, Prof. Dr. Valerie Zakhartchenko, Dr. Barbara Kessler, Dr. Kilian Simmet and Dr. Florian Jaudas for their endless support. Thanks to Max Moraw, Christina Blechinger, Tuna Güngör and Tatiana Schröter for technical assistants, Harald Paul for excellent animal caretaking and to all the fellow graduate students (Laeticia, Nadja, Andreas, Libera, Richard, Johanna, Nicol, Yasmin, Natalie, Hannah, Sarah, Lucie and Martin) for their help.

Finally, I want to thank my family and friends for interest and support.